Translation elongation factor P and its post-translational modification enzyme EpmA

DISSERTATION

der Fakultät für Biologie

der Ludwig-Maximilians-Universität München

vorgelegt von

Miriam Pfab

München, November 2020

Diese Dissertation wurde angefertigt

unter der Leitung von Prof. Dr. Kirsten Jung

im Bereich Mikrobiologie

an der Ludwig-Maximilians-Universität München

Erstgutachterin: Prof. Dr. Kirsten Jung

Zweitgutachter: Prof. Dr. Jörg Nickelsen

Tag der Abgabe: 02. Juli 2020

Tag der mündlichen Prüfung: 11. November 2020

Eidesstattliche Erklärung

Ich versichere hiermit an Eides statt, dass die vorgelegte Dissertation von mir selbstständig und ohne unerlaubte Hilfe angefertigt wurde. Des Weiteren erkläre ich, dass ich nicht anderweitig ohne Erfolg versucht habe, eine Dissertation einzureichen oder mich der Doktorprüfung zu unterziehen. Die folgende Dissertation liegt weder ganz, noch in wesentlichen Teilen einer anderen Prüfungskommission vor.

München, den 23.11.2020

Miriam Pfab

Statutory Declaration

I declare that I have authored this thesis independently, that I have not used other than the declared sources/resources. As well I declare, that I have not submitted a dissertation without success and not passed the oral exam. The present dissertation (neither the entire dissertation nor parts) has not been presented to another examination board.

Munich, 23.11.2020

Miriam Pfab

Table of Content

Eidesstattliche Erklärung III
Statutory Declaration III
Table of Content IV
Nomenclature VII
Abbreviations VIII
Contributions and publications originating from this thesis III
Summary IV
Zusammenfassung V
1 Introduction 1
1.1 Translation as checkpoint for protein production 1
1.2 Bacterial translation elongation factors 3
1.3 Strategies for post-translational modification of EF-P 5
1.4 EF-P modification pathway in *E. coli* 7
1.5 EpmA, a representative of lysyl-tRNA synthetase class II 8
1.6 Aim of the study 11
2 Material and methods 12
2.1 General 12
2.1.1 Strains, primers and plasmids 12
2.1.2 Standard chemicals and cultivation of bacteria 18
2.1.3 Molecular genetic methods and Miscellaneous 19
2.2 Peptide antibody generation 21
2.3 Preparation of bacterial lysates 21
2.4 Cloning strategies for plasmid and strain constructions 22
2.4.1 His_6-SUMO-tagged *efp*s from different organisms 22
2.4.2 His_6-tagged EpmA and its variants A298G, R303I/L/S and His_{10}-tagged EpmB 22
2.4.3 Removal of resistance cassette to create antibiotic-sensitive strains 23
2.5 Overexpression and purification of EF-Ps from *E. coli*, *B. subtilis* and *S. oneidensis* 23
2.6 Electrophoretic methods 25
2.6.1 SDS-polyacrylamide gel electrophoresis 25
2.6.2 Sample preparation for isoelectric focusing 25

2.6.3 Native horizontal isoelectric focusing 26
2.6.4 Denaturating horizontal isoelectric focusing 27
2.6.5 Vertical isoelectric focusing 27
2.7 Silver Staining, Western Blotting and antibodies used in this study 27
2.8 *B. subtilis* swarming assay 29
2.9 Experiments with antibiotic gradient plates 29
2.10 *In vitro* EF-P modification by EpmA 30
2.11 [^{32}P]-AMP formation assay 30
2.12 *In vitro* transcription/translation of RPPP-Nluc 31
2.13 β-galactosidase activity assay 32
2.14 Purification of endogenous EF-P 32
3 Results 34
3.1 Universal antibody against EF-P of a wide range of bacteria 34
3.1.1 Generation of the two EF-P-specific peptide antibodies P68/P69 34
3.1.2 Characterization of antibodies P68/P69 36
3.1.3 Applications of P68/P69 38
3.2 Isoelectric focusing for detection of the post-translational modification status of EF-P *in vivo* 41
3.2.1 General remarks for reproducible IEF results 41
3.2.2 Detection of EF-P$_{E.c.}$ modification status in different growth phases 44
3.3 Modification of EF-P with unnatural substrates by the help of EpmA 46
3.3.1 Copy number balance of EF-P, EpmA and EpmB 46
3.3.2 Identification of functional EpmA amino acid variants 48
3.3.3 Unnatural post-translational modifications of EF-P mediated by EpmA 50
3.3.4 Unnatural EF-P modification *in vivo* 66
3.4 Modification of EF-P in *B. subtilis* and other Firmicutes 70
3.4.1 Modification status of EF-P$_{B.s.}$ during different growth phases 70
3.4.2 Aminotransferases potentially involved in the post-translational modification of EF-P$_{B.s.}$ 71
4 Discussion 73
4.1 Unnatural post-translational modifications of EF-P 73
4.2 New insights into post-translational modification of EF-P in *E. coli* 83
4.3 Promiscuity of EpmA unlocks the enzyme's potential 85
4.4 Modification of EF-P in *Bacillus* 88

4.5 Detection of EF-P for elucidation of new post-translational modifications... 90
5 References..... 95
Acknowledgements 107
Curriculum Vitae 108

Nomenclature

Amino acids are given in the one-letter code (e. g. K for lysine), whereby X is a placeholder for any amino acid (e. g. PPX for proline-proline-amino acid).

The configuration at the stereocenter of an amino acid is given according to Cahn-Ingold-Prelog priority rules (e. g. (*R*/*S*)-lysine) instead of using the historically evolved *D*/*L* configuration derived from the Fischer projection.

Amino acid exchanges are indicated by naming the original amino acid followed by its position in the protein and the new amino acid (e. g. EpmA_A298G: alanine in position 289 of EpmA is replaced by glycine).

N-terminal and C-terminal affinity tags are placed corresponding to their position in relation to the protein (e. g. His_6_*epmA* or *efp*_His_6).

The bacterial origin of a gene or protein is abbreviated and subscripted (e. g. $efp_{E.c.}$, $EF\text{-}P_{B.s.}$). Deletions of genes as well as the mass difference between unmodified and modified EF-P are marked with Δ.

P68 and P69 name the two different peptide antibodies for EF-P from diverse bacteria. Their names are derived from the synthesized peptides no. 1612068 and 1612069 (Eurogentec numbering), respectively.

The incorrect but widely used biological unit m/v% (mass/volume percentage) is renounced.

Antibiotic resistances are indicated by the abbreviated antibiotic followed by superscripted ‘R’ (e. g. Cm^R, Kan^R), whereby sensitivity to the certain antibiotic is indicated by superscripted ‘S’ (e. g. Kan^S).

If not otherwise stated, tests were conducted in biological replicates of at least three individual measurements and are presented by mean and standard error (s.e.m.).

Radioactively labeled compounds are marked with a star (e. g. ATP* for [α-^{32}P]-ATP).

Abbreviations

1D-IEF	one-dimensional isoelectric focusing
A-site	aminoacyl site
aa-AMP	aminoacyl adenylate
aa-tRNA	aminoacyl-tRNA
aaRS	aminoacyl-tRNA synthetase
AB	antibody
AC	aminocapronic acid
AcK	acetyllysine
aIF5A	archaeal translation initiation factor 5A
APS	ammonium peroxodisulfate
ATP	adenosine triphosphate
BCIP	5-bromo-4-chloro-3-indolyl-phosphate
BPP	bromophenol blue
BSA	bovine serum albumin
ddH_2O	double distilled water
CFSB	cell-free synthetic biology
dH_2O	distilled water
CHAPS	3-[(3-cholamidopropyl) dimethylammonio]-1-propanesulfonate
Cryo-EM	Cryogenic Electron Microscopy
Da	Dalton
DAP	diaminopimelic acid
DNase	deoxyribonuclease
DTT	1,4-dithiothreitol
E-site	exit site
EDTA	ethylenediaminetetra-acetic acid
EE	early exponential phase
EF-G	elongation factor G
EF-P	translation elongation factor P
EF-Ts	elongation factor thermo stable
EF-Tu	elongation factor thermo unstable
eIF5A	eukaryotic translation initiation factor 5A
ELISA	Enzyme-Linked ImmunoSorbent Assay
EtOH	ethanol
FDA	U. S. Food and Drug Administration
GTP	guanosine triphosphate
HEPES	2-[4-(2-hydroxyethyl) piperazin-1-yl]ethane sulfonic acid
IEF	isoelectric focusing
IMAC	immobilized metal ion affinity chromatography
IPTG	isopropyl-β-D-thiogalactopyranoside
KAT	lysine acetyltransferases
kb	kilobase
kcal	kilocalorie
kDa	kilodalton
KDAC	lysine deacetylases

KEGG	Kyoto Encyclopedia of Genes and Genomes
KLH	keyhole limpet hemocyanin
K_m	Michaelis constant
LAO	lysine-arginine-ornithine
LB	lysogeny broth
LC	liquid chromatography
LE	late exponential phase
LP	lag phase
LysP	lysine-specific permease
M	molar mass
ME	middle exponential phase
MeOH	methanol
mRNA	messenger RNA
MS	mass spectrometry
Mw	molecular weight
n	amount
N	particle number
N_A	Avogadro constant
NBT	4-nitro blue tetrazolium chloride
NC	nitrocellulose
NCBI	National Center for Biotechnology Information
n. d.	not determined
Nluc	NanoLuc luciferase
NMR	nuclear magnetic resonance
NptI	neomycin phosphotransferase I
NTA	nitrilotriacetic acid
OB	oligonucleotide binding
OD_{600}	optical density at 600 nm wavelength
ON	over night
ORF	open reading frame
P-site	peptidyl site
PAGE	polyacrylamide gel electrophoresis
PCR	polymerase chain reaction
PDB	Protein Data Bank
PEI	polyethylenimine
pI	isoelectric point
PIPES	piperazine-N,N'bis(2-ethanesulfonic acid)
PLMD	protein lysine modification database
PLP	pyridoxal 5'-phosphate
PMSF	phenylmethylsulfonyl fluoride
PTC	peptidyl transferase center
PTM	post-translational modification
RBS	ribosome binding site
R_F	retardation factor
RiPP	Ribosomally synthesized and post-translationally modified peptide
RNA	ribonucleic acid
rpm	rounds per minute
rRNA	ribosomal RNA
RT	room temperature
SAM	*S*-adenosyl methionine

SDS	sodium dodecyl sulfate
s.e.m.	standard error of the mean
SP	stationary phase
sRBS	synthetic ribosome binding site
SUMO	small ubiquitin-like modifier
TAE	Tris-acetate-EDTA
TCA	trichloroacetic acid
TCE	2,2,2-trichloroethanol
TEA	triethanolamine
TEMED	tetramethylethylene-diamine
TLC	thin layer chromatography
Tris	tris(hydroxymethyl)-aminomethane
tRNA	transfer RNA
Ulp	ubiquitin-like protein-processing enzyme
V	volume
v%	volume percent
WT	wild-type
wt%	weight percent

Contributions and publications originating from this thesis

Weblogos presented in Figure 8 were designed by Prof. Dr. Jürgen Lassak. Figure 11B and Figure 16BC are based on data determined in Schmidt *et al.* [1]. Alina Sieber provided His_6-tagged EF-P purified from *E. coli* LF1 P_{lac} *efp* background. Mass spectrometry experiments were performed by Dr. Pavel Kielkowski (TU Munich, Figure 25, Figure 29, Table 6 and Table 7). Structures in Figure 32 were depicted by Dr. Ralph Krafcyzk. Study on using the amber suppression system to modify EF-P with tetrahydrofuran carboxylic acid, butanoic acid, crotonic acid, propionic acid and valeric acid was performed by Dr. Wolfram Volkwein. All other experiments were performed by Miriam Pfab.

Parts of figures, tables and text in Chapter 3.3.3 and 3.3.4 as well as parts of Figure 32 were previously published in a different form in:

Miriam Pfab, Pavel Kielkowski, Ralph Krafczyk, Wolfram Volkwein, Stephan A. Sieber, Jürgen Lassak, Kirsten Jung (2020). Synthetic post-translational modifications of elongation factor P using the ligase EpmA. [published online ahead of print, 2020 Apr 26]. *FEBS J*. 2020;10.1111/febs.15346.

Parts of Figure 14C were previously published in:

Wolfram Volkwein*, Ralph Krafczyk*, Pravin Kumar Ankush Jagtap, Marina Parr, Elena Mankina, Jakub Macošek, Zhenghuan Guo, Maximilian Josef Ludwig Johannes Fürst, Miriam Pfab, Dmitrij Frishman, Janosch Hennig, Kirsten Jung and Jürgen Lassak (2019). Switching the Post-translational Modification of Translation Elongation Factor EF-P. Frontiers in Microbiology 10.

*Authors contributed equally

Summary

Protein translation is a non-uniform process, whereby especially proline-containing motifs lead to ribosome stalling events. Elongation factor P (EF-P) rescues the ribosome by stimulation of peptidyl transfer. The four known subgroups of bacterial EF-Ps either require post-translational modification (PTM) established by EpmABC/EarP/YmfI or are functional without PTM. In *Escherichia coli*, the aminomutase EpmB converts (*S*)-α-lysine into (*R*)-β-lysine, which is subject to a two-step reaction catalyzed by lysyl-tRNA synthetase paralog EpmA. First, (*R*)-β-lysyl-adenylate is formed, from which the β-lysyl moiety is subsequently transferred to the ε-amino group of lysine 34 of EF-P.

This thesis focuses on the interplay of EF-P and EpmA which ensures EF-P functionality *in vivo* and was used to modify EF-P with seven unnatural substrates *in vitro*. To detect PTM status two universal peptide antibodies, nonselective for the bacterial origin of EF-P, were generated and three subtypes of one-dimensional isoelectric focusing were established (native/denaturating horizontal, vertical). EpmA and EF-P protein copy numbers indicated balanced coordination to ensure outright modification status of EF-P during all growth phases, but no mutual regulation. EpmA's donor substrate promiscuity was pinpointed to permit C_6 scaffolds with at least an amino group at α- ((*R*/*S*)-α-lysine, 5-hydroxy-(*S*)-α-lysine), β- ((*R/S*)-β-lysine, (*R*)-3-aminocapronic acid) or ε-position (6-aminocapronic acid). In addition, EpmA variant A298G enabled modification of EF-P with (*S*)-α-ornithine. For the first time, known natural PTMs of EF-P were expanded by seven synthetic PTMs. *In vitro* transcription translation assay demonstrated superiority of (*R*)-β-lysylation in ribosome rescue, explaining its evolutionary selection. Modification of EF-P with (*S*)-α-lysine was successfully achieved *in vivo*, when (*R*)-β-lysine synthesis was impeded (*E. coli* Δ*epmB*) and *epmA*(_A298G) overexpressed.

In *Bacillus subtilis*, the ratio of unmodified-to-modified EF-P varied over time. Out of 13 tested aminotransferase genes *dat*, *epsN*, *gsaB*, *ilvK* and *yhdR* are potentially involved in the yet unsolved modification pathway.

In summary, the present work not only provides new biochemical insights into the functionalization of EF-P, but also paves the way to modify proteins post-translationally using EpmA.

Zusammenfassung

Die Translation von Proteinen ist kein gleichförmiger Prozess. Besonders bei Polyprolinmotiven treten Verzögerungen des Ribosoms auf. Hier übernimmt Elongationsfaktor P (EF-P) eine helfende Funktion und stimuliert den Peptidyltransfer. Die vier bekannten Gruppen von bakteriellen EF-P benötigen entweder posttranslationale Modifikation (PTM) durch EpmABC/EarP/YmfI, oder sind ohne PTM funktional. In *Escherichia coli* wandelt die Aminomutase EpmB (*S*)-α-Lysin in (*R*)-β-Lysin um. Ein Paralog der Lysyl-tRNA-Synthetase, EpmA, katalysiert die folgende zweistufige Reaktion. Erst wird (*R*)-β-Lysyladenylat gebildet, dessen β-Lysylgruppe dann auf die ε-Aminogruppe von Lysin 34 von EF-P übertragen wird.

Diese Dissertation widmet sich dem Zusammenspiel von EF-P und EpmA. Dieses stellt *in vivo* die Funktion von EF-P sicher, *in vitro* erlaubt es die Modifikation von EF-P mit sieben unnatürlichen Substraten. Zur Detektion des PTM Status wurden zwei universelle Peptidantikörper etabliert, die EF-P unabhängig von dessen bakterieller Herkunft detektieren, sowie drei Formen der eindimensionalen Isoelektrischen Fokussierung (nativ/denaturierend horizontal, vertikal). Die Kopienzahlen von EpmA und EF-P sind aufeinander abgestimmt, um vollständige Modifikation von EF-P in allen Wachstumsphasen sicherzustellen. Sie regulieren sich aber nicht gegenseitig. Die Promiskuität von EpmA erlaubt Donorsubstrate mit C_6-Ketten, die zumindest eine Aminogruppe in α- ((*R*/*S*)-α-Lysin, 5-Hydroxy-(*S*)-α-lysin), β- ((*R*/*S*)-β-Lysin, (*R*)-3-Aminohexansäure) oder ε-Position (6-Aminohexansäure) haben. Zusätzlich ermöglicht die Enzymvariante EpmA_A298G (*S*)-α-Ornithylierung von EF-P. Erstmals konnten so die natürlichen PTMs von EF-P um sieben synthetische PTMs erweitert werden. *In vitro* Transkriptions/Translations-Assays zeigten die wirkungsvollste Ribosomen-rettung bei (*R*)-β-lysyliertem EF-P, was dessen evolutionäre Auswahl erklärt. *In vivo* gelang die Modifikation von EF-P mit (*S*)-α-Lysin, wenn die Fähigkeit zur (*R*)-β-Lysinsynthese fehlte (*E. coli* Δ*epmB*) und *epmA*(_A298G) überexprimiert wurde.

In *Bacillus subtilis* variiert das Verhältnis von unmodifiziertem zu modifiziertem EF-P. Von 13 untersuchten Genen, die Aminotransferasen kodieren, sind *dat*, *epsN*, *gsaB*, *ilvK* und *yhdR* möglicherweise am ungeklärten Modifikationsweg beteiligt.

Zusammengefasst liefert die vorliegende Arbeit nicht nur neue biochemische Einsichten in die Funktionalisierung von EF-P, sondern eröffnet auch einen neuen Weg, Proteine mittels EpmA posttranslational zu modifizieren.

1 Introduction

1.1 Translation as checkpoint for protein production

In all domains of life, the fundamental step of protein synthesis presets cellular proteome composition and quality. Coordinated interplay of several cellular compounds is necessary for conversion of a gene into a functional protein. For transcription RNA polymerase, transcription factors and RNA nucleotides are employed to form the pool of messenger RNA. The latter is further processed at the ribosome to translate it by the help of charged tRNA (harboring the anticodon triplets of the genetic code), several translation factors and GTP into a functional protein (Figure 1). The ribosome serves as the central machinery of mRNA-to-protein translation and in bacteria, it consists of three rRNAs (16S, 23S, 5S) and 52 ribosomal proteins itself [2]. Ribosome concentration increases with increasing cell size leading to the conclusion that the ~10,000 ribosomes/cells exclude ribosome availability limitation [2]. This is also reflected in the stable active ribosome fraction of 80 % [3].

All three steps of translation - namely initiation, elongation and termination - but also the co-translational folding are checkpoints on the way to protein synthesis that finally ensures protein homeostasis or stress adaptation. They all aim to work together for optimal protein amount and quality. It is known that transcription and translation speed are coordinated as their rates are equivalent [3]. During initiation the ribosome selects and binds the mRNA and occupies the ribosome binding site (RBS) at the start of the open reading frame (ORF). At this stage, the control point is mainly RBS accessibility supervised by secondary mRNA structures which are induced by protein-, RNA-, metabolite-, and temperature variations [4]. Translation elongation implies aminoacyl-tRNA (aa-tRNA) selection, peptide bond formation in the peptidyl transferase center (PTC) and tRNA/mRNA translocation (Figure 1) [5]. After completed translation of the mRNA into a polypeptide chain, the latter is released from the ribosome which dissociates into its subunits (termination and ribosome recycling) [4].

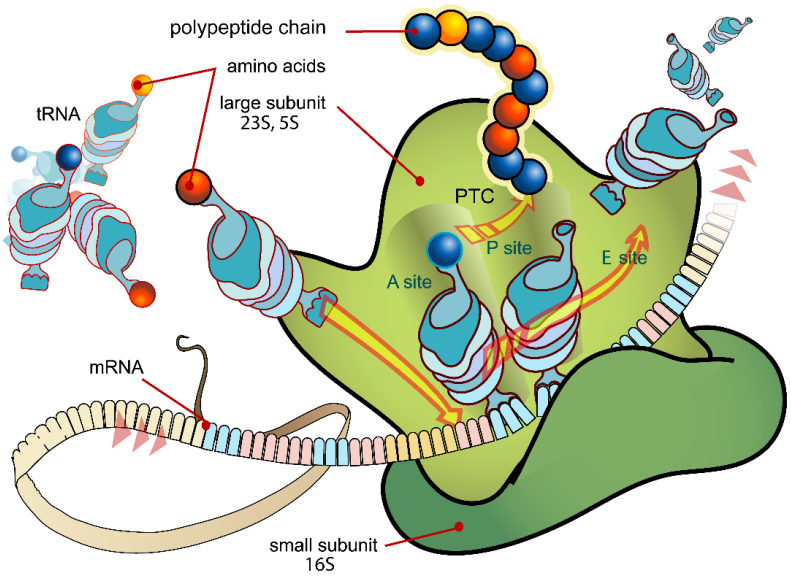

Figure 1: Ribosome during translation of mRNA to form the nascent polypeptide chain. The cartoon is derived from [6]. PTC: peptidyl transferase center.

This thesis focuses on the step of translation elongation, whereby rapidly synthesized stretches can be interrupted by translational pauses, making translation elongation a non-uniform process. In average, 12 to 21 amino acids per second are connected in the widely used laboratory organism *Escherichia coli* but as the translation rate is not uniform, it depends on various factors such as secondary structure elements of the mRNA, tRNA availability, rare codon usage, interactions between ribosome and nascent polypeptide (stalling peptides) and not least of amino acid nature [3, 5, 7]. It is calculated that one aminoacyl-tRNA synthetase (aaRS) aminoacylates 10 cognate tRNAs per second, leading to a tRNA pool with 75 - 90 % charging level on average [2]. Availability of low abundant cognate aa-tRNAs as well as codon choice are factors that can influence local translation elongation rates [4]. For example, there are hints that rare codons are found between protein domains to downregulate translation speed which provides a time delay for correct folding [8, 9]. Translation of a mRNA strand is newly initiated before the ribosome completes translation of the ORF which leads to polysome formation and is reflected by the ratio of ~540 protein copies per one mRNA copy in *E. coli* [10]. Bremer *et al.* reported that increasing growth rates lead to less space between one ribosome on the mRNA and the following one, namely it is reduced from 120 to 60 nucleotides during exponential growth [2]. These “logistic demands” reflect the necessity for high accuracy and smooth progression of translation elongation. The identity of the peptidyl-tRNA in the peptidyl site (P-site) as well as aa-tRNA in the aminoacyl site (A-site) can contribute to decreased elongation rates

because donor and acceptor substrate influence peptidyl transfer [11]. Regarding these amino acid structure effects especially proline sticks out due to rigidity of its pyrrolidine ring. The challenge to translate polyproline sequences arises from poor accommodation of the prolyl-tRNA, the retarded rate of peptide bond formation at proline residues and clashes between the nascent polyproline chain and the exit tunnel [12–14]. This leads to high dependency of elongation speed on the amino acid context surrounding a diproline motif. Explicitly, strong ribosome stalling occurs for example at triproline and D/A-PP or PP-W/D/N/G motifs [15].

To ensure protein homeostasis and bacterial fitness, specialized translation elongation factors are recruited to the ribosome to facilitate peptide bond formation between prolines in bacteria (translation elongation factor P (EF-P), [16]) as well as in eukaryotes (eukaryotic translation initiation factor 5A (eIF5A), [17]), respectively.

To summarize, translation elongation is a non-uniform process. Especially polyproline containing motifs lead to ribosome stalling that requires relief by a specialized translation elongation factor.

1.2 Bacterial translation elongation factors

Translation elongation factors EF-Tu (thermo unstable), EF-Ts (thermo stable) and EF-G support translation independent of the motif to be translated, whereby EF-P is especially recruited to paused ribosomes.

Charged tRNAs (aa-tRNAs) form the ternary complex with EF-Tu and GTP and are subsequently delivered to the ribosome [5]. The ternary complex with the cognate aa-tRNA interacts with the mRNA codon exposed in the A-site of the ribosome. Here, EF-Tu catalyzes hydrolysis of GTP and dissociates from the ribosome. At this stage, EF-Ts acts as the guanine nucleotide exchange factor for EF-Tu. This leads to a change in conformation of the complex and enables the aa-tRNA to align in the A-site and to interact with the nascent peptide chain in the P-site [4]. It is shown for corporation of proline into the nascent peptide chain that the slowest step is performed at the PTC after GTP hydrolysis of EF-Tu [13].

Another elongation factor, EF-G, catalyzes tRNA-mRNA translocation under GTP hydrolysis. The peptidyl-tRNA is moved from A- to P-side and subsequently, deacylated tRNA is repositioned to the exit site (E-site) [5].

In contrast to EF-Tu and EF-G, EF-P is not catalyzing global steps during the protein translation but is specialized for relief of ribosome pausing that is caused by stalling motifs. EF-P is conserved among all bacteria whereby the evolutionary origin is linked to valyl-tRNA synthetase (ValS), which contains PPP in its active site and is essential in all bacteria [18]. EF-P is particularly required in phases of high translation initiation rates that entail the danger of ribosome queuing at PPX motifs [19]. 270 proteins from *E. coli* (total >4000) contain PPP or PPG, whereby transcription factors, metabolic proteins and transporters are more frequently found than basal proteins [20]. It was shown that several other stalling motifs have been selected against, except for PP(X) motifs [21]. EF-P was crystallized (*Thermus thermophilus* [22], in complex with a ribosome [23]; *E. coli*, in complex with EpmA [24]) and thereby shown to contain three β-barrel domains (I, II, III) that are arranged in L-shape and exhibit a negatively charged surface (Figure 2) [22]. N-terminal domain I contains a conserved positive residue at its tip [22].

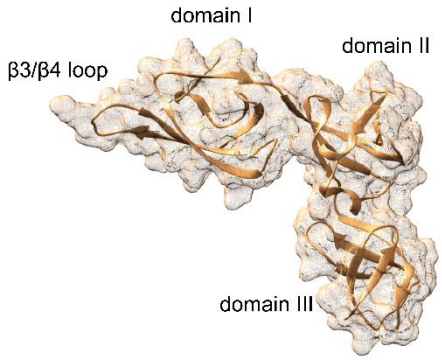

Figure 2: Structure of EF-P. The bacterial elongation factor contains three domains. β3/β4 loop contains the conserved tip residue that is post-translationally modified. The crystal structure is derived from *E. coli* [24].

EF-P spans both ribosomal subunits 30S and 50S and binds between peptidyl-tRNA P-site and the E-site [23]. Stimulation of the peptide bond formation requires functional EF-P reaching with the conserved residue at the tip of EF-P into the PTC [12, 23]. For the vast majority of bacteria it was shown that EF-P needs to be post-translationally modified for full functionality [16, 25]. By that, EF-P stabilizes the peptidyl-Pro-tRNA, decreases the activation energy by ~2.5 kcal/mol and entropically stimulates peptide bond formation [12]. The highly abundant polyproline motifs lead to importance of EF-P for proper protein synthesis in bacterial strains in general but also in pathogens.

1.3 Strategies for post-translational modification of EF-P

Bacteria, eukaryotes and archaea have evolved several distinct ways to post-translationally modify their EF-P (e/aIF5A), whereby they all have in common that the central amino acid residue of the loop between β-strands 3 and 4 (β3/β4 loop) is the position of modification. It leads to a prolongation of the residue that is now able to reach into the PTC and thereby stimulates peptide bond formation between prolines [12].

Translation initiation factor 5A, the ortholog of EF-P in eukaryotes, is modified post-translationally in a two-step process. Deoxyhypusine synthase (DHS) attaches the 4-aminobutyl moiety of spermidine to a conserved lysine residue. Subsequently, deoxyhypusine hydroxylase (DOHH) hydroxylates the PTM to convert lysine into hypusine (N^{ε}-(4-amino-2-hydroxybutyl)-lysine) [26–29]. PTM of aIF5A is similar, but not as detailed studied as for eIF5A [30, 31].

In 2010 it was published that *E. coli* and other γ-proteobacteria modify the conserved K34 of EF-P with (*R*)-β-lysine (Figure 3) [19, 32]. The conserved residue is embedded in the signature sequence PGKG. The substrate of modification is produced from the proteinogenic amino acid lysine ((*S*)-α-lysine) catalyzed by aminomutase EpmB. Subsequently, (*R*)-β-lysine is ligated to EF-P by EpmA and K34 is hydroxylated by EpmC [19, 33]. The detailed mechanism is presented in chapter 1.4.

In 2016, the first PTM of EF-P from a Gram-positive bacterium was published. *Bacillus subtilis* EF-P was shown to have a 5-aminopentanol residue attached to K32 [34]. The latter lays in the corresponding signature motif KPGKG with the second lysine being modified [35]. 5-aminopentanolation is structurally akin to (*R*)-β-lysylation as well as to the hypusination observed in eukaryotes (eIF5A). Nevertheless, the modification pathway in *B. subtilis* and Firmicutes seems to be more complex and is not fully understood to date. Known is, that YmfI catalyzes the last step of modification, the conversion of 5-aminopentanone to 5-aminopentanol at EF-P and is found in 4.5 % of bacteria [35]. How and which precursor is transferred to K32 remains elusive. Nevertheless, Witzky *et al*. proposed that *ynbB* and *gsaB* are required in addition to *ymfI* [36].

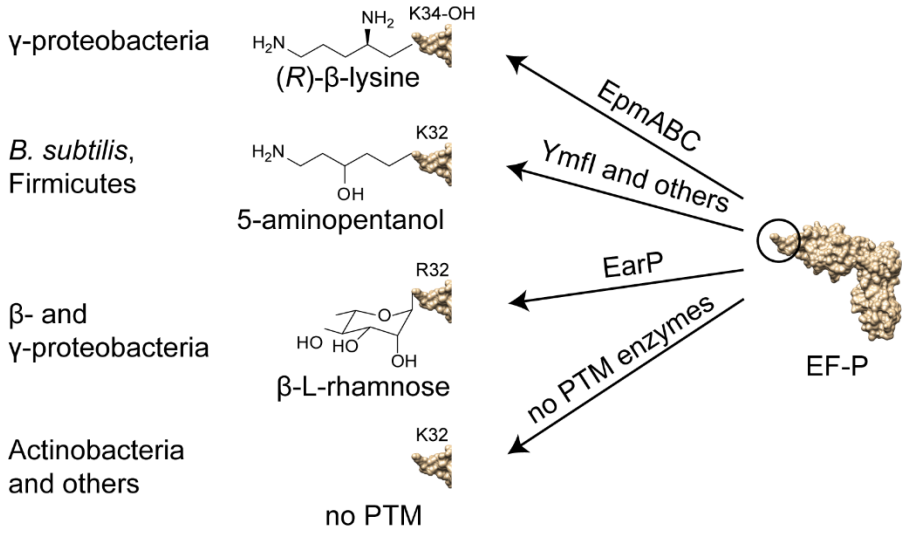

Figure 3: Post-translational modifications of EF-P in bacteria. The conserved tip residue (lysine or arginine) is modified by the help of different PTM systems.

By contrast, the group of bacteria with ring structured PTM stands out. β-proteobacteria and some γ-proteobacteria including *Pseudomonas* mono-rhamnosylate EF-P at the conserved residue R32 [37]. Here, the sequence background of the β3/β4 loop is more variable than found for other EF-P subfamilies but proline is excluded at -2 position to the central arginine [38]. These 9 % of bacteria encode *earP* as their EF-P modification enzyme which rhamnosylates EF-P by N-linked glycosylation [37, 39–41]. The donor substrate for the reaction, dTDP-β-L-rhamnose, is produced in the RmlABCD pathway. In this study, *Shewanella oneidensis* is chosen as model organism to represent the group of EF-P modifiers *via* the EarP pathway.

Recently a whole new clade of bacteria was published that encode EF-P not being post-translationally modified [35]. Instead, structure analysis revealed the palindromic consensus sequence PGKGP to stabilize the loop due to the rigidity of the two bracketing prolines [35]. The central K32 was shown to enable functionality of EF-P by its positively charged side chain, as replacement by arginine kept the ribosome rescue ability of EF-P. This unique subfamily is formed by 11 % of bacteria, including predominantly Actinobacteria but also *Flavobacterium* and *Campylobacter* species [35].

In total, ~40 % of bacteria are known to post-translationally modify their EF-Ps. They all have in common that positively charged amino acids (either lysine or arginine) are modified in a very specific and unusual way. (*R*)-β-lysylation, 5-aminopentanolation and N-linked glycosylation were first discovered on EF-P, so on the one hand, these

evolutionary events seem to be quite unique strategies of protein functionalization and on the other hand, several independent ways to functionalize EF-P at the ribosome are possible. Only around one half of bacterial EF-Ps is solved regarding their PTM and/or modification enzymes. Therefore, study on EF-P is not complete. Especially poorly studied strains require specialized culture conditions and additional expertise. For those bacteria, EF-P detection tools, which lay the foundation for their research, remain elusive. Among them is a universal antibody for EF-P which is sensitive and specific for a preferably large group of bacteria ranging from Gram-negative to Gram-positive bacteria of different phyla.

1.4 EF-P modification pathway in *E. coli*

The most abundant - and for this thesis central - modification is (*R*)-β-lysylation of K34 by the help of modification enzymes EpmABC. This pathway that is utilized by 26 - 28 % of all bacteria [19, 37], including *E. coli* and most other γ-proteobacteria, is depicted in Figure 4.

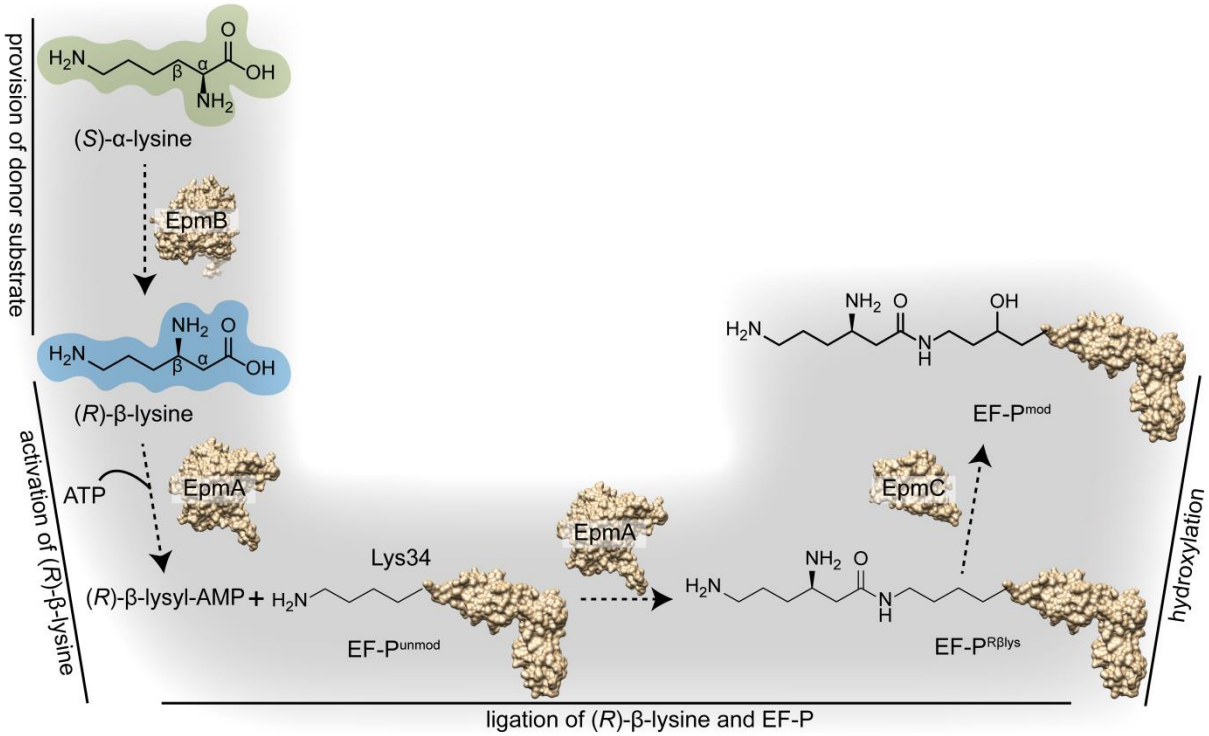

Figure 4: Modification pathway of EF-P by EpmABC. Aminomutase EpmB transfers the proteinogenic amino acid (*S*)-α-lysine into (*R*)-β-lysine. Subsequently, a two-step reaction is catalyzed by EpmA: First, (*R*)-β-lysine as donor substrate is activated by hydrolysis of ATP. Second step is the ligation of (*R*)-β-lysyl-AMP to K34 of EF-P under release of AMP (EF-P$^{R\beta lys}$). The now functional EF-P is further hydroxylated at K34 by EpmC (EF-P^{mod}).

The L-lysine 2,3-aminomutase EpmB (YjeK) provides the natural substrate for EpmA (YjeA, GenX, EF-P – (*R*)-β-lysine ligase, PDB: 3A5Y/Z [24]), as it isomerizes (*S*)-α-

lysine to form (*R*)-β-lysine using a radical mechanism [42]. EpmB requires *S*-adenosyl methionine (SAM), a [4Fe-4S] cluster and pyridoxal 5'-phosphate (PLP) [42]. EpmA catalyzes the central two-step reaction that involves activation of (*R*)-β-lysine to form the high-energy aminoacyl-adenylate (*R*)-β-lysyl-AMP which is subsequently cleaved in a thermodynamically favorable reaction to condensate the activated amino acid with EF-P as acceptor. EpmC (EF-P hydroxylase, YfcM, PDB: 4PDN [43]) finally hydroxylates EF-P [33]. This last step is not essential for EF-P's functionality [16, 18, 20].

It is widely accepted that deletion of *efp*, *epmA* or *epmB* results in similar phenotypes. At first glance this seems to be obvious because either *epmA* or *epmB* deletion leads to EF-P in the unfunctional, unmodified form and phenotypes are often similar to global absence of *efp*. Nevertheless, a detailed look at this subject reveals a divergent situation in the cell whether the EF-P modification pathway is impaired, EF-P is forced to be in the unmodified state (EF-P_K34A) or EF-P lacks completely [44, 45]. Moreover, there are situations reported where EF-P in the unmodified form seems to have an advantageous effect [46]. Therefore, it is necessary to analyze *E. coli* Δ*epmB* more closely regarding the modification status of EF-P *in vivo*, as in this strain (*R*)-β-lysine is unavailable and the natural modification can not be established.

Of all bacterial modification enzymes known to date, EpmA stands out due to its relevance in the most commonly used laboratory bacterium, the wide abundance in bacterial species in general and its central role within the PTM pathway of EF-P as it catalyzes both important reaction steps.

1.5 EpmA, a representative of lysyl-tRNA synthetase class II

In all domains of life aaRSs play a central role in protein expression as they catalyze the esterification of their cognate amino acids to the hydroxyl group at the 3' end of the corresponding tRNAs (Figure 5, upper part) [47]. This correct charging of one of the 20 proteinogenic amino acids enables efficient and accurate translation of the genetic code. aaRS can be divided into two subclasses, whereby composition of the catalytic domain is defining. It is well studied that class I aaRS which contain a catalytic domain with Rossmann fold are predominantly selecting for hydrophobic amino acids and their corresponding tRNAs. The catalytical core structure of class II tRNA synthetases possesses three β hairpins with a large loop between β-strands 2 and 3 which includes the characteristic Motif II [48]. Here, the uniqueness of lysyl-tRNA synthetase (LysRS)

becomes perceptible as class I and class II LysRS both exist and are unrelated to each other [49]. The first-mentioned variant is present in Euryarchaeota, Spirochaetes and *Rickettsia* whereas the last-named is found in eukaryotes, the rest of bacteria and the crenarchaea [49]. For class IIb aaRSs (including aaRS for lysine, aspartate and asparagine), Smith *et al*. suggest that their evolutionary origin lays in a single tRNA synthetase putatively able to recognize an ancient precursor of lysine, an early available and positively charged compound like 2,4-diamino butyric acid or 2,3-diamino propionic acid [48].

However, lysyl-tRNA synthetase class II not only covers LysRS but also the interesting enzyme EpmA [50] that has evolved an entirely new function in a large subset of bacteria. In 1991, EpmA was first described as “new protein resembling a lysyl-tRNA synthetase”. Indeed, EpmA shows 31 % amino acid identity with the C-terminal domain of LysRS from *E. coli* but lacks the N-terminal OB-fold anticodon binding domain [19, 50]. In parallel to aaRSs, two successive reactions are catalyzed by a single enzyme (Figure 5). First, the carboxyl group of an amino acid is activated in an ATP-dependent condensation reaction to form enzyme-bound aminoacyl adenylate (aa-AMP). Specific binding of the correct amino acid is ensured by EpmA’s catalytic pocket amino acid composition, in particular side chain size, charges and hydrogen bonding potential [48]. The second step includes ligation with the acceptor and concurrent AMP release from the catalytic pocket. EF-P as the acceptor molecule admittedly resembles tRNA structure by shape, but remarkably is a protein instead of a RNA molecule [22]. In the case of EpmA the activated amino acid (*R*)-β-lysine is transferred to K34 at the loop of EF-P. As paralog of LysRS, EpmA lost its function to acylate $tRNA^{Lys}$ but has evolved the ability to ligate EF-P and (*R*)-β-lysine [51].

Even before the function of EpmA as PTM enzyme of EF-P was solved, Ambrogelly *et al.* demonstrated EpmA’s promiscuity towards its donor substrate [51]. Enzyme promiscuity is characterized by accidental binding of a non-canonical substrate to the active site and subsequent turn-over. The promiscuous ability provides a fitness advantage during environmental changes and can finally result in new enzymes when gene duplication is followed by divergence [52].

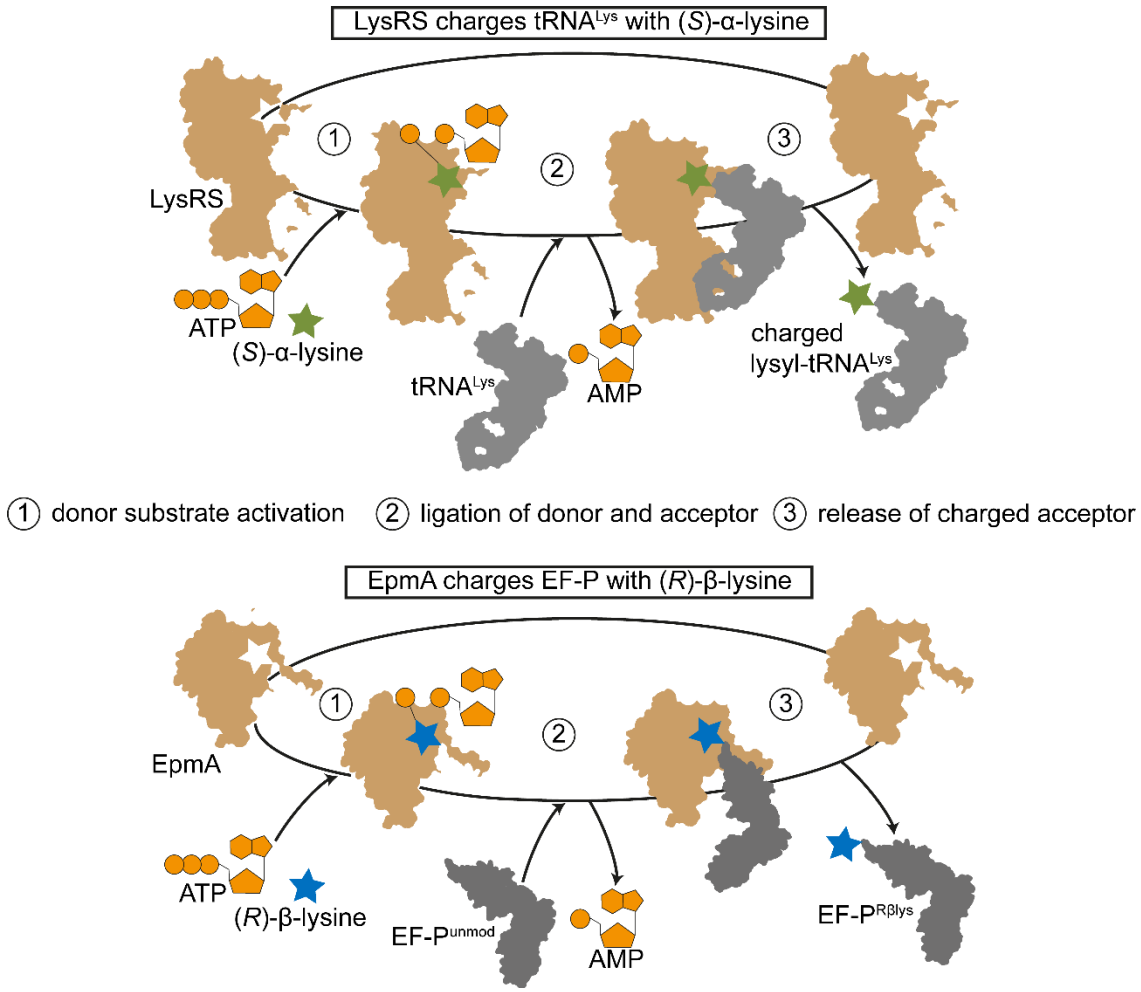

Figure 5: Similarity of LysRS charging tRNA^{Lys} and EpmA charging EF-P. Depicted is the parallelism of protein structures and shapes as well as enzyme mechanisms between aminoacylation of tRNA^{Lys} catalyzed by lysyl-tRNA synthetase (LysRS, upper part) and PTM of EF-P by modification enzyme EpmA (lower part). LysRS and EpmA belong to lysyl-tRNA synthetase class II but at the latter, the anticodon binding domain is missing. Both reaction mechanisms contain the substep of donor substrate activation to form aminoacyl adenylate (aa-AMP) bound to the enzyme and the subsequent transfer of the activated amino acid to the acceptor substrate.

It is known that the specific recognition of the amino acid by a tRNA synthetase as well as by EpmA is error prone [51, 53]. For example, tRNA^{Lys} is mischarged by LysRS with non-cognate substrates like arginine, threonine, methionine, leucine, alanine, serine and cysteine *in vitro* [54]. Moreover, Ambrogelly *et al*. were able to demonstrate substrate promiscuity of EpmA due to activation of 5-hydroxy-L-lysine, (*S*)-α–lysine (L-lysine), diaminopimelic acid (DAP) and thialysine ((*S*)-(2-aminoethyl)-L-cysteine) [51]. Misactivated aa-AMP can be cleaved by the enzyme. In the case of aaRS this distinction between cognate and non-cognate aa-AMP is known as pre-transfer editing [55, 56]. Notably, it is reported that pre-transfer editing is also observed in absence of

the tRNA as acceptor, allowing the two partial reactions to be studied individually [57, 58].

1.6 Aim of the study

Having demonstrated the importance of EF-P for proper translation of proteins containing ribosome stalling motifs and having introduced the dependence on the central PTM enzyme EpmA, the question arises how EF-P and EpmA interplay in *E. coli* to finally ensure EF-P functionality *in vivo*. This lays the foundation and motivation for the research of this thesis. Are the protein copy numbers coordinated to ensure complete modification of EF-P during all growth phases? Which chemical prerequisites need to be fulfilled to serve as EpmA substrate leading to successful binding, activation and finally transfer to K34 of EF-P? Is it possible to use the knowledge on interplay of EF-P and EpmA to artificially modify EF-P to create novel post-translationally modified variants of EF-P? These research questions are tackeled in the following chapters, including development and application of EF-P modification detection techniques.

2 Material and methods

2.1 General

2.1.1 Strains, primers and plasmids

All strains, primers and plasmids used in this study are listed in Table 1, Table 2 and Table 3.

Table 1: Bacterial strains used in this study.

Strain	Feature	Reference
***B. subtilis* 168**	*trpC2*	[59] AG Bramkamp
B. subtilis* Δ*alaT	BKE31400, *yugH trpC2* Δ*yugH*::erm	BGSC
B. subtilis* Δ*dat	BKE09670, *trpC2* Δ*dat*::erm	BGSC
B. subtilis* Δ*efp	*trpC2* Δ*efp*	Jörg Stülke
B. subtilis* Δ*epsN	BKE34230, *trpC2* Δ*epsN*::erm	BGSC
B. subtilis* Δ*frl	BKE32610, *trpC2* Δ*frlB*::erm	BGSC
B. subtilis* Δ*gsaB	BKE08710, *trpC2* Δ*gsaB*::erm	BGSC
B. subtilis* Δ*ilvE	BKE02390, *ybgE trpC2* Δ*ilvE*::erm	BGSC
B. subtilis* Δ*kbl	BKE17000, *trpC2* Δ*kbl*::erm	BGSC
B. subtilis* Δ*mtnE	BKE13580, *trpC2* Δ*mtnE*::erm	BGSC
B. subtilis* Δ*serC	BKE10020, *trpC2* Δ*serC*::erm	BGSC
B. subtilis* Δ*spsC	BKE37890, *trpC2* Δ*spsC*::erm	BGSC
B. subtilis* Δ*yaaO	BKE00270, *trpC2* Δ*yaaO*::erm	BGSC
B. subtilis* Δ*yhdR	BKE09570, *trpC2* Δ*yhdR*::erm	BGSC
B. subtilis* Δ*yhxA	BKE09260, *trpC2* Δ*yhxA*::erm	BGSC
***E. coli* BL21 (DE3)**	*E. coli* B F$^-$ *dcm ompT hsdS* ($r_B^- m_B^-$) *gal*	[60]
***E. coli* BW25113**	Δ(*araD-araB*)*567*, Δ*lacZ4787*(::*rrnB-3*), λ$^-$, *rph-1*, Δ(*rhaD-rhaB*)*568*, *hsdR514*	[61]
E. coli* BW25113 Δ*efp	JW4106, BW25113 *efp*::*npt*, Kan^R	[61]
E. coli* BW25113 Δ*epmA	Resistance free mutant of JW4116 [61], Kan^S	[38]
***E. coli* BW25113 Δ*epmB* Cm^R**	SU1, BW25113 *yjeK643-1029::cat*, Cm^R	[16]

***E. coli* BW25113 Δ*epmB* Cm^S**	Resistance free mutant of SU1 [16], exclusively this *E. coli* Δ*epmB* strain was used for experiments, Cm^S	This study
E. coli* BW25113 Δ*epmC	Resistance free mutant of JW5381 [61], Kan^S	Lassak unpublished
***E. coli* DH5αpir**	*endA1 hsdR17 glnV44* (= *supE44*) *thi-1 recA1 gyrA96 relA1* φ80d*lac*Δ(*lacZ*)M15 Δ(*lacZYA-argF*)U169 *zdg-232*::Tn*10 uidA*::*pir*$^+$	[62]
***E. coli* LF1 P$_{lac}$ efp**	Additional *efp* copy at P$_{lac}$ in LF 1 (F$^-$ λ$^-$ *ilvG rfb50 rph1 rpsL150* P*lac*::*rps-neo-kan::lacZ#*) background	Volkwein unpublished
***E. coli* LMG194**	F$^-$ *ΔlacX74 galE galK thi rpsL* Δ*phoA* Δ*ara714 leu::*Tn*10*	[63]
***E. coli* MG1655**	F$^-$ λ$^-$ *ilvG rfb50 rph-1*	[64]
E. coli* MG1655 Δ*epmB	TK1, MG1655 yjeK$_{643-1029}$::*npt*, Kan^R	[16]
M. luteus		DSM 20030
S. griseus		DSM 40236
***S. oneidensis* MR-1**		[65]
S. oneidensis* Δ*efp	Δ2328	[37]
***S. venezuelae* ATCC 10712**		DSM 40230

Table 2: Oligonucleotides. All primers were purchased from Sigma-Aldrich and diluted to 10 µM stock solutions.

	Oligonucleotide name	Primer sequence (5' - 3')	Restriction site
P1	XbaI_SUMO_efp Bs_fw	TCC TCT AGA AAT AAT TTT GTT T	*XbaI*
P2	XbaI_SUMO_efp Bs_rv	AAC TGA AAT CAT ACC ACC AAT CTG	
P3	HindIII_efpBs_fw	CAG ATT GGT GGT ATG ATT TCA GTT	

P4	HindIII_efpBs_rv	AGC CAA GCT TCT ATG CTC TTG A	*HindIII*
P5	XbaI_SUMO_efpSo_fw	TCC TCT AGA AAT AAT TTT GT	*XbaI*
P6	XbaI_SUMO_efpSo_rv	AGC AGT TTT CAT ACC ACC AAT CTG	
P7	HindIII_efpSo_fw	CAG ATT GGT GGT ATG AAA ACT GCT	
P8	HindIII_efpSo_rv	AGC CAA GCT TTT AAA CGC GCT T	*HindIII*
P9	SacI_sRBS_His6_epmA_fw	ATC GAG CTC AGC GTA AGC CGA GAG AAC TAA GGA GGT CTA AAA TGC ATC ACC ATC ACC ATC ACG GCA GCA GCG AAA CGG CAT CCT GGC A	*SacI*
P10	XbaI_epmA_rv	GAC TCT AGA TTA TGC CCG GTC AAC GCT AAA GGC	*XbaI*
P11	pBAD33_seq_fw	GGC GTC ACA CTT TGC TAT GC	
P12	epmA_A294G_rv	CGA TCA ACA CCT AAA CCC ACG CCG GAA CAG TCA	
P13	epmA_A294G_fw	TGA CTG TTC CGG CGT GGG TTT AGG TGT TGA TCG	
P14	pBAD-HisA-rev	CAG TTC CCT ACT CTC GCA TG	
P15	R303I_rv	CGC CAA CAT CAC CAG AAT ATC AAC ACC TAA TGC	
P16	R303I_fw	GCA TTA GGT GTT GAT ATT CTG GTG ATG TTG GCG	
P17	R303L_rv	CGC CAA CAT CAC CAG AAG ATC AAC ACC TAA TGC	
P18	R303L_fw	GCA TTA GGT GTT GAT CTT CTG GTG ATG TTG GCG	
P19	R303S_rv	CGC CAA CAT CAC CAG ACT ATC AAC ACC TAA TGC	
P20	R303S_fw	GCA TTA GGT GTT GAT AGT CTG GTG ATG TTG GCG	

Check Primer		
epmA_inside_rv	TTC ATT ACG GAA GCT GCG GCA	This study
epmA_seq_fw (yjeA-fw-seq)	GCC CTT GTC AAA AAC TGG AG	S. Ude
epmA_seq_rv (yjeA-rev-seq)	CTG AAA AAT TAC TGA ATT AAC AGC G	S. Ude
epmB_inside_rv	GAT CAC AAT CGG CAG ACG GCT	This study
epmB_seq_fw	GCA CGA TGT AGG CCT GAT AAG CG	This study
epmB_seq_rv	AGA CCA GCA CGA AAA TCG TTG CT	This study
epmB_up50 (up50_yjeK)	CGT TGC CAT AAG GCC CTC TGA AAT TTG TTA ATT GGT AGC TAA GCC ACA AAA ATT AAC CCT	T. Kraxenberger
epmB_down50 (down50_yjek)	AAG CGT AGC GAA TCA GGC AAT TTT AAT GTT TAA CTT CCC TGT TTA ATC AGT AAT ACG ACT	T. Kraxenberger
T7_prom	TAA TAC GAC TCA CTA TAG GG	S. Ude
E. coli EF-P fw	GGC CTC GAG ATG GCA ACG TAC TAT AGC AAC GAT TTT C	This study
E. coli EF-P rv	AAG ATC GGA TCC TTA GTG ATG GTG ATG GTG ATG CTT CAC GCG AGA GAC GTA TTC ACC AGA	This study
pET16b_chk_fw	AAC AAA TAG GGG TTC CGC	This study

Table 3: Plasmids used in this study.

Plasmid name	**Feature**	**Reference**
p3LC-TL30-3P-CCG	Equivalent to pBBR1_MCS3_TL30_ 3*CCG_*lacZ*, TL30 fragment of *cadC* fused to 3 x CCG (coding for a triproline motif) and *lacZ*, Tet^R	[16]
pACycDuet_AcKRST	Contains the gene for acetyllysyl-tRNA-synthetase (AcKRS), a variant of	[66]

	pyrrolysyl-tRNA-synthetase (PylRS) from *Methanosarcina mazei*, Cm^R	
pBAD/HisA_GIWPPP_*nptI*	Triproline motif cloned upstream of neomycin phosphotransferase I (kanamycin resistance cassette), arabinose-inducible pBAD/HisA, Amp^R, Kan^R	Volkwein unpublished
pBAD24_sRBS_efp_{Eco} K34TAG_His_6	C-terminally His_6-tagged *E. coli efp* containing the amber codon TAG at position K34, synthetic ribosome binding site, arabinose-inducible pBAD24, Amp^R	[67]
pBAD24-efp_{Eco} K34R	C-terminally His_6-tagged *E. coli efp,* coding for the amino acid substitution variant EF-P_K34R, arabinose-inducible pBAD24, Amp^R	[38]
pBAD24_His_{10}_*epmB*	N-terminally His_{10}-tagged *E. coli epmB,* arabinose-inducible pBAD24, Amp^R	[68]
pBAD33	Expression vector with pACYC184/p15A origin of replication, arabinose-inducible P_{BAD}, Cm^R	[63]
pBAD33_*epmA*	*E. coli epmA,* arabinose-inducible pBAD33, Cm^R	[38]
pBAD33_His_6_*efp*	N-terminally His_6-tagged *E. coli efp*, arabinose-inducible pBAD33, for production of unmodified EF-P in *E. coli* Δ*epmA*, Cm^R	[37]
pBAD33_His_6_*efp*_ *epmAB*	N-terminally His_6-tagged *E. coli efp*, *epmA* and *epmB*, arabinose-inducible pBAD33, for production of post-translationally modified EF-P, Cm^R	[38]
pBAD33_His_{10}_*epmB*	N-terminally His_{10}-tagged *E. coli epmB,* arabinose-inducible pBAD33, Cm^R	This study
pBAD33_sRBS_His_6_ *epmA*	N-terminally His_6-tagged *E. coli epmA*, arabinose-inducible pBAD33, synthetic ribosome binding site, Cm^R	[67]

pBAD33_sRBS_His_6_*epmA*_A298G	N-terminally His_6-tagged *E. coli epmA,* coding for the amino acid substitution variant EpmA_A298G, arabinose-inducible pBAD33, synthetic ribosome binding site, Cm^R	[67]
pBAD33_sRBS_His_6_*epmA*_R303I	N-terminally His_6-tagged *E. coli epmA,* coding for the amino acid substitution variant EpmA_R303I, arabinose-inducible pBAD33, synthetic ribosome binding site, Cm^R	This study
pBAD33_sRBS_His_6_*epmA*_R303L	N-terminally His_6-tagged *E. coli epmA,* coding for the amino acid substitution variant EpmA_R303L, arabinose-inducible pBAD33, synthetic ribosome binding site, Cm^R	This study
pBAD33_sRBS_His_6_*epmA*_R303S	N-terminally His_6-tagged *E. coli epmA,* coding for the amino acid substitution variant EpmA_R303S, arabinose-inducible pBAD33, synthetic ribosome binding site, Cm^R	This study
pBAD33_SUMO_*efp*$_{E.c}$	N-terminally His_6-SUMO-tagged *E. coli efp,* arabinose-inducible pBAD33, Cm^R	This study
pBAD33_SUMO_*efp*$_{B.s}$	N-terminally His_6-SUMO-tagged *B. subtilis efp,* arabinose-inducible pBAD33, Cm^R	This study
pET	Expression vector with pBR322 origin of replication, IPTG-inducible P_{T7}, Kan^R	[69]
pET_SUMO-*efp*$_{Eco}$	C-terminally His_6-SUMO-tagged *E. coli efp,* IPTG-inducible pET, Kan^R	[38]
pET_SUMO-*efp*$_{Eco}$ K34R	C-terminally His_6-SUMO-tagged *E. coli efp,* coding for the amino acid substitution variant EF-P_K34R, IPTG-inducible pET, Kan^R	[38]
pET_SUMO-*efp*$_{Eco}$ P32S	C-terminally His_6-SUMO-tagged *E. coli efp,* coding for the amino acid substitution	[38]

	variant EF-P_P32S, IPTG-inducible pET, Kan^R	
pET_SUMO_*efp*$_{S.o.}$	N-terminally His_6-SUMO-tagged *S. oneidensis efp*, IPTG-inducible pET, Kan^R	This study
pET16b_RPAP_*nluc*	Nonstalling motif RPAP cloned upstream of *nluc*, IPTG-inducible pET16b, Amp^R	Pinheiro unpublished
pET16b_RPPP_*nluc*	Arginine-triproline motif cloned upstream of *nluc*, IPTG-inducible pET16b, Amp^R	[67]
pET16b_SUMO_*efp*$_{E.c.}$	N-terminally His_6-SUMO-tagged *E. coli efp*, IPTG-inducible pET16b, Amp^R	This study
pRED/ET AmpR	λ-RED recombinase, arabinose-inducible pBAD24, Amp^R	Gene Bridges

2.1.2 Standard chemicals and cultivation of bacteria

Acetic acid, acetone, ammonium peroxodisulfate (APS), L(+)-arabinose, L-arginine hydrochloride, CHAPS, 1,4-dithiothreitol (DTT), ethylenediaminetetraacetic acid (Na_2EDTA), ethanol (EtOH), 2-[4-(2-hydroxyethyl)piperazin-1-yl]ethanesulfonic acid (HEPES), glycerol, glycine, (*S*)-α-lysine hydrochloride, methanol (MeOH), $MgCl_2$, piperazine-N,N'bis(2-ethanesulfonic acid) (PIPES), SDS, sodium bicarbonate ($NaHCO_3$), D(+)-sucrose, TCA, tetramethylethylenediamine (TEMED) and tris(hydroxymethyl)-aminomethane (Tris) were purchased from Roth. Adenosine 5'-triphosphate disodium salt (ATP), (*R*)-3-aminohexanoic acid hydrochloride, (*S*)-3-aminohexanoic acid hydrochloride, 6-AC, bromophenol blue (BPP), deoxyribonuclease I from bovine pancreas (DNase), 2,6-diaminopimelic acid (DAP), KCl, lysozyme, phenylmethylsulfonyl fluoride (PMSF), (*S*)-α-ornithine hydrochloride, TCE and urea were purchased from Sigma-Aldrich. (*RS*)-5-hydroxy-(*S*)-α-lysine, (*R*)-α-lysine hydrochloride and thiourea were provided by Fluka. Isopropyl-β-D-thiogalactopyranoside (IPTG) and NaCl was purchased from PanReac AppliChem and L-glutamine from Serva.

(3*R*)-3,5-diaminopentanoic acid dihydrochloride ((*R*)-β-ornithine) was provided by AKos GmbH. (*R*)-β-lysine was synthesized by Carbolution Chemicals, (*S*)-β-lysine was

purchased from PepTech Corporation. All lysine derivatives were dissolved in ddH_2O (SG Ultra Clear UV plus Watersystem).

TEA buffer: 20 mM triethanolamine hydrochloride (Sigma), pH 7.5

HEPES buffer: 50 mM HEPES, 100 mM NaCl, 50 mM KCl, 10 mM $MgCl_2$, 5 v% glycerol, pH 7.0

M. luteus, *S. griseus*, and *S. venezuelae* were cultivated at 30 °C in LB medium (10 g/L NaCl, 10 g/L tryptone/peptone ex casein (Roth), 5 g/L Bacto Yeast Extract (BD), pH 7.0) supplemented with 0.5 v% glycine. *S. oneidensis* was grown at 30 °C in LB medium. *B. subtilis* and *E. coli* were cultivated at 37 °C using LB medium. When necessary the medium was solidified using 30 mg/mL Difco agar (BD) and supplemented with antibiotics in the following concentrations: 100 µg/mL ampicillin sodium salt (Roth), 100 µg/mL carbenicillin disodium salt (Roth), 50 µg/mL kanamycin sulphate (Roth), 34 µg/mL chloramphenicol (Roth), or 12.5 µg/mL tetracycline hydrochloride (Sigma).

Optical density at 600 nm wavelength (OD_{600}) of cultures were measured using Ultrospec 2100 pro (Amersham Biosciences). The growth curve of BW25113 Δ*epmB* transformed with the plasmids pBAD33 and p3LC-TL30-3P-CCG was recorded using Spark 20M multimode microplate reader (Tecan) at 37 °C. Here, the LB medium was supplemented with varying amounts of (*R*)-3-AC (0.02 to 10 mM) and OD_{600} was measured every 15 min for 14 h.

2.1.3 Molecular genetic methods and Miscellaneous

Plasmids were reproduced by transformation of *E. coli* DH5α and subsequent plasmid isolation procedure using the Hi Yield Plasmid Mini Kit (Süd-Laborbedarf). Genomic DNA was extracted using UltraClean Microbial DNA Isolation Kit (MO BIO Laboratories) according to instructions. Samples were stored at -20 °C.

Standard DNA techniques like restriction (different enzymes, NEB), ligation (T4 DNA ligase, NEB) and PCR (OneTaq Polymerase, Q5 High-Fidelity DNA Polymerase, both NEB) were performed according to manufacturer's instructions. DNA fragments were separated in 10 mg/mL agarose (Serva) electrophoresis gel supplemented with Midori Green Advance Stain (NIPPON Genetics Europe) which was placed in a Bio-Rad Horizontal DNA gel electrophoresis chamber for 20 min at 120 V and using TAE buffer (20 mM acetic acid, 1 mM EDTA, 40 mM Tris, pH 8) as running buffer. Prior to loading

samples were mixed with 6X DNA loading dye (0.3 mg/mL BPP, 0.3 mg/mL xylene cyanol FF (Serva), 60 v% glycerol, 10 mg/mL SDS, 10 mM EDTA). 2-Log DNA Ladder (0.1 - 10.0 kb) was purchased from NEB. Gel Doc EZ Gel Documentation System (Bio-Rad) was used to save agarose gel pictures. Subsequent DNA extraction was conducted using Hi Yield PCR Clean-Up & Gel-Extraction Kit (Süd-Laborbedarf). DNA as well as protein concentrations were measured using NanoDrop ND-1000 (NanoDrop Technologies).

Chemically competent *E. coli* cells were obtained by inoculation (1:100) of 200 mL LB medium with ON culture. When the culture has grown to OD_{600} = 0.3 – 0.6 it was placed on ice for 10 min. After centrifugation for 10 min at 4 °C at 5,000 rpm (Eppendorf 5415R, rotor FA-45-24-11) the pellet was resuspended in 100 mL transformation buffer (50 mM $CaCl_2 \cdot 2\ H_2O$ (Baker), 15 v% glycerol, 10 mM PIPES, pH 6.6) and stored on ice for 20 min. After repeated centrifugation, the pellet was resuspended in 10 mL transformation buffer, split in 250 µL aliquots and stored at -80 °C.

For transformation 1 - 5 µL of plasmid were mixed with 250 µL chemically competent *E. coli* cells. After 30 min storage on ice a heat shock was conducted at 42 °C for 90 sec. 1 mL LB medium was added and agitated for 1 h at 37 °C. A part of the culture was finally exposed to a LB agar plate supplemented with the corresponding antibiotic for selective colony growth at 37 °C ON.

Newly designed plasmids and strains were subjected to colony PCR using OneTaq polymerase according to manufacturer's instructions and sequenced by LMU Sequencing Service. Samples were processed on ABI 3730 capillary sequencers with 50 cm capillary length.

PDB entries of crystal structures shown in this work are the following:
EF-P of *P. aeruginosa* in Figure 7: 3OYY
EpmA (GenX, YjeA) of *E. coli* in complex with EF-P in Figure 2, Figure 4, Figure 18C, Figure 19, Figure 21: 3A5Z
EpmC (YfcM) of *E. coli* in Figure 4: 4PDN
LysRS of *E. coli* in Figure 5: BBU
$tRNA^{Asp}$ of *E. coli* in Figure 5: 1EFW

Theoretical pI values were calculated using ExPASy pI/Mw tool [70].

The Phyre2 web portal for protein modeling, prediction and analysis [71] was used to analyze secondary structure elements of EF-P and to predict structure of EpmB (YjeK) of *E. coli* in Figure 4.

Molecular graphics and analyses were performed with UCSF Chimera, developed by the Resource for Biocomputing, Visualization, and Informatics at the University of California, San Francisco, with support from NIH P41-GM103311 [72].

Chemical structures were designed using ChemDraw Professional (version 16.0.0.82, PerkinElmer Informatics).

When necessary, grey density analysis was performed using ImageJ [73].

Sequencing results, amino acid alignments and primer design was conducted using CLC Genomics Workbench 7.7 (https://www.qiagenbioinformatics.com/).

Graphs, K_m calculations and two-tailed t-tests were created and performed using GraphPad Prism version 5.03 for Windows, GraphPad Software, La Jolla California USA, www.graphpad.com.

2.2 Peptide antibody generation

Peptides NH_2-C+TEPGVKGDTAGGTKP-$CONH_2$ and NH_2-C+VPLFINEGEKIKVDT-$CONH_2$ were selected for the Eurogentec Anti-Peptide Polyclonal Antibody program AS-SUPR-DXP (AS-SUPR-DX + 2 x 5 mL purify). The two peptides were synthesized and conjugated to the carrier keyhole limpet hemocyanin (KLH). Each of two rabbits was immunized with two peptides. After 28 days that included four injections and three bleeds, blood was harvested, and serum collected. ELISA test determined and compared the titer in preimmune serum and large bleed serum. Affinity purification with the synthesized peptides removed unspecific antibodies and yielded polyclonal peptide antibodies P68 and P69, respectively.

2.3 Preparation of bacterial lysates

If not otherwise mentioned, strains were grown ON and harvested the next day. OD_{600} was set using TEA or HEPES buffer. DNase was added and incubated 30 min at RT. For Gram-positive bacteria, 1 mg/mL lysozyme was included at this incubation step. Small volumes (< 10 mL) were lysed using BRANSON Digital Sonifier (30 % amplitude, 0.5 sec pulse, 0.5 sec pause for 2 x 30 sec) under constant ice-cooling. Larger volumes were lysed using a cell disruptor (Constant Systems Ltd, iX T4A, 3 x

at 1.35 kbar). After 20 min of centrifugation at 4 °C and 5,000 rpm (Eppendorf Centrifuge 5804 R, rotor A-4-44), the clear supernatant was used for further analysis.

For characterization of antibodies P68/P69 OD_{600} of *E. coli* BW25113, *B. subtilis* and *S. oneidensis* (WT and Δ*efp* each) was set to 50 using TEA buffer. Additionally, 0.5 mM PMSF was added. *E. coli* and *S. oneidensis* cells were lysed by vortexing with MicroBeads (from UltraClean Microbial DNA Isolation Kit, MO BIO Laboratories) for 10 min. MicroBeads were spinned down and the supernatant was mixed with 5X SDS loading dye, heated for 10 min to 95 °C and centrifuged for 10 min.

2.4 Cloning strategies for plasmid and strain constructions

2.4.1 His_6-SUMO-tagged *efp*s from different organisms

His_6-SUMO was fused to the N-terminus of *efp* and subsequently following plasmids were constructed: pBAD33_SUMO_$efp_{E.c.}$, pET16b_SUMO_$efp_{E.c.}$, pBAD33_SUMO_$efp_{B.s.}$ and pET_SUMO_$efp_{S.o.}$. Cleavage by SUMO protease Ulp allowed for production of the native protein.

For the first-mentioned plasmids, pET_SUMO_efp_{Eco} was digested using *XbaI* and *HindIII* as restriction sites. The resulting fragment was subsequently ligated to pBAD33 and pET16b backbone, respectively. For pBAD33_SUMO_$efp_{B.s.}$ construction, the His_6-SUMO fragment was amplified from pBAD33_SUMO_$efp_{E.c.}$ using the primer pair P1/P2. Genomic DNA of *B. subtilis* 168 served as template for amplification of *efp* using primers P3/P4. Overlap extension PCR led to a fragment that was subsequently digested using restriction enzymes XbaI and HindIII. These restriction sites were used to insert His_6-SUMO-$efp_{B.s.}$ into plasmid backbone pBAD33. Accordingly, pET_SUMO_$efp_{S.o.}$ was constructed following a similar procedure for *S. oneidensis* MR-1 using primers P5 – P8 and plasmid backbone pET.

2.4.2 His_6-tagged EpmA and its variants A298G, R303I/L/S and His_{10}-tagged EpmB

pBAD33_*epmA* was used as template for construction of pBAD33_sRBS_His_6_*epmA* using P9/P10. The synthetic ribosome binding site was calculated using RBS Calculator (https://salislab.net/software/, De Novo DNA). *SacI* and *XbaI* restriction sites were used for digest of fragment and backbone. It must be noted that the His_6-tag was also introduced C-terminally but this variant was non-functional (not shown). Subsequently, amino acid exchange A298G was introduced by overlap PCR using

P11 – P14. Amino acid substitutions of R303 were conducted by overlap PCR using pBAD33_sRBS_His_6_*epmA* as template and primer pair P11/P15 P16/P14 for R303I, P11/P17 P18/P14 for R303L and P11/P19 P20/P14 for R303S. The fragments were digested using *SacI* and *XbaI* and ligated to pBAD33.

His_{10}-tagged *epmB* fragment was amplified from pBAD24_His_{10}_*epmB* using P11/P14 and digested at restriction sites *NsiI* and *XbaI*. The resulting fragment was ligated to pBAD33 to yield pBAD33_His_{10}_*epmB*.

2.4.3 Removal of resistance cassette to create antibiotic-sensitive strains

The selection marker of BW25113 Δ*epmB* Cm^R (SU1) was removed by FLP/FLPe expression from pRED/ET AmpR. Quick & Easy *E. coli* Gene Deletion Kit (Gene Bridges) was used according to the manufacturer's instructions to create BW25113 Δ*epmB* Cm^S. This strain was used throughout the whole study.

2.5 Overexpression and purification of EF-Ps from *E. coli*, *B. subtilis* and *S. oneidensis*

For production of untagged EF-Ps of *E. coli*, *B. subtilis* and *S. oneidensis*, inducible plasmids pBAD33_SUMO_$efp_{E.c.}$, pET_SUMO-efp_{Eco} K34R/P32S**,** pBAD33_SUMO_ $efp_{B.s.}$ and pET_SUMO_$efp_{S.o.}$ were used, respectively. BW25113 (for modified EF-$P_{E.c.}$), BW25113 Δ*epmA* (for unmodified EF-$P_{E.c.}$ and EF-$P_{B.s.}$) and BL21 (for all pET vectors) were transformed with one of these plasmids and grown to exponential growth phase. Gene expression was induced by addition of 2 g/L arabinose (for pBAD) or 1 mM IPTG (for pET). After 5 h, cultures were harvested by centrifugation (20 min, 4 °C, 5,000 rpm, Beckman Coulter Avanti JXN-26, rotor JLA-8.1000). The pellet was resuspended in TEA buffer to yield a concentration of 0.2 g/mL. After addition of 10 mg DNase incubated at RT for 30 min, cells were lysed using a cell disruptor (Constant Systems Ltd, iX T4A, 3 x at 1.35 kbar). Ultracentrifugation was conducted for 1 h at 45,000 rpm (Beckman Coulter Optima L-90K, Rotor 50.2 Ti). His_6-SUMO-tagged EF-P was purified using Ni-NTA agarose (nitrilotriacetic acid, Qiagen) according to the following quick protocol. 1 mL beads were washed and resuspended one time with ddH_2O and two times with TEA buffer. After each round, centrifugation at 4 °C for 3 min at 2,000 rpm (Eppendorf Centrifuge 5804 R, rotor A-4-44) was conducted. The equilibrated beads were incubated with the supernatant from the ultracentrifugation step for 1 h at 4 °C. The IMAC column (immobilized metal ion affinity chromatography FLEX-COLUMNS, Thermo Fisher) was washed with ddH_2O (1 x) and with TEA buffer

(2 x). The bead suspension was added to the column and subsequently, flow-through was collected for SDS-PAGE analysis. Washing steps were performed twice using 10 mL of TEA buffer + 20 mM imidazole (Roth) and the final elution was conducted using 400 mM imidazole. Samples were dialyzed (SERVAPOR dialysis tubing MWCO 12,000 – 14,000, Serva, cooked in 20 g/L $NaHCO_3$ + 0.37 g/L EDTA and stored in 1 mM EDTA) two times for 4 h to remove imidazole. 15 wt% (compared to total protein mass) of SUMO protease (Ulp, Invitrogen, [74, 75]) was added and incubated for 5 h at 30 °C. After incubation with fresh and equilibrated Ni-NTA agarose beads for 1 h, chromatography flow-through was collected to yield untagged EF-P. Successful purification of the target protein was ensured by SDS-PAGE, visualized by TCE staining (Chapter 2.6.1) and when necessary by vertical IEF (Chapter 2.6.5).

For overexpression and purification of His_6-tagged EF-P of *E. coli* in different modification states, His_6_*efp* was overexpressed from pBAD33_His_6_*efp* in BW25113 Δ*epmA* (unmodified EF-P), from pBAD33_*efp*_*epmAB* in BW25113 (modified EF-P) or from pBAD33_His_6_*efp* in BW25113 Δ*epmC* (unhydroxylated EF-P).

For production of EF-P with acetyllysine at position 34, C-terminally His_6-tagged *efp* was overexpressed from pBAD24_sRBS_efp(Eco)K34TAG_His_6 in *E. coli* LMG194. Moreover, the strain was transformed with pACycDuet_AcKRST to allowed for amber suppression with the acetyllysine-tRNA synthetase (AcKRS) described by Volkwein *et al*. [66]. LB medium was supplemented with 5 mM Nε-acetyl-L-lysine (Sigma-Aldrich) and 1 mM nicotinamide (Sigma-Aldrich) to prevent deacetylation by CobB [76].

Amino acid exchange variant K34R was overexpressed from pBAD24-efp_{Eco} K34R in BW25113 Δ*epmA* (modification prevented) or WT. Here, additional *epmA* overexpression was conducted using pBAD33_sRBS_His_6_*epmA* (modification stimulated). The above-mentioned procedure was varied by using HEPES buffer instead of TEA buffer for pellet resuspension and purification. Moreover, Ulp digest and the following second purification step was omitted.

Parallel overexpressions of His_6_*efp*_K34R and His_6_*epmA* require an additional separation step due to the similar protein tags. Therefore, EpmA and EF-P were separated by Size Exclusion Chromatography performed at ÄKTA pure chromatography system (GE) equipped with a Superdex 200 Increase 10/300 GL column (GE). The fraction containing EF-P but not EpmA was elucidated by SDS-

PAGE analysis and concentrated using sucrose. To do so, a highly concentrated sucrose gel was prepared in a 250 mL flask filled with sucrose up to the 150 mL mark. Then, HEPES buffer was added up to the 250 mL mark and the solution was stirred at 4 °C ON and stored until use. The protein sample was filled in a dialysis tube (SERVAPOR dialysis tubing MWCO 12,000 – 14,000, Serva, cooked in 20 g/L $NaHCO_3$ + 0.37 g/L EDTA and stored in 1 mM EDTA) and covered with sucrose solution. The remaining volume was checked every hour until considerable decrease was reached.

2.6 Electrophoretic methods

2.6.1 SDS-polyacrylamide gel electrophoresis

For separation and visualization of proteins, SDS-PAGE was conducted according to Lämmli [77]. The stacking gel contained 4.8 v% acrylamide (Roth) and the separating gel contained 12.5 v% acrylamide. 0.5 v% TCE was added for protein visualization using the Gel Doc EZ Gel Documentation System (Bio-Rad) [78]. Polymerization of the gels was induced using APS and TEMED. By default, samples were mixed with 5X SDS loading dye (250 mM Tris, 0.1 g/mL SDS, 5 mg/mL BPP, 50 v% glycerol, 500 mM DTT, pH 6.8), heated to 95 °C for 10 min and subsequently, 15 to 20 µL were loaded per lane. Lonza ProSieve Color Protein Marker (FisherScientific) or Roti-Mark (Roth) was used as size standard. Proteins were separated using PerfectBlue SDS-PAGE chambers (Peqlab) filled with Lämmli buffer (25 mM Tris, 200 mM glycine, 1 g/L SDS, pH 8.2 - 8.3) at 200 V.

2.6.2 Sample preparation for isoelectric focusing

To prepare *E. coli* lysates for native horizontal IEF, cells were grown in 1 L LB medium. Samples (at least 5 mL) were taken at different time points. Cells were harvested and stored at -20 °C. The pellets were washed (10 mM Tris, 250 mM sucrose, pH 7.0), whereby high-salt buffers were avoided in accordance with Westermeier [79]. OD_{600} was set to 10 and subsequently, 0.5 mM PMSF was added and incubated for 30 min at RT. Cell lysis was conducted using BRANSON Digital Sonifier (30 % amplitude, 0.5 sec pulse, 0.5 sec pause for 2 x 30 sec) under constant ice-cooling. 20 µL of each growth curve sample were subjected to SDS-PAGE. Proteins of each lane were visualized using TCE staining and quantified using Image Lab Software 4.1 (Bio-Rad). Normalized protein amounts were used for native horizontal IEF gel. 10X loading buffer contained 50 v% glycerol and 10 mg/mL BPP.

To prepare *B. subtilis* lysates for denaturating horizontal IEF the procedure described above was slightly modified. Cell pellets were lysed using 0.5 mM PMSF and 1 mg/mL lysozyme. Sonification was conducted 5 x 30 sec and an additional protein precipitation step was included. Therefore, 750 µL were mixed with 187.5 µL ice-cold 50 v% TCA and stored on ice for 15 min. After centrifugation at 2 °C for 15 min at full speed the pellet was resolved in 500 µL ice-cold acetone. After 15 min on ice followed by centrifugation, remaining acetone was facilitated to evaporate by removal of the cap for 30 min. Solubilization was conducted ON using 75 µL of solubilization mix according to Westermeier (7 M urea, 2 M thiourea, 40 mg/mL CHAPS, 10 mg/mL DTT, 0.8 v% carrier ampholyte (Pharmalyte, GE), 20 µg/mL BPP) [79].

2.6.3 Native horizontal isoelectric focusing

The GelPool (GE) was washed with distilled water to make sure it is clean and dust-free. Rehydration solution (1.1 g D-sorbitol (Roth), 820 µL Pharmalyte pH 4 - 6.5 (GE) ad 11 mL) was prepared freshly and pipetted along the long side of the GelPool. The precast gel (CleanGel IEF (GE)) was placed with the gel side down into the rehydration solution, carefully avoiding bubbles. The gel was rehydrated for 1 h on a rocker, whereby the gel was moved during the first 15 min to avoid clogging. Pharmacia Biotech Multiphor II was equipped with MultiTemp III Thermostatic Circulator (Pharmacia Biotech) to ensure constant cooling to 10 °C and connected to a high voltage source (Pharmacia Electrophoresis Power Supply EPS 3500). Gel surface was cleaned with a filter paper. 2 mL SERVA Cooling Fluid were pipetted onto the gridline. The IEF gel was placed on the cooling platform gel side up and aligned to the gridline of the Multiphor II. Platin electrodes were cleaned, dried and placed on the edges of the gel. During the prefocusing phase the pH gradient was established (350 V 6 mA 8 W, 20 min). The gel surface was dried with a filter paper when necessary. Small filter papers were placed on the cathode side of the gel and soaked with protein samples. The latter were transferred to the gel by applying 250 V for 20 min (4 mA 8 W). Main focusing was conducted at 1,000 V (7 mM 14 W) for 4 h, whereby filter papers were removed after 2 h. Band sharpening was conducted for 10 min (1250 V 7 mM 18 W). A metal wire was placed between gel and plastic sheet which had been placed on a 1 L Schott bottle (Figure 6). After the gel was carefully removed from its plastic sheet it could be subjected to Silver Staining or Western Blotting.

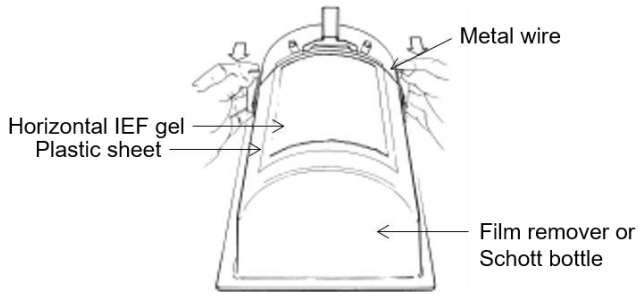

Figure 6: Film remover apparatus to separate IEF gel from plastic sheet. Horizontal IEF gels require separation from its plastic sheet before Western Blotting can be conducted. The figure is adapted from GE Multiphor II manual.

2.6.4 Denaturating horizontal isoelectric focusing

Due to the usage of urea for denaturating conditions the protocol described in chapter 2.6.3 was modified as follows: CleanGel IEF (GE) or Blank FocusGel 24S (Serva) was rehydrated for at least 2 h. For the first-mentioned gel the solubilization mix without BPP was used. The SERVA gel was rehydrated according to manufacturer's instructions using 12.84 g urea, 4.65 g thiourea, 2.46 mL Pharmalyte 4 - 6.5 (GE), 1.28 g CHAPS, 0.32 g DTT ad 32 mL. The rehydrated gel could be stored in a plastic bag ON. To avoid crystallization of urea the focusing temperature was kept at 15 °C. For sample application, small filter paper stripes or a silicone applicator strip were used at the cathode side of the gel.

2.6.5 Vertical isoelectric focusing

0.5 µg of purified protein was mixed with 2X IEF Sample Buffer (Serva). PerfectBlue SDS-PAGE chamber (Peqlab) was filled with SERVA IEF Cathode Buffer 3 - 10 (inner tank) and SERVA IEF Anode Buffer (outer tank) and connected to a high voltage source (Pharmacia Electrophoresis Power Supply EPS 3500). Wells of the precast native vertical IEF gel with a pH gradient range of 4 - 7 (SERVA*Gel*) were rinsed with cathode buffer. For clearly distinct bands 5 µL of 2X IEF Sample Buffer without protein were loaded in the lanes between two samples. Focusing was conducted at 4 °C for 1 h at 50 V, 1 h at 200 V and finally bands were sharpened for 40 min at 500 V. The gel could be subjected to Coomassie, InstantBlue (Expedeon) or Silver Staining as well as Western Blotting.

2.7 Silver Staining, Western Blotting and antibodies used in this study

When a staining method with excellent sensitivity was needed, Silver Staining was conducted. Therefore, the IEF or SDS-PAGE gel was incubated for at least 1 h in fixing solution (50 v% MeOH, 12 v% glacial acetic acid, freshly added 0.05 v% of 37 %

formaldehyde (Roth)). Subsequently, the gel was washed with 50 % EtOH (3 x 20 min or ON), incubated 1 min in thiosulfate solution (1.25 mM $Na_2S_2O_3$, Sigma), and washed with dH_2O (3 x 20 sec). Freshly prepared incubation solution (0.03 mM $AgNO_3$ (Roth), 0.075 v% of 37 % formaldehyde) was added and incubated for 20 min. After another washing step with dH_2O (3 x 20 sec), development solution (550 mM Na_2CO_3 (Roth), 2 % thiosulfate solution, 0.05 v% of 37 % formaldehyde) was incubated for 3 - 10 min. The gel was shortly washed with dH_2O and incubated in stop solution (65 mM EDTA) for at least 15 min.

For Western Blotting, proteins were transferred to a nitrocellulose membrane (Amersham Protran 0.45 µm NC, GE) prewetted with blot buffer (25 mM Tris, 192 mM glycine, 20 v% MeOH) using the Trans-Blot Turbo Transfer System (Bio-Rad). Subsequently, the membrane was blocked in buffer A (50 mM Tris, 150 mM NaCl, pH 7.4) + 30 mg/mL BSA (albumin from bovine serum, Sigma). A suitable primary antibody was added and incubated for a defined time. The blot was washed with buffer A (3 x 5 min) and incubated with Anti-RABBIT IgG (alkaline phosphatase conjugated) as secondary antibody (0.1 µg/mL) for 1 h. After washing with buffer A (3 x 10 min), the blot was incubated in development solution (50 mM sodium carbonate buffer, pH 9.5, 1 mg/mL NBT (4-nitro blue tetrazolium chloride, biomol), 10 mg BCIP (5-bromo-4-chloro-3-indolyl-phosphate, PanReac AppliChem)) until visible color development.

Table 4: Antibodies used in this study

Antibody name	Feature	Supplier
Anti-EF-P "P68"	Primary, polyclonal peptide antibody against a consensus motif of a wide range of bacterial EF-Ps, produced in rabbit NH_2-C+VPLFINEGEKIKVDT-$CONH_2$	Eurogentec
Anti-EF-P "P69"	Primary, polyclonal peptide antibody against a consensus motif of a wide range of bacterial EF-Ps, produced in rabbit NH_2-C+TEPGVKGDTAGGTKP-$CONH_2$	Eurogentec
Anti-EF-P$_{E.c.}$	Primary antibody against *E. coli* EF-P, produced in rabbit	Eurogentec
Anti-EF-P$_{B.s.}$	Primary antibody against *B. subtilis* EF-P, produced in rabbit	Eurogentec

Anti-RABBIT	Secondary antibody against rabbit, conjugated to alkaline phosphatase, produced in goat	Rockland

2.8 *B. subtilis* swarming assay

25 mL of 2X LB were mixed with 6.7 mL of 2X agar and filled to 50 mL for a 0.4 % swarming plate. The mixture was poured into a square petri dish (Greiner Bio-One) and dried for 5 min in a laminar flow hood. Six colonies were picked, spotted on the plate and incubated at 37 °C ON. An image of the plates was recorded, and the swarming halos were quantified using Adobe Photoshop Elements 2.0.

2.9 Experiments with antibiotic gradient plates

To obtain kanamycin gradient plates, 35 mL of LB agar supplemented with 100 µg/mL kanamycin and appropriate other antibiotics was poured into a square petri dish plate (Greiner Bio-One) which was placed in a slanted position. 45 mL of LB agar containing antibiotics but no kanamycin was poured on the dried, first layer and the plate was evenly positioned. 50 µL fresh ON culture of BW25113 Δ*epmB* transformed with pBAD/HisA_GIWPPP_*nptI* and pBAD33_sRBS_His_6_*epmA* was striked out on the whole plate and incubated at 37 °C ON. The five colonies able to grow at highest kanamycin concentrations were used to inoculate LB medium. The next day, OD_{600} was set to 0.5 and subsequently, 10 µL were striked along the length of a fresh gradient plate. Clones that still exhibited a growth advantage on kanamycin were subjected to plasmid extraction followed by sequencing of *epmA* using P11/P14. Moreover, colony PCR was used to amplify *efp* fragment with primer pair *E. coli* EF-P fw/rv which was sequenced to elucidate possible mutations.

The procedure described above was slightly adjusted to yield gentamicin gradient plates. Here, 5 µg/mL gentamicin was added to the first and 2 g/L arabinose to both LB agar layers. BW25113 Δ*epmB* and MG1655 Δ*epmB* were transformed with pBAD33_sRBS_His_6_*epmA* and plated on independent plates. Different EpmA amino acid exchange variants were also tested on kanamycin gradient plates. Therefore, BW25113 Δ*epmB* was transformed with pBAD/HisA_GIWPPP_*nptI* and either pBAD33, pBAD33_sRBS_His_6_*epmA* or pBAD33_sRBS_His_6_*epmA*_A298G/R303I/R303L/R303S. 20 µL were striked out alongside the kanamycin plate.

2.10 *In vitro* EF-P modification by EpmA

For *in vitro* EF-P modification, 25 µM unmodified His_6-tagged EF-P, 2 mM ATP (in HEPES buffer, pH 7.0), 5 µM His_6-tagged EpmA or its variant EpmA_A298G and 10 mM lysine derivative were mixed in HEPES buffer and incubated ON at RT. Following lysine derivatives were used: 6-AC, (*R*)- and (*S*)-3-aminohexanoic acid hydrochloride, (*S*)-arginine hydrochloride, (3*R*)-3,5-diaminopentanoic acid dihydrochloride, 2,6-diaminopimelic acid, (*RS*)-5-hydroxy-(*S*)-α-lysine, (*S*)-glutamine, (*R*)- and (*S*)-α-lysine hydrochloride, (*R*)- and (*S*)-β-lysine, (*S*)-α-ornithine hydrochloride. On the next day, samples were either mixed with 2X IEF buffer (Serva) and stored at 4 °C for IEF analysis or stored at -20 °C for intact protein MS conducted by collaboration partners (Pavel Kielkowski, TUM).

For the (*R*)-β-ornithine/lysine competition assay, the assay described above was performed with different concentrations of (*R*)-β-lysine and (*R*)-β-ornithine. *In vitro* modified EF-P was analyzed by intact protein MS.

2.11 [^{32}P]-AMP formation assay

Hydrolysis of ATP by EpmA in the presence of various amounts of lysine derivative was monitored in HEPES buffer for time course experiments and K_m determination. The instruction published by Chen *et al.* [80] was adapted as follows.

For time course experiments 10 or 100 mM 6-AC, 0 or 5 µM unmodified His_6-EF-P, 5 mM DTT, 3 mM [α-^{32}P]-ATP (20 Ci/mol, PerkinElmer) were incubated at 37 °C (timepoint 0 min) and the reaction was started by addition of 1 µM His_6-EpmA. Aliquots were taken at 2, 5, 10, 30 and 60 min and quenched with four volumes of 200 mM sodium acetate (Merck, pH 5.0). 1 µL of the mixture was analyzed by thin layer chromatography (TLC) in duplicates on PEI cellulose plates (Merck Millipore, pre-washed with water). The dried plates were developed in a TLC glass chamber using 0.1 M ammonium acetate (Roth), 5 v% acetic acid. [α-^{32}P]-ATP and [^{32}P]-AMP were visualized and quantified by phosphor imaging using Typhoon TRIO Variable Mode Imager (Amersham Biosciences) equipped with a red laser (633 nm) and ran with the Typhoon Scanner Control v5.0. Acquisition mode was set to “Storage Phosphor” and Pixel Size to “100 microns”. Grey densities of the [^{32}P]-AMP (AMP^*) spots were compared to the grey density of a known [α-^{32}P]-ATP (ATP^*) amount using ImageJ. Equation 1 was used for analysis. The reaction was conducted using 3 mM ATP and

20 mM [α-^{32}P]-ATP (Stock solution of Perkin Elmer with 3000 Ci/mmol, 10 mCi/mL, 3.3 µM).

Equation 1: Calculation of amount *n* and concentration *c* of released AMP during *in vitro* EpmA substrate activation.

$$n(ATP^*) = c(ATP^*) \cdot V = 20\ nM \cdot \frac{1.5\ \mu L}{1.5\ \mu L + 6\ \mu L} = 4\ fmol$$

$$n(AMP^*) = \frac{intensity(AMP^*)}{intensity(ATP^*)} \cdot 4\ fmol$$

$$n\left(AMP_{ges}\right)[nmol] = n(AMP^*)[fmol] \cdot \frac{c(ATP) + c(ATP^*)}{c(ATP^*)} \cdot 10^{-6}$$

$$= n(AMP^*)[fmol] \cdot \frac{3\ mM + 20\ nM}{20\ nM} \cdot 10^{-6}$$

$$c\left(AMP_{gesamt}\right)[mM] = \frac{n\left(AMP_{ges}\right)[nmol] - n(blank)[nmol]}{V[\mu L]}$$

$$= \frac{[n\left(AMP_{ges}\right) - n(blank)][nmol]}{0.2\ \mu L}$$

For K_m determination the lysine derivative concentration was varied from 0 to 100 mM for high K_m substrates and from 0 to 2.5 mM for low K_m substrates. Moreover, reaction mixtures contained 5 mM DTT, 3 mM [α-^{32}P]-ATP (20 Ci/mol, PerkinElmer) and were incubated at 37 °C until initiation with 1 µM EpmA or EpmA_A298G, respectively. After 15 min the reaction was quenched and processed as described. K_m values were estimated using nonlinear fitting (least squares (ordinary) fit) of the Michaelis-Menten equation that was performed using GraphPad Prism version 5.03 for Windows, GraphPad Software, La Jolla California USA, www.graphpad.com.

2.12 *In vitro* transcription/translation of RPPP-Nluc

The PURExpress *In Vitro* Protein Synthesis Kit (NEB) was used according to instructions using pET16b_RPAP_*nluc* or pET16b_RPPP_*nluc* and unmodified EF-P, *in vivo* modified EF-P (positive control, EF-P$^{R\beta lys}$) or *in vitro* modified EF-P (Materials and methods, Chapter 2.5). For a 12.5 µL reaction mixture 5 µL PURExpress solution A, 3.75 µL PURExpress solution B, 0.25 µL RNase inhibitor Murine (NEB), 5 µM EF-P and 1 ng pET16b_RPA/PP_*nluc* was incubated at 37 °C at 300 rpm agitation. At 0, 2.5, 5, 7.5, 10, 12.5, 15, 20, 25 and 30 min a 1 µL aliquot was quenched with 1 µL 50 mg/mL kanamycin and stored on ice. Afterwards, 2 µL Nano-Glo Luciferase Assay

(Promega) Reagent and 18 µL ddH_2O were added to induce luminescence development which was detected by the Infinite F500 microplate reader (Tecan). At least three independent replicates were analyzed, and significance of the results were determined by two-tailed t-test using GraphPad Prism.

2.13 β-galactosidase activity assay

BW25113 and deletion mutants BW25113 Δ*epmA* and BW25113 Δ*epmB* were transformed with the plasmid p3LC-TL30-3P-CCG described by Ude *et al.* [16]. Here, truncated *cadC* was fused to an EF-P-dependent triproline stalling motif and *lacZ*. The plasmid-encoded complementation of the deletion mutants as well as cross-complementation was performed using pBAD33_sRBS_His_6_EpmA, pBAD33_sRBS_His_6_EpmA_A298G or pBAD33_His_{10}_*epmB*, respectively.

To compare the effects of the different lysine derivatives *in vivo*, BW25113 Δ*epmB* was transformed with p3LC-TL30-3P-CCG and pBAD33, pBAD33_sRBS_His_6_EpmA or pBAD33_sRBS_His_6_EpmA_A298G. Here, 10 mM lysine derivative was added to the medium. (*S*)-β-lysine was used in the concentration of ~0.25 mM. Concentration of (*R*)-3-AC was reduced to 1 mM due to a growth defect at higher concentrations.

Co-transformed cells were grown in LB medium ON and harvested by centrifugation. Pellets were resuspended in sodium phosphate buffer according to instructions [81]. β-galactosidase activities were determined for at least three independent experiments and are given in Miller units, which were calculated according to Miller [82].

2.14 Purification of endogenous EF-P

BW25113 co-transformed with p3LC-TL30-3P-CCG and pBAD33 as well as BW25113 Δ*epmB* co-transformed with p3LC-TL30-3P-CCG and pBAD33_sRBS_His_6_EpmA or pBAD33_sRBS_His_6_EpmA_A298G, respectively, were grown in 1 L of LB medium at 37 °C to exponential growth phase. Expression of *epmA* was induced by 2 g/L arabinose and cells were grown at 18 °C ON. Cells were harvested, and the pellet was resuspended in TEA buffer. After 30 min of incubation with DNase and PMSF, cells were disrupted by a continuous-flow cabinet from Constant Systems Ltd. at 1.35 kb. The resulting lysates were clarified by centrifugation for 1.5 h at 4 °C at 235,000 x *g*. Anion Exchange Chromatography was performed using an ÄKTA pure chromatography system (GE Healthcare) equipped with Mono Q 10/100 GL and the fraction collector F9-C at a salt gradient of 0 to 1 M KCl. The fraction with the highest

EF-P concentration was determined by SDS-PAGE followed by Anti-EF-P$_{E.c.}$ Western Blotting. Size Exclusion Chromatography was performed using a Superdex 200 Increase 10/300 GL column. Samples were not analyzed regarding their activity but regarding their EF-P modification status, on the one hand by IEF followed by Western Blotting, and on the other hand by MS analysis performed by collaboration partners (Pavel Kielkowski, TUM).

3 Results

3.1 Universal antibody against EF-P of a wide range of bacteria

The widely used molecular biological technique of Western Blotting is hinged on the availability of specific antibodies. The order of polyclonal antibodies against EF-P from an unexplored strain is a time- and cost-intensive approach, which is therefore not suitable for initial screening experiment. Due to the fact that approximately half of all known bacteria are not understood regarding function and modification of EF-P, there is a need for an antibody that is specific for EF-P as target protein but at the same time nonselective in terms of its bacterial origin.

EF-Ps of different bacteria show structure and sequence conservation. Primary, secondary and tertiary structures of a large set of bacterial EF-Ps were analyzed to identify sequence motifs of EF-P that are conserved among as many bacteria as possible and at the same time are present on the protein's surface to represent the accessible epitope for an antibody. From these, peptide antibodies were produced which were specific, sensitive and universal. The latter can be used to correlate Western Blot band intensities and protein amount to finally determine endogenous EF-P copy number. Moreover, the antibody is required for detection of EF-P from newly studied bacteria on an IEF gel. Separation of endogenous and recombinant EF-P according to their charges elucidates occurrence and nature of a potential post-translational modification. Thereby the universal EF-P antibody subjoins the toolbox enabling EF-P research in Gram-positive and Gram-negative bacteria.

3.1.1 Generation of the two EF-P-specific peptide antibodies P68/P69

First, the amino acid sequences of EF-P from 1345 different species were downloaded from NCBI Knowledgebase [83] in FASTA format. Next, these sequences were aligned using two different tools. Clustal W [84] followed by clean-up of sequences with Bioedit [85] (excluding sequences with missing domains, improvement of gap alignment) identified amino acids with > 90 % conservation. Using CLC Genomics Workbench 7.7 (https://www.qiagenbioinformatics.com/) consensus sequence was obtained (Figure 7A). Using The Phyre2 web portal for protein modeling, prediction and analysis [71] and the available EF-P crystal structures, four different regions with high density of conserved residues were identified that were moreover easily available for antibody binding due to their location at the EF-P protein surface (Figure 7B).

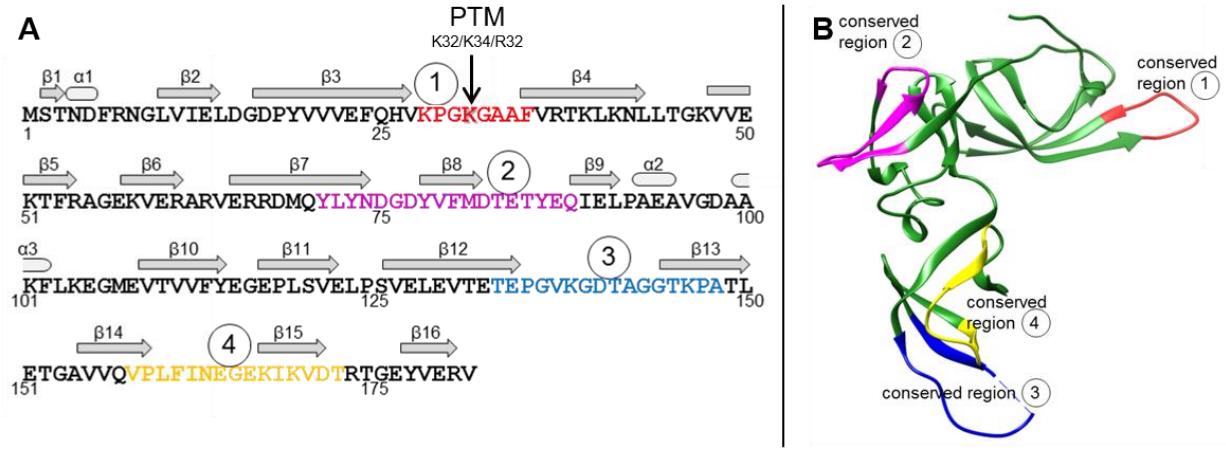

Figure 7: The four conserved regions of EF-P identified by amino acid alignment of 1345 bacterial EF-Ps. Regions 1 - 4 show accumulation of conserved amino acids in the EF-P sequence alignment and are highlighted in color. (A) EF-P consensus sequence and secondary structure elements. Region 1 contains the residue which is post-translationally modified. Regions 3 and 4 represent loops between β-strands and were chosen for peptide antibody generation. (B) Exemplary EF-P structure (*P. aeruginosa*) shows accessibility of all four identified regions at the protein surface.

Conserved region 1 (Figure 7, red) consists of the loop between β-strands β3 and β4 which contains the PTM site, the conserved K32, K34 or R32, respectively. The PTM could block the antibody binding and lead to false-negative results. Consequently, this region was not taken into consideration for peptide design and synthesis which serve as preliminary steps for antibody production. Peptides of regions 2 - 4 included β-strands and disordered regions. They were analyzed by Eurogentec with respect to their predicted antibody quality. As a result, peptides 3 (NH_2-C+TEPGVKGDTAGGTKP-$CONH_2$) and 4 (NH_2-C+VPLFINEGEKIKVDT-$CONH_2$) were selected for the Eurogentec Anti-Peptide Polyclonal Antibody program and finally yielded antibodies P68 and P69, respectively (Figure 8, Material and Methods 2.2).

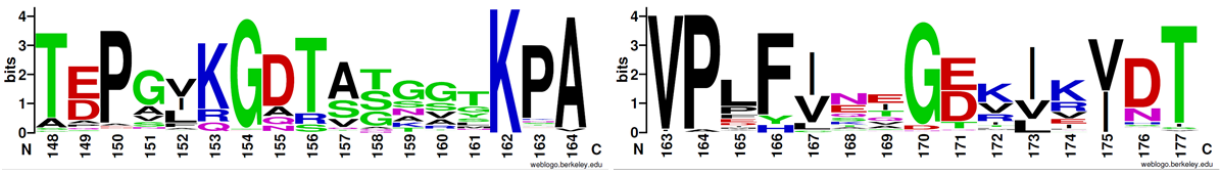

peptide „**P68**“
derived from conserved region 3

peptide „**P69**“
derived from conserved region 4

Figure 8: Weblogos [86] of the two peptide sequences (P68 and P69) that were chosen for peptide antibody production. The high degree of sequence conservation is visualized which formed the basis to design the universally applicable EF-P antibodies P68/P69.

3.1.2 Characterization of antibodies P68/P69

The obtained antibodies P68 and P69 as well as their 1:1 mixture were applied in Western Blot analysis of purified EF-P from different bacteria. Antibody concentration and incubation time were adjusted to define the optimal conditions for laboratory application. Moreover, protein amounts were gradually decreased to determine the sensitivity for different model organism EF-Ps.

E. coli, *B. subtilis* and *S. oneidensis* were selected as model organisms, not only because of their importance in laboratory and commercial work but also due to the fact that they encompass three important bacterial PTM types. *E. coli* as representative of the Gram-negative γ-proteobacteria with EpmABC as modification enzymes modifies K34 with (*R*)-β-lysine that is further hydroxylated. *B. subtilis* was recently postulated to be modified with aminopentanol, whereby the full modification pathway is unknown [34]. *S. oneidensis* represents the arginine-type EF-P with R32 being modified with rhamnose by the modification enzyme EarP [37].

Untagged *efp*s of *E. coli*, *B. subtilis* and *S. oneidensis* were overexpressed and purified by affinity chromatography. The pure protein as well as bacterial lysates of WT and Δ*efp* mutant strains were subjected to SDS-PAGE and subsequently, to Western Blot analysis. Three different universal EF-P antibody solutions (P68, P69, and a mixture of them) were used in different dilutions (1:100, 1:1,000 and 1:10,000) and incubated for different durations (1 h, ON). This detailed antibody characterization is shown in Figure 9 and optimal conditions are framed in red.

For *E. coli* (Figure 9, upper part), it can be concluded that P69 performed better than P68 because here, bands appeared to be more intensiv. Primary antibody in a final dilution of 1:1,000 (0.55 µg/mL) and subsequent incubation ON led to the best results. EF-P antibodies P68 and P69 were both very sensitive for EF-$P_{B.S.}$. In this case, a mixture used at the highest dilution tested (0.04 µg/mL) was enough to detect EF-P from cell lysate. Notably, higher antibody concentrations led to recognition of unspecific bands (not shown). Both antibodies P68 and P69 detected *S. oneidensis* EF-P only in the purified and therefore higher concentrated form, whereby P69 at a dilution of 1:1,000 (0.55 µg/mL) exhibited the best results after ON incubation.

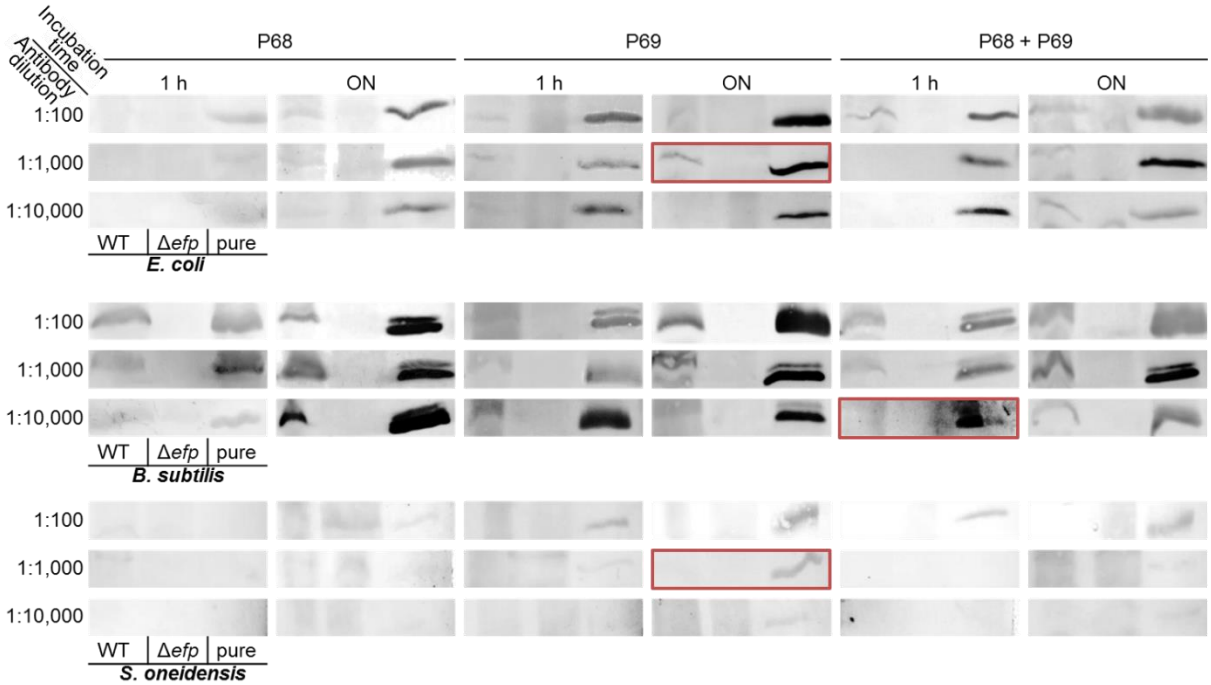

Figure 9: Characterization of EF-P antibodies P68 and P69 to find optimal application recommendation. SDS-PAGE gel lanes 1 (WT) and 2 (Δ*efp* mutant strain) were loaded with lysate of 6·10^8 cells of *E. coli* (BW25113, upper part), *B. subtilis* (middle part) or *S. oneidensis* (lower part), respectively. Each third lane was loaded with 0.5 µg of purified, untagged EF-P. Dilution of primary antibody solution was varied, whereby dilution 1:10,000 corresponds to 0.04 µg/mL of primary antibody. Optimal antibody dilution and incubation time for each bacterium is framed in red. Anti-RABBIT was used as secondary antibody.

After determination of the best antibody usage conditions for three model organisms (also summarized in Table 9), they were applied to quantify the antibody sensitivity. Thereby, serial dilution of EF-P starting from 1 µg per SDS-PAGE lane and using a dilution factor of two was conducted. Figure 10 shows that EF-P$_{E.c.}$ was successfully detected by P69 down to 31 ng (9·10^{11} molecules) when a dilution of 1:1,000 was used, whereas a higher EF-P amount (125 ng) was necessary for proper detection at an antibody dilution of 1:10,000. The antibody mixture was highly sensitive towards EF-P$_{B.s.}$ as it detected down to 15 ng (4·10^{11} molecules). For clear detection of EF-P$_{S.o.}$, at least 125 ng (4·10^{12} molecules) were required. Therefore, I suggest this antibody for detection of concentrated EF-P.

The characterization of universal EF-P antibodies P68/P69 showed that both were able to specifically detect EF-P of different species. *B. subtilis* as model organism of Gram-positive bacteria was sensitively detected by the EF-P antibodies P68/P69. Regarding the EF-Ps of the Gram-negative bacteria *E. coli* and *S. oneidensis*, P69 clearly outreaches P68. *S. oneidensis* is best detected in the purified form using >0.25 µg of protein.

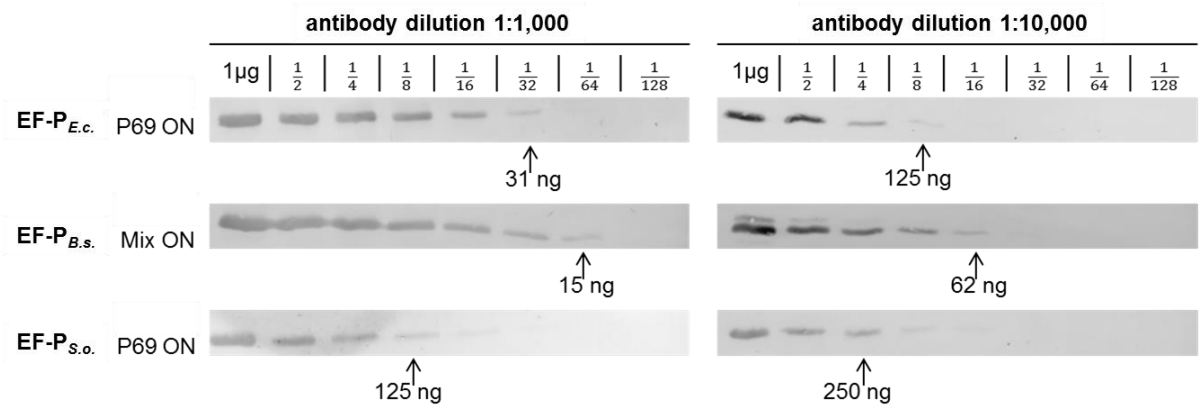

Figure 10: Determination of universal EF-P antibody sensitivity towards EF-Ps of *E. coli*, *B. subtilis* and *S. oneidensis*. Serial dilution starting at 1 µg of EF-P and reduction by a factor of two per lane in the SDS-PAGE gel revealed the minimal EF-P amount necessary for detection by the universal EF-P antibody. Optimal antibody and incubation time for the different bacteria was determined above and is indicated on the left.

By that an alternative to the available, organism-specific EF-P antibodies was found which does not recognize a tag but endogenous motifs of EF-P that are conserved among bacterial species.

3.1.3 Applications of P68/P69

3.1.3.1 Determination of endogenous EF-P copy numbers

Applications of the newly available EF-P antibodies to bacterial lysates enable determination of endogenous EF-P copy numbers.

An EF-P dilution row starting from 1 µg of purified protein as well as bacterial lysate with known optical density was loaded on a single SDS-PAGE gel. Grey density analysis of the anti-EF-P Western Blot bands were plotted against the corresponding EF-P amounts. Exemplary, this is shown for *E. coli* and *B. subtilis* in Figure 11A.

The latter depicts the proportionality between EF-P amount and Western Blot band intensity over a wide range. Therefore, the universal EF-P antibodies were suitable to determine the linear fit which enables calculation of the amount of EF-P in the WT lysate m_{EF-P}. Application of Equation 2 reveals the number of EF-P per cell N_{EF-P}.

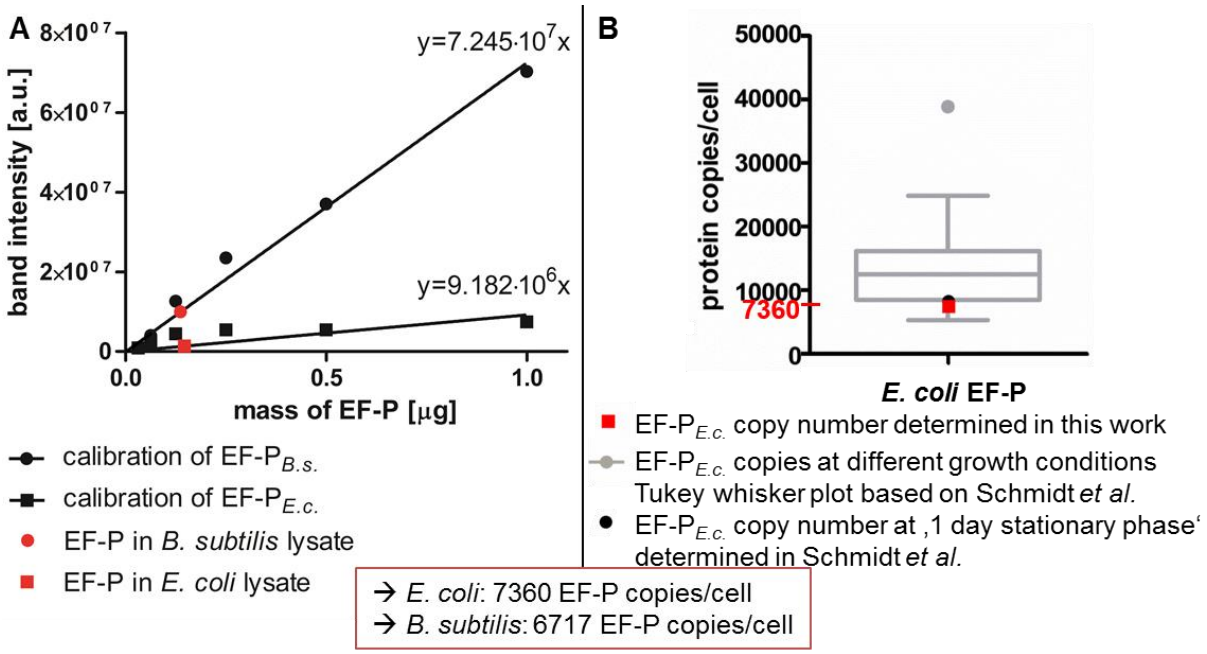

Figure 11: Determination of endogenous EF-P copy numbers. (A) EF-P calibration curves for *E. coli* (P69, 1:1,000) and *B. subtilis* (Mix, 1:10,000) generated from serial dilution rows shown in Figure 10 (single replicate). Grey densities of Western Blot bands were quantified using ImageJ. Band intensities for WT lysates of $6 \cdot 10^8$ cells are highlighted in red. Copy numbers were calculated according to Equation 2. (B) Comparison of EF-P copy number for *E. coli* (red) with 22 literature values (grey) determined at different conditions and derived from Schmidt *et al*. [1]; represented as Tukey whisker plot. Copy number determined at '1 day stationary phase' is shown in black.

Equation 2: Calculation of endogenous EF-P copy number.

$$N_{EF-P}\left[\frac{molecules}{cell}\right] = \frac{m_{EF-P}[g] \cdot N_A\left[\frac{molecules}{mol}\right]}{10^9\left[\frac{cells}{mL}\right] \cdot OD_{600} \cdot V_{per\ lane}[mL] \cdot M_{EF-P}\left[\frac{g}{mol}\right]}$$

Using Equation 2 the number of EF-Ps per cell was found to be 7360 for *E. coli* and 6717 for *B. subtilis* and therefore exhibited similar quantities. Schmidt *et al.* determined EF-P copies at 22 different growth conditions of *E. coli* [1]. Figure 11B shows that EF-P copies determined at '1 day stationary phase' by them (8323 EF-P/cell) match the determined number in this thesis very well. Muntel *et al*. analyzed the proteome of *B. subtilis* during exponential growth in an amino acid based medium and found a low number of 2274 EF-P/cell [87]. The difference to the value determined in this study could origin from divergent cultivation.

A quick and accurate approach for EF-P copy number determination is shown for, but is not limited to, *E. coli* and *B. subtilis*.

3.1.3.2 Extension of the universal EF-P antibody application to other bacteria

The newly available antibodies P68/P69 were applied to EF-Ps from organisms with little research on their EF-Ps.

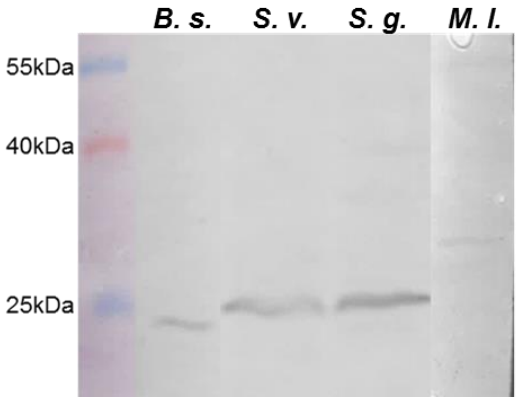

Figure 12: Application of the universal EF-P antibodies on different bacterial lysates. Bacterial lysates ($4 \cdot 10^8$ cells) of *Bacillus subtilis* (*B. s.*, control), *Streptomyces venezuelae* (*S. v.*), *Streptomyces griseus* (*S. g.*) and *Micrococcus luteus* (*M. l.*) were subjected to SDS-PAGE. Western Blot was conducted with P68/P69 antibody mixture used in a dilution of 1:1,000 each and incubated ON. A sensitive and highly specific reaction is achieved for two *Streptomyces* species and *M. luteus*. Anti-RABBIT was used as secondary antibody.

Figure 12 shows that *Streptomyces venezuelae*, *Streptomyces griseus* and *Micrococcus luteus* EF-P were detectable from bacterial lysate using a P68/P69 mixture and simultaneously proof the high specificity of the antibodies as only a single band appears on the Western Blot at the expected ~25 kDa size. It is frequently observed that some bacterial EF-Ps (*S. oneidensis*, *M. luteus*, …) appear at higher positions in an SDS-PAGE gel than expected from their amino acid chain length.

Application of the generated antibodies to other bacterial lysates showed, that especially EF-P from Gram-positive bacteria represented by the phyla Firmicutes and Actinobacteria were robustly detected. As EF-Ps of these branches of bacteria are not adequately studied to date, the universal antibody provides a suitable new tool.

3.2 Isoelectric focusing for detection of the post-translational modification status of EF-P *in vivo*

The electrophoresis method IEF separates proteins on the basis of their different pI values. As separation of unmodified and modified EF-P/eIF5A ((*R*)-β-lysylated [32], 5-aminopentanolated [36], hypusinated [88]) has been described it appears to be an useful technique in the research on PTMs. Nevertheless, a detailed analysis of the opportunities and possibilities offered by this technique in the research on PTMs, and especially on EF-P is lacking to date. Therefore, I established the IEF method in our laboratory. There are vertical, native horizontal and denaturating horizontal IEF, all three different techniques being necessary to satisfy the demands of diverse samples. This study reveals the intrinsic characteristics of each technique as well as their field of application.

3.2.1 General remarks for reproducible IEF results

In general, horizontal IEF was preferred over vertical IEF when a complex protein mixture is analyzed like it is the case for bacterial lysates. The advantage of vertical IEF in comparison to horizontal IEF laid in its easier handling, versatile and cheap equipment and shorter focusing time. For reproducible results the experimental setup was important for the final position of the protein band to be studied. Consequently, a protein standard ladder was found not to be useful in IEF of EF-P because narrow pH gradients were applied (e.g. pH 4 - 7 for vertical, pH 4 – 6.5 for horizontal IEF). Instead, positions of the bands should always be compared to known controls (EF-P^{unmodified}, (*R*)-β-lysylated EF-P (EF-P$^{R\beta lys}$), …). Not least because of the connection between temperature and pI it is important to maintain constant and uniform heat transport which was ensured by use of a thermostatic circulator (horizontal IEF) or by operating the gel in a cold room (vertical IEF). Moreover, it is known that the temperature in electrode regions can rise especially during the prefocusing phase of a horizontal gel in which the pH gradient is established [89]. Therefore, samples were applied after the prefocusing step to prevent them from overheating. Although proteins can travel in both directions between cathode and anode in this electrophoretic technique, it is very important to find the appropriate sample application location. By applying cell lysates to different gel regions (cathode side, middle, anode side), it became very clear that lysates should always be applied at the cathode side to ensure good resolution of the different protein bands (not shown). In general, the application location should be kept

at a distance of at least 1 cm to the electrodes to avoid extreme pH, and optimally lays near the place where the interesting protein band was about to settle.

The native horizontal IEF gels shown in Figure 13BC reveal the positioning of the EF-P band in a gel with established pH gradient from 4 - 6.5 (rehydration of the gel with Pharmalyte (GE), see Materials and Methods 2.6.3). It shows that (*R*)-β-lysylation of EF-P is clearly distinguishable from unmodified EF-P in the purified samples (B) and in the lysate (C) due to the fact that it settles in closer proximity to the cathode than the variant without PTM.

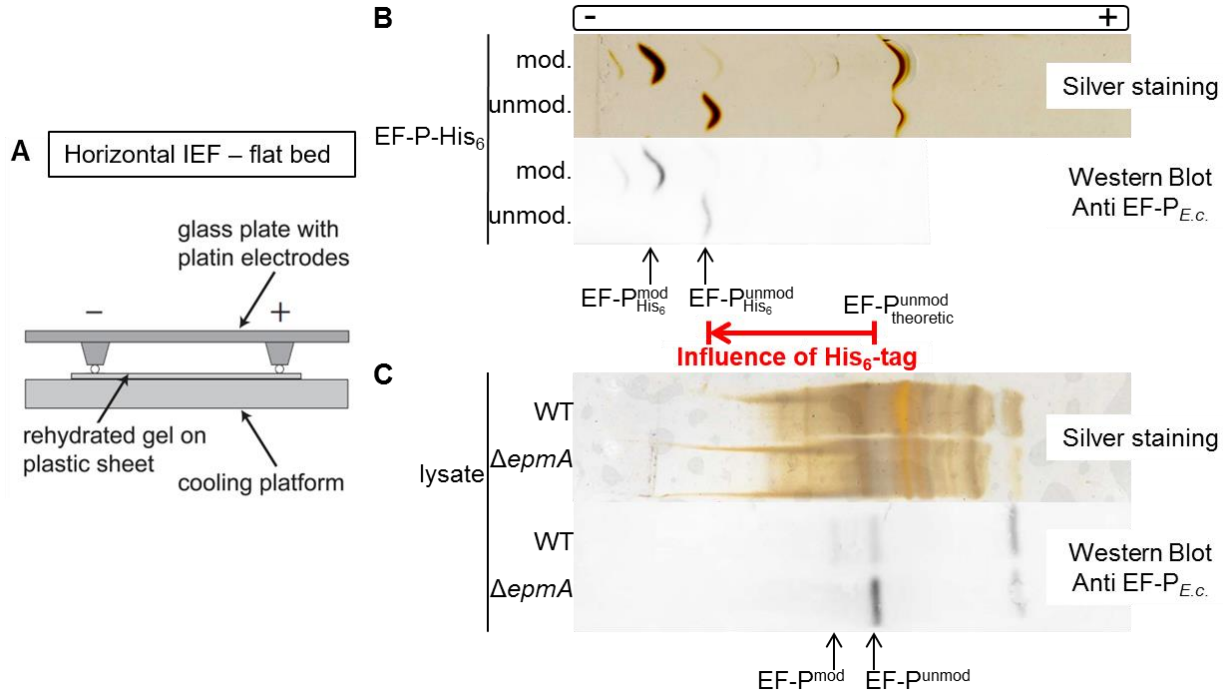

Figure 13: Native horizontal IEF of EF-P from *E. coli* BW25113. (A) Schematic depiction of horizontal IEF performed in flat-bed apparatus. Horizontal gels are appropriate for ambitious specifications like gel rehydration with urea or other supplements. The figure is adapted from Serva Electrophoresis Seminar (02.03.2017). (B, C) The entire width of the native horizontal IEF gel is shown to reveal the exact positioning of EF-P in the tagged/endogenous and unmodified/modified form. Proteins were stained unspecifically by Silver Staining (upper part) or subjected to Western Blot incubated with Anti EF-P$_{E.c.}$ (lower part). The theoretical pI value 5.17 of endogenous unmodified EF-P is indicated. (B) 2 µg of purified, His$_6$-tagged EF-P overproduced in WT or *E. coli* Δ*epmA* were loaded per lane. (C) Lysate of 1·10^8 cells of WT and *E. coli* Δ*epmA* were loaded per lane.

Although only a single additional positive charge originating from the β-amino group of the PTM is present, which does not influence the theoretical pI value so much, the electrophoretic behavior is altered which leads to distinguishable bands and makes the IEF technique very useful for PTM research. The theoretical pI value of EF-P^{unmod} in the endogenous and His$_6$-tagged form vary by only 0.01 pH units (calculated by

ExPASy pI/Mw tool). Unexpectedly, it becomes obvious from Figure 13BC that untagged and tagged protein have a distinct settling point in the gel.

Due to high influence of the protein tag on the electrophoretic behavior in the IEF gel it is necessary to purify EF-P in unaltered form to use it as control in experiments involving lysates. If, however, the status of tagging or PTM of purified EF-P should be determined, vertical IEF is conducted (Figure 14A).

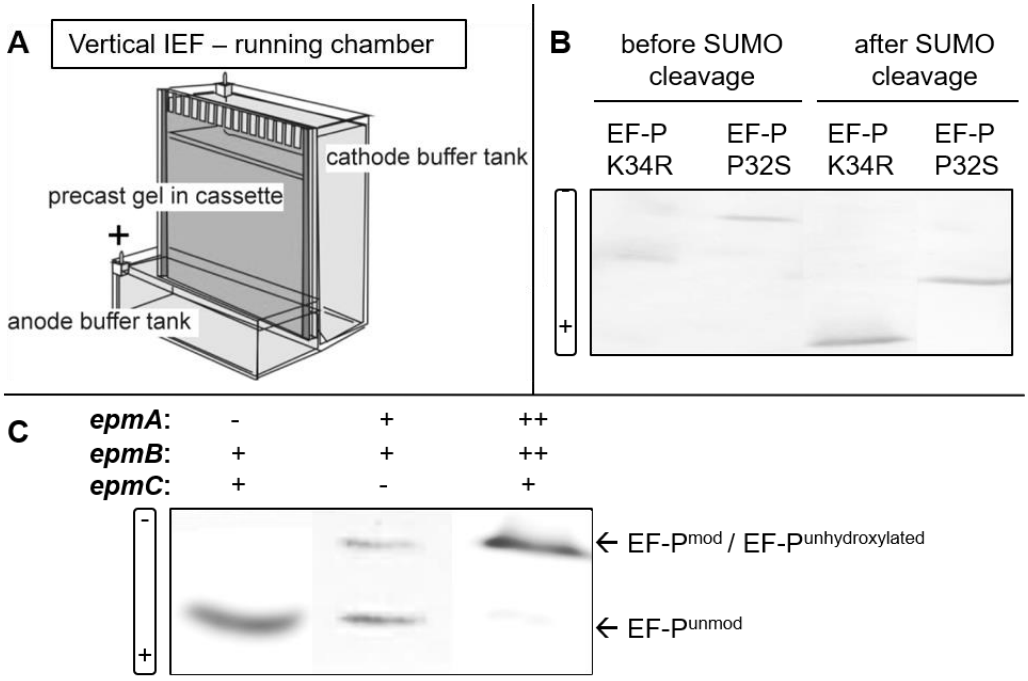

Figure 14: Vertical IEF reveals status of purified EF-Ps. (A) Schematic depiction of a vertical IEF chamber. The vertical system is suitable for quick and easy applications. The figure is adapted from GE Multiphor II manual. (B) Verification of amino acid replacements (K34R, P32S, 5 µg EF-P per lane) and completed protease digest. (C) Modification status detection of EF-P expressed in different *E. coli* strains (3 – 10 µg per lane). In an e*pmA* deletion (-) strain, fully unmodified EF-P was produced (+, endogenous expression). Deletion of *epmC* (-) led to production of unhydroxylated EF-P but also to a similar portion of unmodified EF-P. Plasmid-based overexpression (++) of *epmA* and *epmB* ensures PTM of EF-P.

Due to the finding of distinct running behaviors of tagged and untagged EF-P, protein SUMOylation was chosen to produce untagged EF-P in high amounts (see Material and Methods 2.4). Affinity purification of His_6-SUMO-EF-P was followed by scar free cleavage by the help of SUMO protease Ulp (ubiquitin-like protein-processing enzyme) to finally produce untagged EF-P. The latter can be used as control for analysis of EF-P modification status during different *E. coli* growth phases (Chapter 3.2.2).

Moreover, Figure 14B shows the successful and complete cleavage of the SUMO-tag which was ensured by quick and easy application of vertical IEF. Different EF-P variants of *E. coli* (K34R, P32S) were shown to be unmodified before these variants

could be used for interaction studies with EarP from *P. putida.* Depending on the overexpression strain, EF-P of *E. coli* can exhibit a different PTM status. As already shown above, *efp* expression in *E. coli* Δ*epmA* exclusively yields EF-P in the unmodified state (Figure 14C). Simultaneous overexpression of *efp* and *epmA* primarily leads to unmodified EF-P (reported in [24]), whereby primarily modified EF-P is examined when modification systems *epmAB* were overexpressed (Figure 14C).

Deletion of *epmC* leads to unhydroxylated EF-P, which reportedly has no negative impact on EF-P functionality [16, 20]. Interestingly, vertical IEF reveals that EF-P is in the modified as well as in the unmodified state suggesting a potential role of the hydroxylation in the protection of the PTM.

Horizontal IEF is the technique of choice, when lysates need to be analyzed regarding the modification status of EF-P whereas vertical IEF is the suitable tool for analysis of purified EF-P samples.

3.2.2 Detection of EF-P$_{E.c.}$ modification status in different growth phases

Newly biosynthesized EF-P in the cytosol of *E. coli* is transmitted to EpmA and accepts (*R*)-β-lysine to be ligated to K34. Either repletion of EpmA and EpmB ensures complete EF-P modification during all phases of growth, or a bottleneck on the PTM pathway occurs, which would lead to partially unmodified endogenous EF-P. To test this, five representative *in vivo* samples, namely from lag phase, exponential growth phase and stationary phase were collected (Figure 15A). Proteins from corresponding lysates were resolved by SDS-PAGE (Figure 15C) and subsequently, grey density analysis revealed the relative protein amount per lane that is equalized in the next step. Then, the lysates were subjected to native horizontal IEF (pH 4 - 6.5). Figure 15D reveals that during all phases, EF-P is present in the post-translationally modified form.

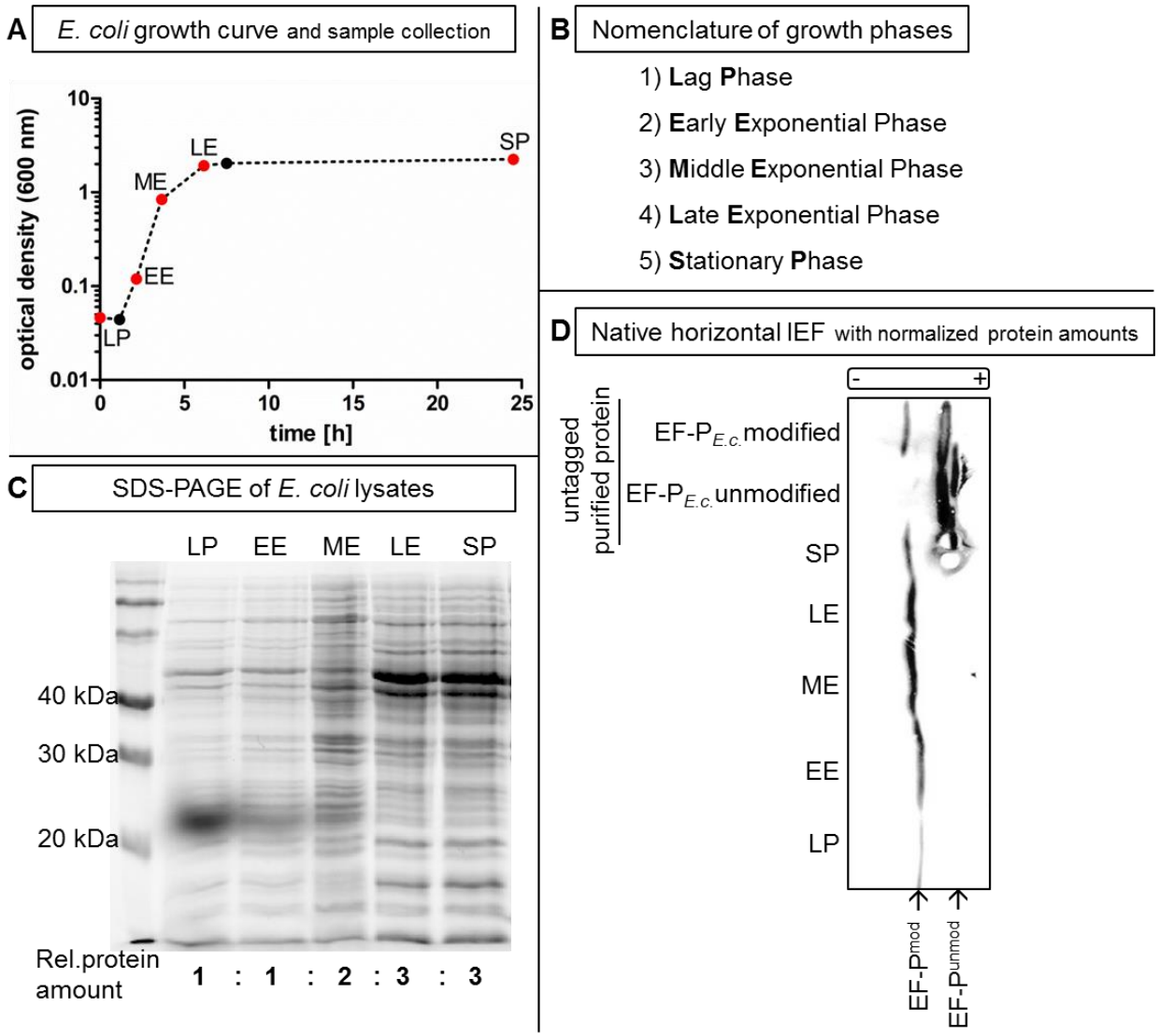

Figure 15: Native horizontal IEF reveals modification status of *E. coli* EF-P during different growth phases. (A) Growth curve of *E. coli* BW25113 with sample collection over 24 h. Five timepoints were chosen for further analysis (highlighted in red) which represent the different growth phases. OD_{600} of lysates were set to 10. (B) Abbreviations of growth phases. (C) SDS-PAGE ($1.6 \cdot 10^8$ cells per lane) with protein visualization by TCE (2,2,2-trichloroethanol) staining [78]. Relative protein amounts were determined by Image Lab Software 4.1 (Bio-Rad) to load equal protein amounts on the IEF gel. (D) Western Blot of native horizontal IEF gel. Pure untagged EF-P (5 µg per lane) in the modified and unmodified form served as controls. All five analyzed endogenous EF-P samples show complete PTM. Anti-EF-$P_{E.c.}$ was used to detect EF-P.

3.3 Modification of EF-P with unnatural substrates by the help of EpmA

3.3.1 Copy number balance of EF-P, EpmA and EpmB

Analysis of the EF-P modification state *in vivo* at different growth phases of *E. coli* showed complete PTM at all growth stages. Therefore, the question arises if EpmA and EF-P copy numbers are finely tuned or if excess of EpmA prevents the occurrence of EF-P in the unmodified state. Therefore, EF-P-to-EpmA ratios were varied in *E. coli* and subsequently, EF-P's modification status was analyzed by vertical IEF. Moreover, the EF-P amino acid variant K34R was included to test acceptor substrate specificity of EpmA. Then, EF-P-to-EpmA/EpmB ratios at different growth conditions from literature values were summarized.

Figure 16A (previously partially published in [38]) shows that deletion (-) of *epmA* in the expression strain led to fully unmodified EF-P. A 2:1 ratio of EF-P-to-EpmA was investigated by chromosomal introduction of a second EF-P copy. The latter was made possible using *E. coli* LF1 P_{lac} *efp* as this strain harbored an additional, His_6-tagged *efp* copy at P_{lac} locus. Interestingly, endogenous levels of EpmA (+) only modify half of the EF-P portion, when a second copy of EF-P was introduced (2x). Here, vertical IEF gel exhibited two bands with similar strength indicating 50:50 distribution of $EF\text{-}P^{mod}$/$EF\text{-}P^{unmod}$. This result underlines that EpmA und EF-P copies were finetuned to ensure complete modification in WT cells at the same time avoiding energy consuming oversupply with modification enzyme. Endogenous EpmA amounts were not sufficient to post-translationally modify EF-P, when the gene was overexpressed using an arabinose-inducible promoter, whereas additional EpmAB overproduction ensured complete modification which is shown in the vertical IEF gel by appearance of a single band shifted towards the cathode.

By contrast, amino acid variation of K34 to arginine, which is the corresponding amino acid in EarP modifying bacteria, prevented PTM at this residue in *E. coli* independent of EpmA-to-EF-P ratio. This indicates the acceptor substrate specificity of EpmA.

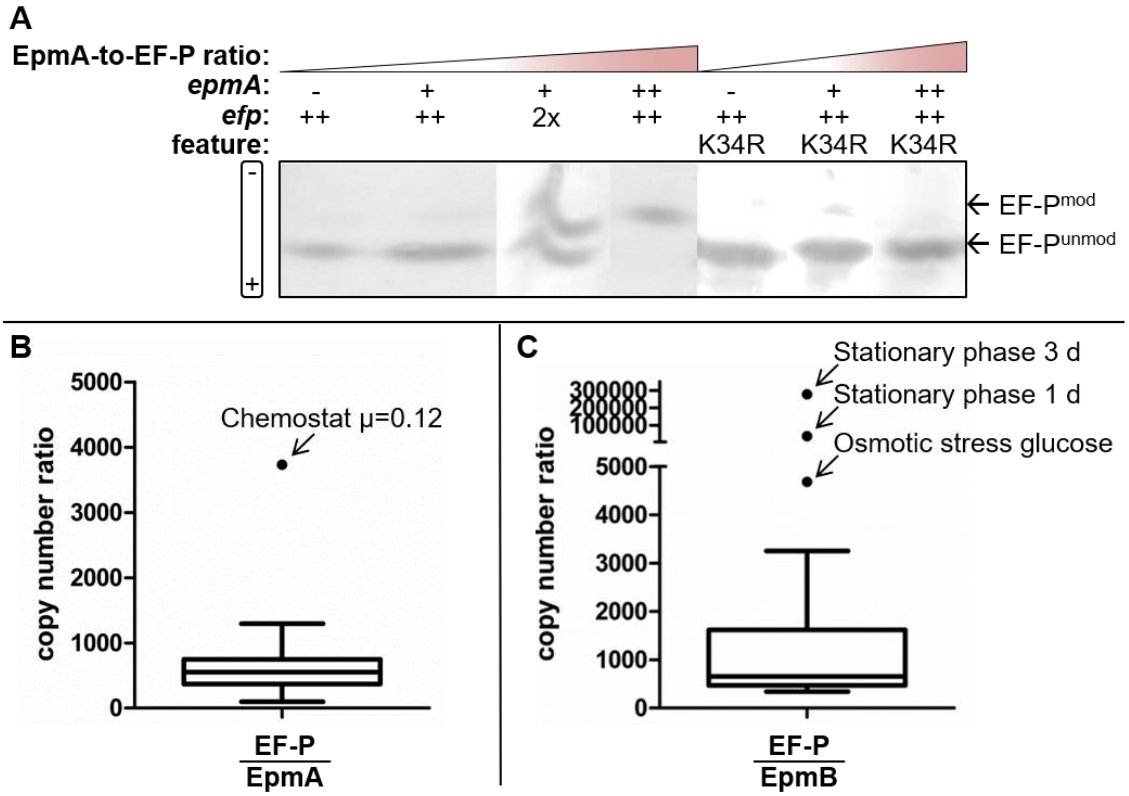

Figure 16: EF-P and EpmA copy numbers are balanced to each other. (A) Variation of EF-P-to-EpmA copy numbers with subsequent analysis of EF-P modification state by vertical IEF. 0.5 µg of EF-P was loaded per lane. EF-P and EpmA copy numbers were modulated by gene deletion (-), endogenous expression (+), introduction of an additional gene copy (2x) and plasmid-based overexpression of EpmAB (++). In addition to *E. coli* EF-P, the amino acid variant EF-P_K34R was tested. Modified and unmodified EF-Ps were separated in the vertical IEF gel and visualized by Western Blotting incubated with Anti-EF-P$_{E.c.}$. (B, C) Copy number ratios of EF-P and EpmAB determined by Schmidt *et al.* [1]. EF-P-to-EpmA (B) and EF-P-to-EpmB (C) copy numbers of 22 growth conditions were determined by Schmidt *et al.* and ratios are presented as whisker plot. Here, outliers are labeled with the specific growth condition.

Schmidt *et al.* [1] analyzed copy numbers of EF-P, EpmA and EpmB at 22 different growth and stress conditions in *E. coli*. Their results are graphically represented in Figure 16BC and show that there is one EpmA molecule per approximately 550 EF-Ps (median of the whisker plot). This value is quite stable at all tested conditions except for growth in the chemostat reactor with the specific growth rate of µ=0.12, because here copy numbers are low in general. EF-P-to-EpmB ratios vary more drastically. At average conditions, one EpmB molecule supplies 650 EF-Ps (median of the whisker plot). Interestingly, EpmB was not found in every cell at stationary phase, leading to the high calculated ratio in Figure 16C. After one and three days, 0.2 and 0.03 copies per cell were measured, respectively [1]. Therefore, the question arises how and if EF-P is modified when EpmB is not present in the cell and can not ensure supply with (*R*)-β-lysine.

In summary, the copy numbers of EF-P and EpmA appear to be finely tuned in *E. coli*.

3.3.2 Identification of functional EpmA amino acid variants

It is known that LysRS is the most promiscuous of all aaRSs, which is underlined by the fact that $tRNA^{Lys}$ is mischarged with arginine, threonine, methionine, leucine, alanine, serine and cysteine *in vitro* [54]. Yanagisawa *et al*. [24] and Roy *et al*. [32] reported several amino acid to alanine substitutions of EpmA which led to loss of function or significantly reduced lysylation activity. Outstanding is the alanine 298 (*E. coli* numbering) to glycine variant because here, donor substrate affinity is altered from (*R*)-β- to (*S*)-α-lysine by just exchanging one amino acid in the catalytic pocket [32].

The aim was to identify more functional EpmA variants by an adaptive evolution experiment using *E. coli* Δ*epmB* that is unable to produce (*R*)-β-lysine. The dependence on functional EF-P for fitness was achieved by introduction of an additional triproline motif which was cloned upstream of the neomycin phosphotransferase I gene (*nptI*) that is responsible for resistance to kanamycin. A LB agar plate with gradually increasing kanamycin concentration was coated with *E. coli* Δ*epmB* transformed with the above described plasmid as well as a plasmid-based copy of *epmA*. Growth at higher kanamycin concentrations was possible for clones that overcame the strong ribosome stalling motif by bringing EF-P into the functional form without having (*R*)-β-lysine, then properly translating *nptI* and thereby gaining resistance to kanamycin. By that approach, five clones were identified that were able to grow at higher kanamycin concentrations (Figure 17A) and those were subjected to a second round of growth on the kanamycin gradient plate. Figure 17B shows that only colonies 2, 4 and 5 retained the phenotype. Sequencing of genomic *efp* and the extracted plasmid neither revealed mutations causing amino acid alterations in EF-P nor in the catalytic pocket of EpmA. Beside the opportunity of mutating PPP-*nptI*, it has already been described that there are ways to bypass EF-P dependence. For example, it was proposed in *Erwinia amylovora* that *hrpA3* deactivation decelerates mRNA degradation at stalled ribosomes to allow more time for translation processes [90].

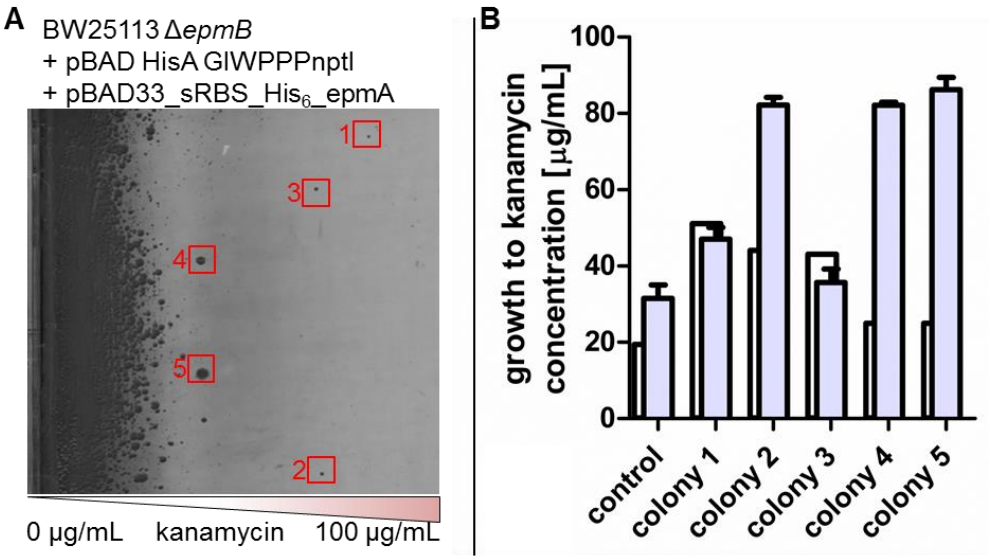

Figure 17: Directed evolution experiment to identify functional EpmA variants. (A) BW25113 Δ*epmB* was double transformed with a plasmid harboring the kanamycin resistance gene *nptI* that included a triproline motif, and a plasmid-based copy of *epmA*. During the first round of selection, five colonies (encircled in red) were able to grow at higher kanamycin concentrations. (B) Bar graph. Colonies from (A) were quantified (white bars) as well as their performance in a second round of growth on a kanamycin gradient plate (grey bars). Colony 2, 4 and 5 kept the kanamycin resistance phenotype in the second round but sequencing showed that neither *efp* nor the catalytic pocket of *epmA* was mutated. For the second round, standard errors of technical duplicates are shown.

Due to the unsatisfying results from the approach with PPP-*nptI* and to avoid the opportunity of mutating the triproline motif as strategy to relieve the EF-P dependence, gentamicin sensitivity was chosen as evolutionary pressure and fitness advantage readout. It was reported that Δ*epmA* and Δ*epmB* mutants of *Salmonella enterica* serovar Typhimurium 14028s are more susceptible to the aminoglycoside gentamicin than the WT strain [44, 91]. Again, *E. coli* Δ*epmB* was used to prevent (*R*)-β-lysine attachment by EpmA, instead substrate promiscuity of EpmA should be utilized to functionalize EF-P in a non-cognate way. Therefore, EpmA copy number was increased by addition of arabinose to the agar plate that ensured additional expression of *epmA* from pBAD vector.

The seven colonies that grew at highest gentamicin concentrations were picked from gradient plates incubated with BW25113 Δ*epmB* and MG1655 Δ*epmB*, respectively. Sequencing proved that *efp* was unmutated in all these colonies. Interestingly, amino acid residue R303 which is part of the catalytic pocket of EpmA was mutated in several of the colonies at the first two codon positions (Figure 18A). By these mutations, three amino acid exchanges were indicated, namely R303 to serine, leucine or isoleucine. Figure 18B illustrates proximity of this residue to the activated donor substrate (*R*)-β-

lysyl-AMP. All these *epmA* mutants with amino acid exchanges were cloned into pBAD33 and were subjected to kanamycin gradient plates containing an additional plasmid with PPP-*nptI*. As results from Figure 18C indicate, PPP-*nptI* was expressed equally well in all strains except for EpmA which was able to grow at slightly higher kanamycin concentrations. Unfortunately, none of the EpmA variants tested exhibited increased antibiotic resistance and therefore EpmA and the reported EpmA_A298G enzyme variant were used in the following study.

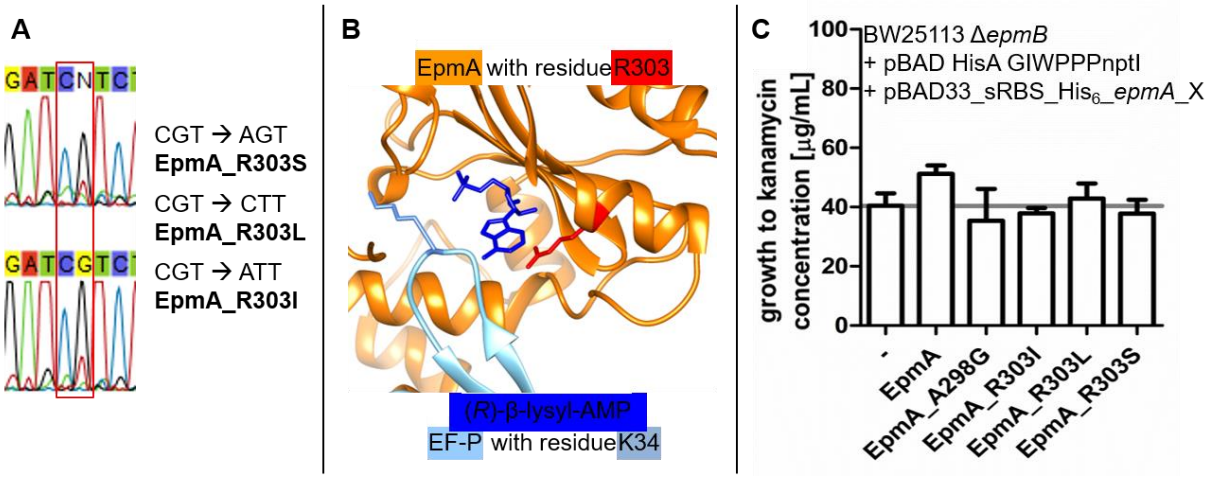

Figure 18: Determination of functional EpmA variants. (A) Exemplary sequencing result of colonies obtained at high gentamicin concentrations in *E. coli* Δ*epmB* background. EpmA residue R303 is encoded by CGT and shown to be mutated at the first and second codon. As consequence, plasmids with *epmA* containing the amino acid exchange mutations R303 to serine, leucine and isoleucine were created. (B) View into the catalytic pocket of EpmA shows the proximity between EpmA (orange) residue R303 (red), EF-P (light blue) and the ligand (*R*)-β-lysine (dark blue). (C) Bar graph of the growth behavior of different strains on kanamycin gradient plates. -: empty pBAD vector. Shown is the standard error of biological duplicates.

3.3.3 Unnatural post-translational modifications of EF-P mediated by EpmA

Ambrogelly *et al.* [51] analyzed the substrate spectrum of LysRS paralog EpmA, without knowing the cellular function of this enzyme. Accordingly, they selected different α-amino acids like 5-hydroxy-(*S*)-α-lysine, (*S*)-α-lysine, DAP and thialysine ((*S*)-(2-aminoethyl)-L-cysteine) [51]. Having demonstrated the substrate promiscuity to be valid for these compounds, I now analyzed the substrate specificity in detail because the role of EpmA in EF-P modification pathway and the fact that (*R*)-β-lysine serves as donor substrate has been solved [19, 32]. The question arises which chemical groups of the cognate substrate (*R*)-β-lysine are necessary for recognition and conversion by EpmA. Comprehensive approaches depicted in Figure 19 were selected to get a deep understanding of the sterical prerequisites necessary for EpmA

to recognize, activate (aa-AMP formation) and finally transfer the donor substrate to acceptor EF-P of *E. coli*.

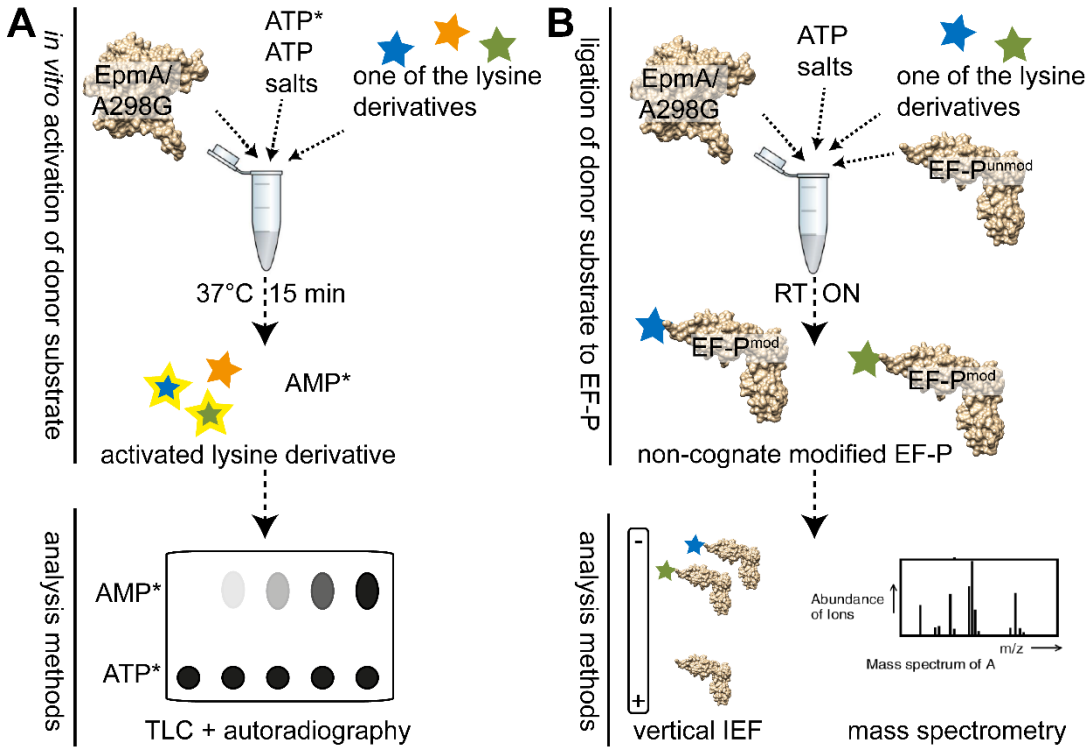

Figure 19: Schematic depiction of *in vitro* modification reaction to create synthetically modified EF-P. (A) *In vitro* activation of non-cognate substrates (indicated by colored stars) by EpmA and EpmA_A298G. Progress of the reaction was visualized by separation of [α-^{32}P]-ATP (ATP*) from [^{32}P]-AMP (AMP*) which indicates hydrolysis of ATP that occurs parallel to aminoacyl adenylate (glowing stars) formation. Quantification by thin layer chromatography (TLC) followed by autoradiography enabled K_m determination. (B) *In vitro* ligation of non-cognate donor substrates to EF-P. 25 µM purified unmodified EF-P, 5 µM pure EpmA(_A298G) and 10 mM potential donor substrate were incubated ON. Successful *in vitro* modification of EF-P is visualized by distinct running behavior on the vertical IEF gel or by MS analysis.

Several different compounds structurally derived from (*R*)-β-lysine were subjected to *in vitro* activation by EpmA. The formation of aminoacyl adenylate occurs in parallel to hydrolysis of radioactively labeled ATP. Therefore, occurrence of radioactively labeled AMP could be separated from ATP by TLC which is followed by autoradiography and therefore enables quantification of activation of the non-cognate substrates of EpmA. In a second experiment, the successfully activated lysine derivatives were subjected to *in vitro* EF-P modification (Figure 19B).

3.3.3.1 Selection of enzyme variants and several possible EpmA substrates for *in vitro* EF-P modification reaction

To elucidate which part or moiety of the natural substrate (*R*)-β-lysine is important for recognition and activation by EpmA, the set of lysine derivatives depicted in Figure 20 was chosen. The sterical variations compared to the natural substrate are indicated and their biological relevance revealed.

Beside both enantiomers of α- and β-lysine substrates with shortened carbon chain ((*S*)-α-ornithine, (*R*)-β-ornithine) were included in the study. Polarity was altered by hydroxylation (5-hydroxy-(*S*)-α-lysine) or by deamination of the natural EpmA substrate (3- and 6-hexanoic acid (capronic acid, AC)). Also here, enantiopure substrates ((*R*)-3-AC, (*S*)-3-AC) were used to elucidate stereoselectivity of EpmA. Moreover, DAP being an important precursor for lysine biosynthesis in bacteria was tested. The list includes highly abundant cellular compounds like (*S*)-α-lysine (0.4 mM) and (*S*)-α-ornithine (0.01 mM) [92] but also compounds which are to the best of my knowledge unknown in bacteria.

	Name	Alterations compared to (*R*)-β-lysine	Feature
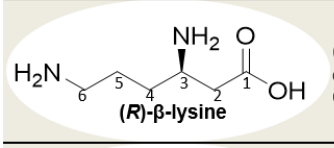	(*3R*)-3,6-diaminohexanoic acid CAS No.: *51703-81-2*	-	Natural substrate of EpmA which transfers it to K34 of EF-P in several γ-proteobacteria
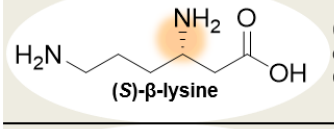	(*3S*)-3,6-diaminohexanoic acid CAS No.: 504-21-2	Enantiomer	Naturally produced by KamA in *Clostridium, Fusobacterium,* and *Porphyromonas* species and others [93]
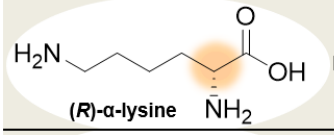	D-lysine	Amino group shifted to α-position	Produced from (*S*)-α-lysine by lysine racemases Lyr and ArgR in several bacteria like *Proteus vulgaris*, *E. coli* and *P. putida* [94]
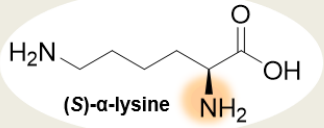	L-lysine	Amino group shifted to α-position	Proteinogenic amino acid Is transferred into (*R*)-β-lysine by EpmB
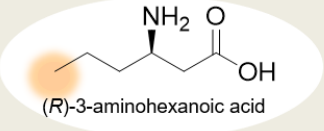	(*R*)-3-aminocapronic acid **(*R*)-3-AC**	No ε-amino group	Unknown in bacteria*
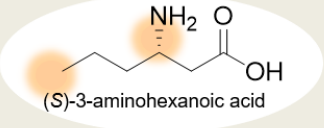	(*S*)-3-aminocapronic acid **(*S*)-3-AC**	No ε-amino group	Unknown in bacteria*
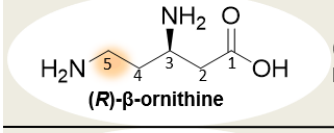	(*R*)-3,5-diamino pentanoic acid	C-chain shortening	Unknown in bacteria*
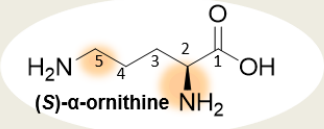		C-chain shortening	Important metabolic intermediate in bacteria, e. g. part of the urea cycle In *E. coli* synthesized from L-glutamate lysine/arginine/ornithine ABC transporter (HisPMQArgT)
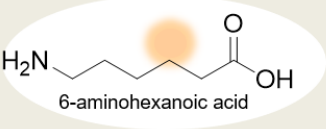	6-aminocapronic acid **6-AC**	No β-amino group	Degradation product in caprolactam degrading bacteria including *Pseudomonas*, *Alcaligenes* and *Acinetobacter* [95] Serves as hydrophobic spacer to couple a tag, a fluorophore, etc. to a peptide [96, 97]
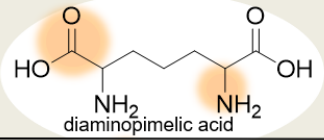	**DAP**	Diamino acid	Direct metabolic precursor of lysine Part of cell wall peptidoglycan in *E. coli* and other gram-negative bacteria [98]
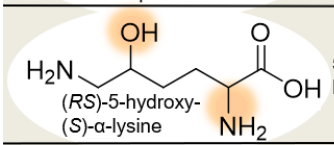	**5-hydroxy-(*S*)-α-lysine**	Additional negatively charged group	Not known to be relevant in the free form in bacteria [99] In the bound form in collagen of vertebrates [100]

*Unknown according to KEGG COMPOUND Database [101]

Figure 20: Potential EpmA substrates tested in this study. Chemical structure, trivial name and biological relevance are listed. Structural alterations compared to (*R*)-β-lysine are highlighted in orange. Carbon chain shortening is indicated by C-atom numbering. Names or abbreviations used in this study are indicated in bold.

Having selected potential substrates for EpmA, EpmA_A298G was also chosen as enzyme variant to get a deeper understanding of the interplay between the amino acid residues of EpmA's catalytic pocket and the ligand.

It is known that LysRS and EpmA differ in two relevant amino acids in the catalytic pocket. The amino acid residues alanine 298 and serine 76 of EpmA are crucial for specificity, substrate recognition, substrate binding and enzymatic activity [32]. Here, mutation of serine 76 to alanine abolishes EpmA functionality [32]. The amino acid residue at position 298 is determining the structure of the ligand which is also demonstrated schematically in Figure 21AC. WT EpmA with alanine 298 (Figure 21A) has evolved towards (*R*)-β-lysine as enzyme-ligand spacings are adapted to each other. Absence of the methyl group as amino acid side chain - like it is the case in LysRS or in the EpmA variant with glycine at position 298 - creates space for α–lysine and its structural derivatives (Figure 21C). A sterical clash between the methyl group of alanine 298 and the amino group of an α amino acids is unfavored.

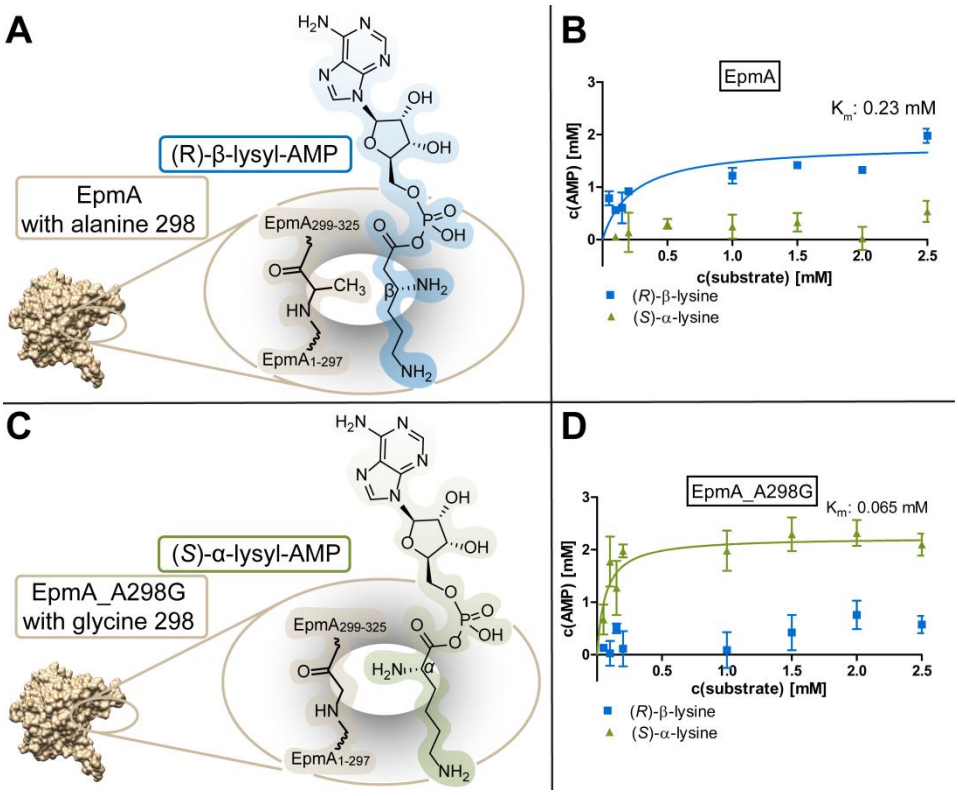

Figure 21: Residue 298 of EpmA regulates donor substrate specificity. K_m determination and zoom into the catalytic pocket of EpmA (A, B) and EpmA_A298G (C, D). (A) Schematic zoom into the catalytic pocket of the WT enzyme-substrate combination: EpmA and (*R*)-β-lysine. The white halo enlightens residue 298. (B) *In vitro* activation of (*R*)-β-lysine (blue) and (*S*)-α-lysine (green) were detected by hydrolysis of ATP forming AMP. K_m of (*R*)-β-lysine for EpmA laid in the low mM range. (C) Amino acid variation A298G created free space in the catalytic pocket of EpmA that led to increased affinity toward (*S*)-α-lysine compared to WT EpmA. (D) Substrate specificity of EpmA_A298G was shifted toward (*S*)-α-lysine representing this enzyme's low K_m substrate.

This was demonstrated when kinetics were determined using the *in vitro* substrate activation assay which is equally structured than tRNA charging assays of aaRSs (Figure 19A, described in detail in the following chapter). Successful activation of the substrate by EpmA or EpmA_A298G was indicated by release of AMP. Figure 21B shows that addition of (*R*)-β-lysine (shown in blue in all figures) as substrate led to detectable AMP release at low millimolar concentrations, whereas in this concentration range, activation of (*S*)-α-lysine (shown in green) was undetectable. K_m of the natural enzyme-substrate combination was determined to be 0.23 mM. Induced by amino acid substitution A298G, the substrate specificity from (*R*)-β- to (*S*)-α-lysine was shifted and is visualized in Figure 21D. K_m for (*S*)-α-lysine was low (0.065 mM) and activity was shifted at the expense of affinity towards (*R*)-β-lysine. 11 potential donor substrates were selected to be tested in combination with EpmA (low K_m substrate: (*R*)-β-lysine) and EpmA_A298G (low K_m substrate: (*S*)-α-lysine).

3.3.3.2 Determination of kinetic parameters for *in vitro* activation of non-cognate substrates by EpmA

The most important steady state kinetic assays for aaRSs are the pyrophosphate assay and the aminoacylation assay, respectively [102]. Both options were tested, and it was found that Pyrophosphate Assay Kit II (Fluorometric, Abcam) responded to EpmA without substrate as well as to substrate without having added any enzyme (not shown) and is therefore not applicable for the purpose of this thesis. Therefore, the classical assay for tracking of tRNA charging already established decades ago [56] was used in which purified enzyme (aaRS/EpmA), donor substrate (amino acid), ATP and a portion of [α-^{32}P]-ATP was incubated at 37 °C. The reaction was quenched subsequently. Activation of the donor substrate led to simultaneous ATP hydrolysis. Unreacted [α-^{32}P]-ATP and newly formed [^{32}P]-AMP were separated by TLC and detected by autoradiography. Grey density quantification of the autoradiography plates, exemplary shown in Figure 22, revealed several findings.

First, detectable AMP release over time shows that 6-AC was accepted as substrate by EpmA. The latter readily activated 6-AC although at this compound, a β-amino group is absent. Therefore, EpmA tolerates structural alterations of its natural substrate (*R*)-β-lysine and obviously does not require the β-amino group for substrate recognition.

Second, it is demonstrated that the aa-AMP intermediate is formed independently of an acceptor substrate (0 or 5 µM EF-P), so addition of EF-P did not alter the amino acid activation by EpmA. This fact was also reported by Francklyn *et al.* for most aminoacylation reactions examined, except for GlnRS, GluRS and ArgRS [102]. It allows focus on the first substep of EpmA catalysis excluding acceptor substrate effects and is important for understanding prerequisites of donor substrate binding or exclusion in detail.

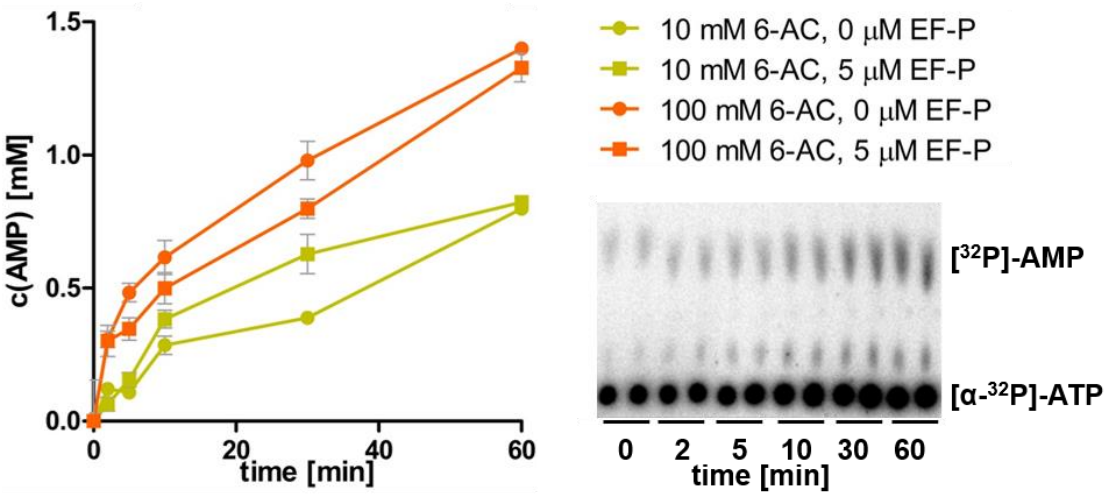

Figure 22: tRNA charging assay implemented to detect non-cognate substrate activation by EpmA. Exemplary, 6-AC was chosen as substrate. *In vitro* aa-AMP formation catalyzed by EpmA was followed over time (0 - 60 min). Technical duplicates of each time point were spotted to TLC plates. Grey densities of the audiographs (right side, representative) were analyzed. For quantification, Equation 1 (Material and Methods, Chapter 2.11) was used. 6-AC was activated by EpmA, irrespective if EF-P was absent (dots) or added (squares).

Having shown that the tRNA charging assay described above is suitable for determination of kinetic parameters for substrate activation by EpmA, 15 min was chosen as fixed timepoint and simultaneously substrate concentration was varied. ATP was present in excess which allowed approximation of the enzymatic reaction to a single-substrate mechanism. This allowed for K_m determination by fitting the obtained curve according to Michaelis-Menten equation [103]. In addition to the cognate enzyme-substrate pairs (already shown in Figure 21, substrate concentration 0 - 2.5 mM), concentrations of non-cognate substrates were varied between 0 and 100 mM to follow the progress of the *in vitro* substrate activation (Figure 23).

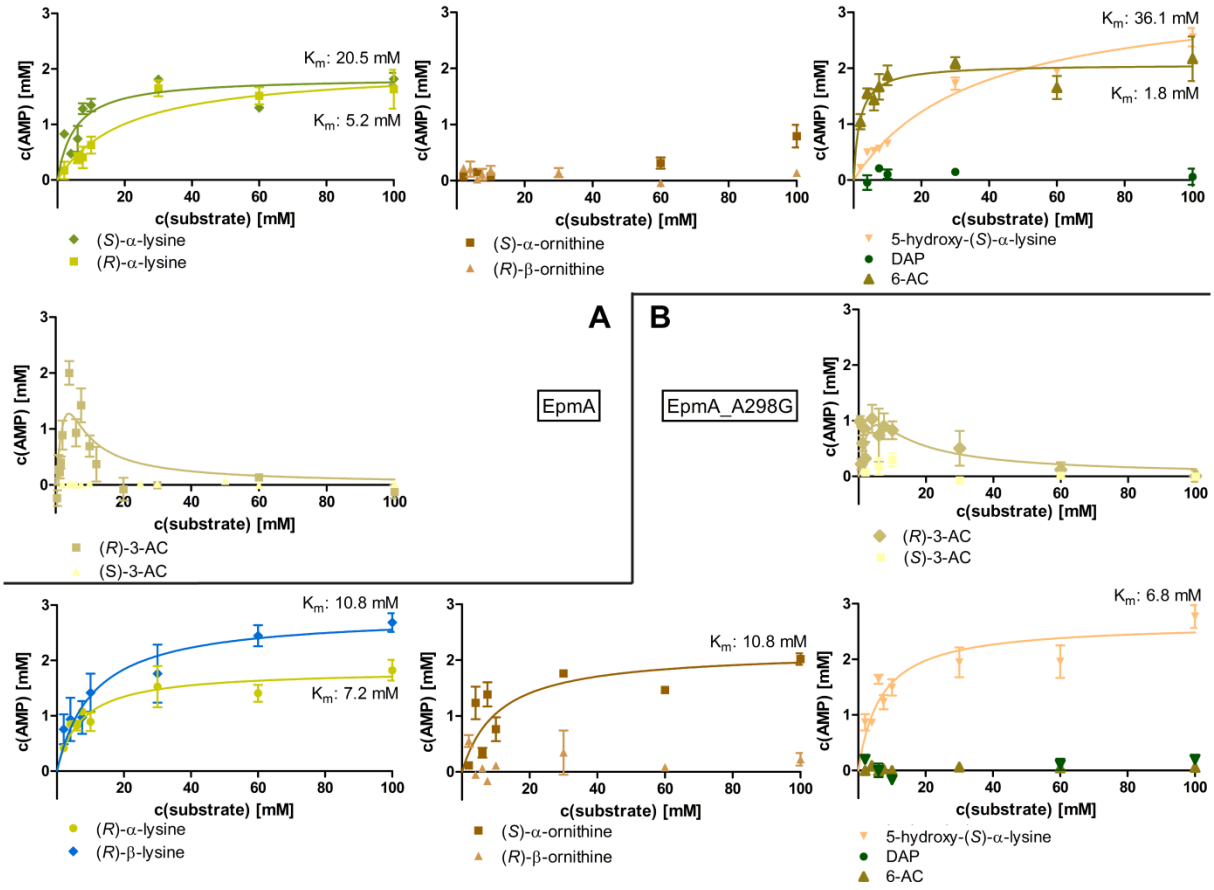

Figure 23: K_m value determination for EpmA and EpmA_A298G. Michaelis-Menten kinetics are shown for EpmA (A) and EpmA_A298G (B) for different lysine derivatives. Whenever possible, K_m value was determined. Although (*R*)-3-AC served as substrate for EpmA, K_m determination was not accurately possible for EpmA as well as EpmA_A298G because of substrate inhibition effects at high (*R*)-3-AC concentrations and improper saturation at low substrate concentrations. Plotted is the standard error of technical duplicates.

From these kinetic curves it became apparent that (*R*)- and (*S*)-α-lysine, 5-hydroxy-(*S*)-α-lysine, (*R*)-3-AC and 6-AC can be activated beside the natural EpmA substrate because for all of them distinct amounts of [^{32}P]-AMP were released. Only (*S*)-α-ornithine, (*R*)-β-ornithine, DAP and (*S*)-3-AC showed no detectable activation by EpmA in the explored concentration range. These data underline the stereoselective choice that EpmA was able to make as it activated (*R*)- but not (*S*)-3-AC.

Table 5 summarizes the completive set of K_m values for the 11 tested substrates and the two different enzyme variants. The EpmA_A298G variation was previously shown to reduce the K_m value towards (*S*)-α-lysine by 96 % compared to WT [32]. Fittingly, only the enzyme-substrate pairs EpmA + (*R*)-β-lysine and EpmA_A298G + (*S*)-α-lysine exhibited K_m values below 1 mM, all other unnatural substrates showed K_m values in the millimolar range. K_m[(*S*)-α-lysine] of 5 mM (EpmA) and 65 µM (EpmA_A298G) were in line with data from Roy *et al*. who found 9 mM (EpmA) and 344 µM

(EpmA_A298G) [32]. In the same publication they found quite similar K_m values for (*R*)-β-lysine regarding both enzyme variants (213 and 414 µM). The values determined here varied by a factor of 60 which appears consistent and explicable. (*R*)-β-lysine exhibited a K_m value of 18 µM for EpmA and a much higher value of 11 mM for EpmA_A298G because here, substrate specificity is shifted towards (*S*)-α-lysine at the expense of (*R*)-β-lysine.

Table 5: K_m values for different substrates of EpmA and EpmA_A298G.

K_m [mM]	enzyme	
	EpmA	**EpmA_A298G**
(*R*)-β-lysine	0.23 (±0.07)	10.8 (±4.0)
(*S*)-β-lysine	Not determined	
(*R*)-α-lysine	20.5 (±9.3)	7.2 (±2.0)
(*S*)-α-lysine	5.2 (±1.3)	0.065 (±0.032)
(*R*)-3-aminohexanoic acid	Not estimable	
(*S*)-3-aminohexanoic acid	No reaction	
(*R*)-β-ornithine	No reaction	
(*S*)-α-ornithine	No reaction	10.8 (±4.1)
6-aminohexanoic acid	1.8 (±0.8)	No reaction
diaminopimelic acid	No reaction	
5-hydroxy-(*S*)-α-lysine	36.1 (±6.4)	6.8 (±1.7)

K_m values for (*R*)-3-AC and for (*S*)-β-lysine could not be determined. (*R*)-3-AC exhibited substrate inhibition effects *in vitro* that led to a reduction of AMP formation at concentrations above ~10 mM. As a result, saturation was not reached which prohibited exact curve fitting and K_m determination. Moreover, it induced a growth defect *in vivo* (Figure 24). For (*S*)-β-lysine, determination of the stock solution concentration was not accurately possible. The K_m value was determined in [32] to be 6.95 mM.

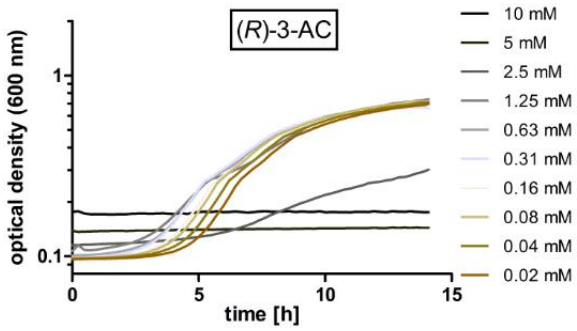

Figure 24: Growth of *E. coli* BW25113 Δ*epmB* in LB medium supplemented with different concentrations of (*R*)-3-AC. Cells exhibit a growth defect at concentrations above 1.25 mM.

The detailed analysis of K_m values furthermore shows that regarding the α-amino acid derivates (*R*/*S*)-α-lysine and 5-hydroxy-(*S*)-α-lysine, K_m values were significantly lower (factor 3 – 80) for EpmA_A298G than for EpmA. Even more striking, (*S*)-α-ornithine could not be activated by the WT enzyme but only by EpmA_A298G. The latter evolved towards α-amino acids but remarkably the shortage of the carbon chain by one carbon atom affected the K_m value by several orders of magnitude as K_m[(*S*)-α-lysine] = 65 µM and K_m[(*S*)-α-ornithine] = 10 mM. EpmA_A298G not only tolerated the α-amino group at different lysine derivatives, it even seemed to require it for activation of the substrate. This was indicated by 6-AC, a compound where no α- nor β-amino group was present. It was readily activated by EpmA (even exhibiting a low K_m value around 2 mM) but showed no reaction when EpmA_A298G was present. Absence of the ε-amino group, represented by (*R*)-3-AC, did not abolish function of EpmA and EpmA_A298G.

By determination of kinetics for activation of 11 lysine derivatives by EpmA and EpmA_A298G useful insights into the amino acid promiscuity and specificity of the enzymes regarding the successful condensation reaction with AMP were gained. They lead to the conclusion that activation by EpmA requires a 6-atom carbon chain with either ε- (6-AC), β- ((*R*)-β-lysine, (*R*)-3-AC) or α- ((*R*/*S*)-α-lysine, 5-hydroxy-(*S*)-α-lysine) amino group. EpmA_A298G explicitly preferred substrates with α-amino groups ((*R*/*S*)-α-lysine, (*S*)-α-ornithine, 5-hydroxy-(*S*)-α-lysine), tolerates substrates with β-amino groups ((*R*)-β-lysine, (*R*)-3-AC), but excludes 6-AC.

3.3.3.3 Creation of new, unnaturally modified EF-P variants

The selection mechanisms of aaRSs are performed at the stage of amino acid activation (pre-transfer editing) as well as subsequent to transfer of an incorrect amino acid (post-transfer editing). For the first-mentioned method, non-cognate amino acids are eliminated by rejecting false ternary complexes at the ribosome [5]. In contrast,

non-cognate amino acids which were already incorporated into the nascent peptide are sorted out by recruitment of release factors [104].

In Chapter 3.3.3.2 seven lysine derivatives were shown to be activated by EpmA and/or EpmA_A298G. (*S*)-3-AC, DAP and (*R*)-β-ornithine were excluded from activation (pre-transfer editing). Therefore, the question arises if substrate activation constitutes the bottleneck of the reaction and consequently all aminoacyl adenylates can be transferred to EF-P, or post-transfer editing prevents EF-P modification with these unnatural substrates. To elucidate this second substep of EF-P modification, the ligation reaction, lysine derivatives were tested in combination with one of the two purified enzyme variants in the *in vitro* modification assay (schematically depicted in Figure 19B). When the lysine derivative is successfully attached to EF-P, its charged groups (in this case mostly amino groups) contribute to the pI value of the protein and lead to a shift towards the cathode compared to the unmodified input EF-P.

The Western Blot in Figure 25 confirms that EF-P was successfully modified *in vitro* by (*R*)- and (*S*)-β-lysine catalyzed by both enzyme variants because the heights of the bands corresponded to the positive control (EF-$P^{R\beta lys}$, *in vivo* modified). This leads to the conclusion that the enantiomer of the natural EpmA substrate was readily activated and subsequently ligated to EF-P although the β-amino group at the chirality center points in a different direction. (*S*)-α-lysine exhibited a slightly lower but undoubtedly EF-P-attached band. This is explicable by the fact that α-amino acids in general show a lower pK_a value than β-amino acids (e. g. pK_a[α-alanine] = 9.87 [105], pK_a[β-alanine] = 10.24 [106]) because of the stronger inductive effect (*–I*) of the carboxyl group in the case of α-amino acids. EpmA_A298G ligated both α-lysine enantiomers to EF-P whereas EpmA only transferred (*S*)-α-lysine, apparently requiring the amino group to point into the same direction than it is the case at the natural substrate.

The pI value for EF-P modified with 5-hydroxy-(*S*)-α-lysine was only slightly higher than for EF-P in the unmodified state because here the pI elevating effect of the α- and ε-amino groups were reduced by the diminishing effect of the hydroxyl group. In line with expectations, 5-hydroxy-(*S*)-α-lysine was transferred to EF-P to a certain extent by EpmA resulting in an unmodified and a modified band with similar intensities in the IEF gel, whereas for the amino acid variant EpmA_A298G the reaction was complete.

(*S*)-glutamine and (*S*)-arginine were not transferred to EF-P by either of the enzymes. This is important for the cell because intracellular concentrations of these compounds are high (3.8 and 0.6 mM [92], respectively) and should therefore be excluded by EpmA to avoid invalid, energy-consuming EF-P modification.

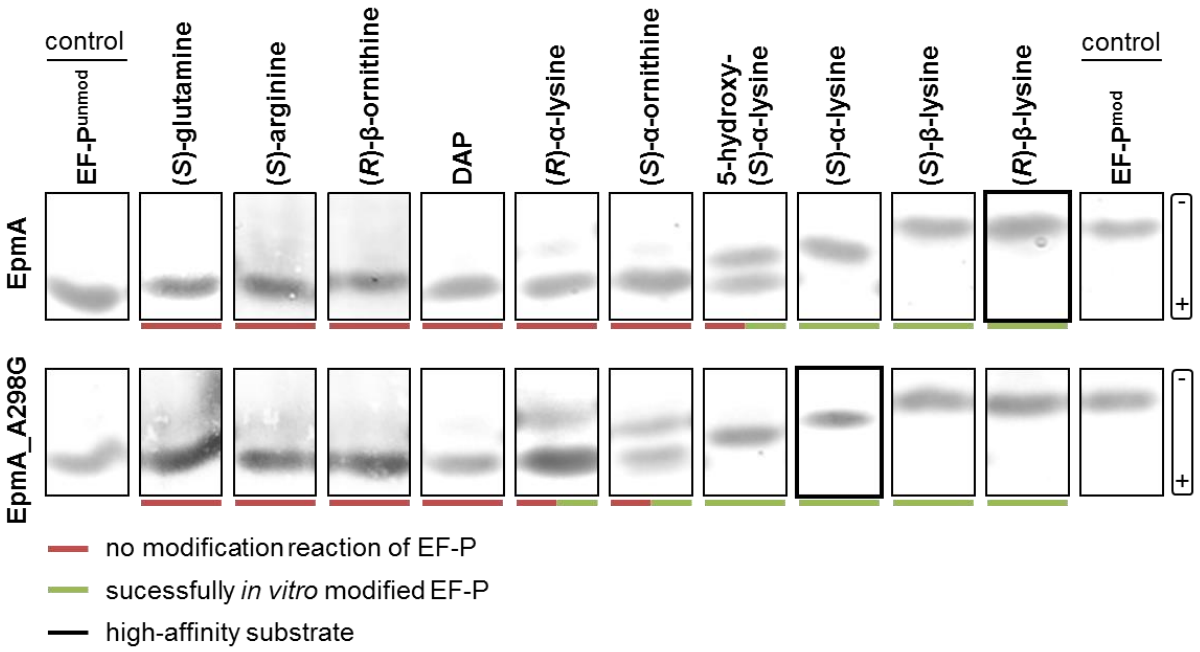

Figure 25: Vertical IEF shows the non-cognate *in vitro* modification of EF-P by EpmA and EpmA_A298G. For *in vitro* reaction purified unmodified EF-P and purified enzyme were incubated with 10 mM substrate ON. 1.5 µg of EF-P was loaded per lane. Unmodified (marked in red) and modified (marked in green) EF-Ps were separated in an IEF gel and visualized by Western Blotting (EF-P$_{E.c.}$ antibody). *In vivo* modified EF-P served as positive control.

For all tested substances, the modification status of EF-P was also confirmed by MS analysis. This was essential for the substrates 3-AC and 6-AC because they do not contain additional charged groups compared to K34 so their attachment to EF-P is invisible by IEF technique. The mass of unmodified EF-P was subtracted from the measured mass resulting in the detected mass shift Δ which is presented in Table 6. Therefore, $\Delta_{measured}$ ~1 stands for unmodified EF-P whereas a number ~130 constitutes EF-P in the modified form.

Equation 3: Calculation of mass shift $\Delta_{measured}$ caused by *in vitro* EF-P modification

$$\Delta_{measured} = m(measured) - m(EF\text{-}P^{unmodified})$$

Table 6: EF-P *in vitro* modification was elucidated by determination of the additional mass *Δ*. MS analysis conducted with intact EF-P after *in vitro* EF-P modification reveals that eight substrates were successfully attached (indicated in green) by either EpmA or EpmA_A298G. Two numbers in a lane point up the presence of both modified and unmodified EF-P and therefore stand for incomplete PTM status.

substrate	Mass shift of succesfull PTM $\Delta_{theoretical}$	Mass shift detected after *in vitro* modification $\Delta_{measured}$		
		EpmA		EpmA_A298G
(*R*)-β-lysine	129.19	129.24		129.23
(*S*)-β-lysine	129.19	129.24		129.24
(*R*)-α-lysine	129.19	1.13		129.21 1.97
(*S*)-α-lysine	129.19	130.24		129.23 0.14
(*R*)-3-aminohexanoic acid	114.17	113.27		114.22
(*S*)-3-aminohexanoic acid	114.17	1.18		1.14
(*R*)-β-ornithine	115.14	1.14		1.14
(*S*)-α-ornithine	115.14	1.13		114.08
6-aminohexanoic acid	114.17	114.22		0.13
Diaminopimelic acid	173.09	1.1.4		1.1.3
5-hydroxy-(*S*)-α-lysine	145.19	145.22 1.12		145.22
(*S*)-arginine	157.20	1.14		1.15
(*S*)-glutamine	129.15	1.14		1.14

In line with results from aa-AMP formation, (*S*)-3-AC does not serve as substrate for EpmA or its variant, whereas the (*R*)-enantiomer was activated and transferred to EF-P. This leads to the conclusion that alterations at the C3 stereocenter and concurrent absence of the terminal amino group were not tolerated by EpmA. Nevertheless, alteration of either the β- (6-AC) or the ε-amino group ((*R*)-3-AC) was tolerated, so both positively charged groups were recognized by EpmA. As 6-AC is only transferred by EpmA and not by its variant, contact of the ε-amino group from the substrate with amino acids in the catalytic pocket was not enough for conversion by EpmA_A298G.

DAP and (*R*)-β-ornithine were the only compounds tested that were neither transferred nor activated by both of the ligases. DAP is a direct precursor of lysine in its synthesis pathway of most bacteria, leading from aspartate to DAP which is subsequently

converted to lysine by the decarboxylase LysA [107]. However, the chemical composition of DAP differs from (*R*)-β-lysine in many ways, not least because of the large additional carboxyl group. The negative result for (*R*)-β-ornithine is not as obvious. Table 7 shows, that (*R*)-β-ornithine was neither activated by EpmA nor inhibiting the enzyme. Different concentrations of (*R*)-β-ornithine with and without additional (*R*)-β-lysine as competitor were tested for *in vitro* EF-P modification. The latter was analyzed by MS. At very high (*R*)-β-ornithine concentrations, EF-P was also not modified with (*R*)-β-ornithine by EpmA or EpmA_A298G, respectively, *in vitro*. When (*R*)-β-lysine was added to the reaction mixture, EF-P was fully modified by it, regardless of the (*R*)-β-ornithine concentration.

Table 7: Concentration of (*R*)-β-ornithine and (*R*)-β-lysine in *in vitro* EF-P modification reaction. Mass shift due to modification of EF-P was detected by MS analysis.

	EpmA_A298G	**EpmA**					
(*R*)-β-ornithine	500 mM	10 mM	500 mM	-	5 mM	10 mM	20 mM
(*R*)-β-lysine	-	-		10 mM			
$\Delta_{measured}$	1.1	1.1	1.1	128.2	129.2	128.2	129.2

Nevertheless, this result is in line with literature as it is known that $tRNA^{Lys}$ is mischarged by LysRS with non-cognate substrates like arginine, threonine, methionine, leucine, alanine, serine and cysteine, but interestingly not with ornithine *in vitro* [54]. Jakubowski *et al*. suggested an efficient editing mechanism including cyclization of ornithyl adenylate. Here, the δ-amino group attacks the activated carbonyl group to yield AMP and ornithine lactam (3-aminopiperidin-2-one), which exhibits a quite stable 6-atom ring [54]. Having this in mind, it is conclusive that despite high relatedness of (*R*)-β-lysine and (*R*)-β-ornithine, the latter is not activated by EpmA.

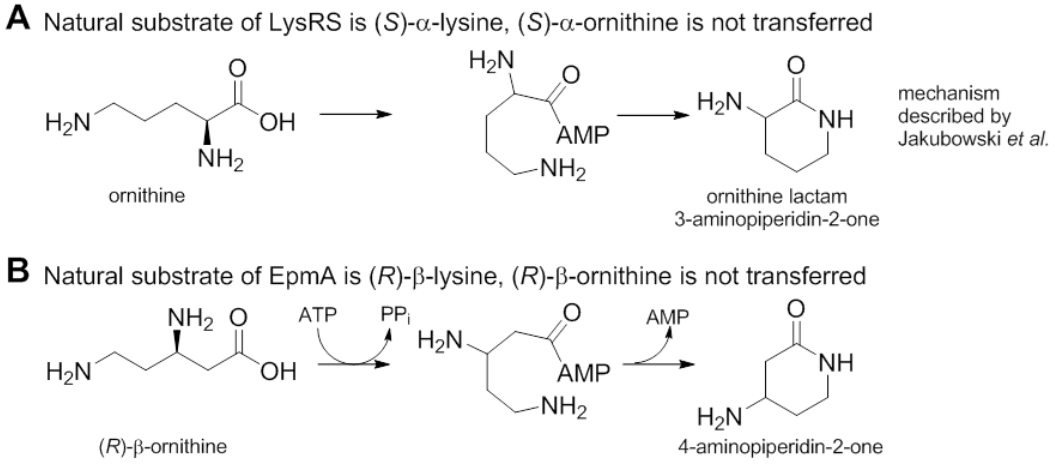

Figure 26: Hypothetical mechanism of lactam formation of activated ornithine. (A) For the unnatural LysRS substrate (*S*)-α-ornithine Jakubowski *et al*. postulated a ring formation that

prevents it from transfer to tRNA [54]. (B) The hypothetical pathway can be transferred to (*R*)-β-ornithine.

Taken together, eight of the 13 tested substances were transferred to EF-P by at least one of the enzyme variants in the *in vitro* approach. As all the substrates which could be activated were subsequently transferred to EF-P it can be concluded that the first substep is the bottleneck of EpmA catalysis and pre-transfer editing is performed.

3.3.3.4 Performance of synthetically modified EF-Ps in *in vitro* translation

Having created seven synthetically modified EF-Ps the question arises whether they perform equally well as (*R*)-β-lysylated EF-P at the ribosome. They all exhibit the elongated tip of EF-P at K34, but it is questionable if orientation and charge conditions enable optimal interplay with the PTC of the ribosome.

To test whether the novel PTMs can support EF-P mediated rescue of polyproline-stalled ribosomes an *in vitro* transcription/translation system reconstituted from purified components (PURExpress, NEB Biolabs) was set up. As readout for translation efficiency NanoLuc luciferase (NLuc), a small protein (19.1 kDa) that can convert furimazine into furimamide and thereby emits light, was used. Naturally, the enzyme lacks any diproline motif. Accordingly, *nluc* ORF was extended 5' by a short codon motif encoding RPAP as control or RPPP to cause a translational arrest being alleviated by modified EF-P (Figure 27AB) [16]. Hence, the more efficient ribosome rescue is, the faster Nluc is translated and the more light is produced in a time-dependent manner (Figure 27B). Figure 27C shows the bar graph of RPPP-*nluc* expression after 30 min. *In vitro* transcription/translation reaction was accelerated 4.5-fold when (*R*)-β-lysylated EF-P instead of unmodified EF-P was added to the reaction mixture. This result was also confirmed by Ude *et al*. who found a similar ratio [16]. By contrast, none of the EF-P variants charged with a non-cognate substrate reached a translational speed which was equal or higher than observed for EF-P$^{R\beta lys}$. In this context it was not decisive if the modification has been attached *in vitro* or *in vivo* as there was no statistically significant difference in *nluc* expression (Figure 27C).

EF-P modified with (*R*)-β-lysine was superior to all tested non-cognate substrates so only this EF-P optimally performed at the ribosome in the context of EF-P orientation and charge conditions at the elongated tip of EF-P at K34.

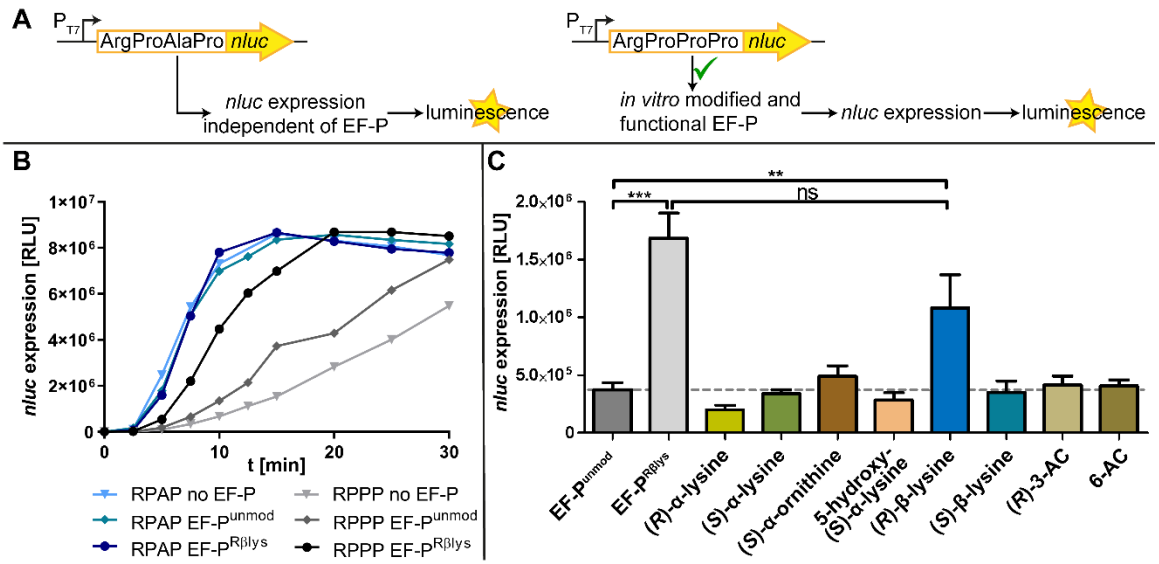

Figure 27: *In vitro* transcription/translation efficiency of RPPP-Nluc using synthetically modified EF-Ps. (A) Schematic depiction of the cell-free transcription/translation experiment with either a RPAP or a RPPP motif upstream of *nluc*. The latter requires functional EF-P for robust translation of NanoLuc Luciferase. Consequently, functionality of the *in vitro* modified EF-Ps can be detected by luminescence readout. (B) Time course of RPAP-*nluc* and RPPP-*nluc* expression with either no, unmodified or *in vivo* modified EF-P over 30 min. RPPP-*nluc* expression was impeded in the presence of no or unmodified EF-P. One exemplary replicate is shown. (C) Bar graph of RPPP-*nluc* expression after 30 min. Successfully *in vitro* modified EF-Ps (verified by IEF or MS analysis), unmodified EF-P (negative control) and *in vivo* modified EF-P (positive control, EF-P$^{R\beta lys}$) were subjected to *in vitro* transcription/translation assay. RPPP-Nluc translation efficiencies were determined for at least three independent samples. Only EF-P modified *in vitro* (blue) or *in vivo* (light grey) with (*R*)-β-lysine exhibited significantly higher *nluc* expression than when unmodified EF-P (grey dashed line) was added to the reaction mixture. Results of the two-tailed t-test are indicated **: p < 0.01, ***: p < 0.001.

Reportedly, the ε-amino group of the protruding EF-P lysine gets acetylated *in vivo* when the modification system is missing [36]. This is proven for EF-P of *B. subtilis,* but lysine acetylation is a widespread PTM [108]. Consequently, this protein variant was included in the study. Chemical biology provides the possibility to obtain a post-translationally modified protein when the corresponding transfer enzyme is unknown or difficult to prepare. Therefore, acetylated EF-P was generated utilizing the AcKRS/tRNA^{Pyl} dependent amber suppression system described by Volkwein *et al.* [66]. Here, *efp* was mutated with a nonsense mutation TAG at position 34. Upon suppression with acetyllysine utilizing the aaRS/tRNA pair AcKRS/tRNA^{Pyl} the EF-P variant bearing an acetyl group at K34 was produced (EF-P^{AcK}) and successful expression confirmed by vertical IEF (Figure 28A). Nevertheless, this variant did not result in better *in vitro* transcription/translation efficiency than it is the case for EF-P in the unmodified form (Figure 28B).

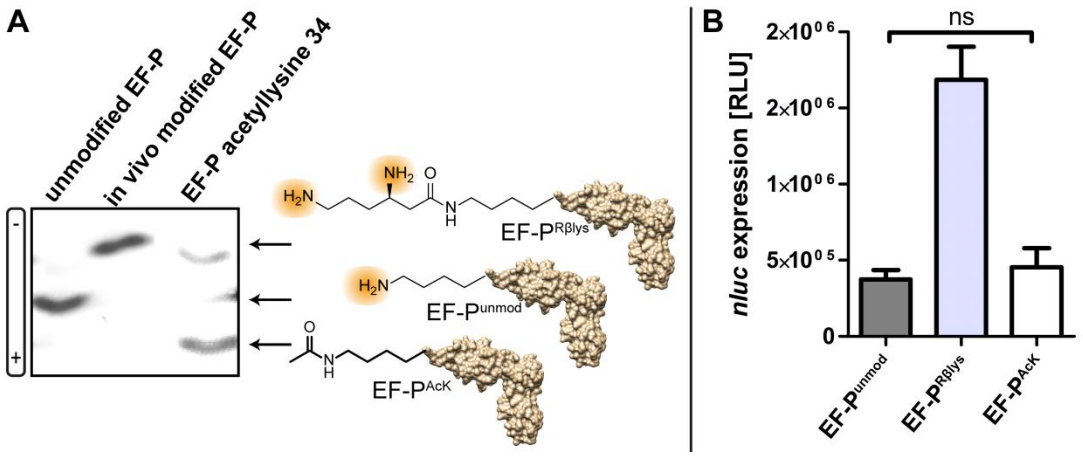

Figure 28: EF-P modified with acetyllysine 34. (A) EF-P was produced with acetyllysine at position 34 using amber suppression [66]. (B) *In vitro* transcription translation of RPPP-Nluc is not stimulated by EF-P with acetyllysine at position 34.

In conclusion, translation of proteins containing a triproline motif was not stimulated by synthetically modified EF-Ps and thereby showed the exceptional achievement of (*R*)-β-lysylated EF-P during translation explaining its evolutionary selection.

3.3.4 Unnatural EF-P modification *in vivo*

Undoubtedly, promiscuity of EpmA towards its donor substrate was shown. Using the natural enzyme EpmA, EF-P was diversely modified in the presence of lysine derivatives. As *B. subtilis* it is known to exhibit an incomplete modification status (5-aminopentanol, hydroxypentanone, pentanone attachment [36]), I aimed to elucidate the modification status of *E. coli* EF-P *in vivo* when *epmB* was deleted. As there is no metabolic pathway known to circumvent *epmB* deletion, the canonical donor substrate of EpmA was missing and it was questionable, if EpmA transfers other substrates *in vivo*.

First, functionality of EF-P in *E. coli* Δ*epmB* was tested using a system described by Ude *et al.* [16]. Truncated *cadC* was fused to a triproline motif and *lacZ* and subsequently introduced to a plasmid backbone (Figure 29A). EF-P in its functional form was necessary to result in *lacZ* expression that could be detected by β-galactosidase activity and quantified in Miller Units. *E. coli* WT, *epmA* and *epmB* deletion strains were transformed with this PPP-*lacZ* containing plasmid and their β-galactosidase activities compared in Figure 29B (white bars). Irrespective which of the EF-P modification systems was deleted, Δ*epmA* and Δ*epmB* showed similar phenotypes with a drastic reduction of β-galactosidase activity compared to WT. Overproduction of EpmA or EpmA_A298G in *E. coli* Δ*epmB* (blue frame) showed no

significant increase in β-galactosidase activity indicating inactivity of EF-P in these cases. Complementations of the deletion phenotypes by *epmA* or *epmB* expression from an integrated plasmid were successful and interestingly also *epmA*_A298G complements Δ*epmA* phenotype.

As EF-P is unfunctional in *E. coli* Δ*epmB* – irrespective of plasmid-encoded *epmA* or *epmA*_A298G addition to assist transfer of non-cognate substrates based on their substrate promiscuities – the question arises whether addition of different lysine analogs can lead to uptake, activation, transfer and finally functionality of EF-P *in vivo* (Figure 29 strategy 1, blue).

β-galactosidase activity was repeated with *E. coli* Δ*epmB* transformed with the PPP-*lacZ* plasmid and a plasmid containing *epmA*, *epmA*_A298G or none of these (framed blue in Figure 29B). This time, LB medium was supplemented with one of the 11 lysine derivatives in a concentration of 10 mM, if not otherwise mentioned. This concentration was chosen because K_m values depicted in Table 5 are in the low millimolar range and because it is much higher than the intracellular lysine derivative concentrations, which are e. g. 0.4 mM for (*S*)-α-lysine and 0.01 mM for (*S*)-α-ornithine [92]. Therefore, *E. coli* Δ*epmB* unable to produce (*R*)-β-lysine was used to check whether supplementation with lysine derivatives helps to overcome the Δ*epmB* phenotype by modifying EF-P with a non-cognate substrate *in vivo*.

Figure 29C shows the bar graphs for each of the possible substrates at natural EpmA production levels (plain bar) and - to provoke substrate promiscuity of EpmA - for subsequent overproduction of EpmA (dotted bar) and EpmA_A298G (squared bar), respectively.

Supplementation with (*R*)-β-lysine led to a 9 - 12 times higher β-galactosidase activity than in LB without additional substrate, on the one hand indicating the improvement of translation by successfully post-translationally modified EF-P, but on the other hand also indicating promiscuity of *E. coli* amino acid transport systems. From all other tested substrates, the enantiomer (*S*)-β-lysine was the only one which detectably improved EF-P compared to EF-P^{unmod}. Here it is assumed that the magnification factor of 1.2 - 1.4 could be enhanced by higher (*S*)-β-lysine concentration in the medium (> 0.25 mM).

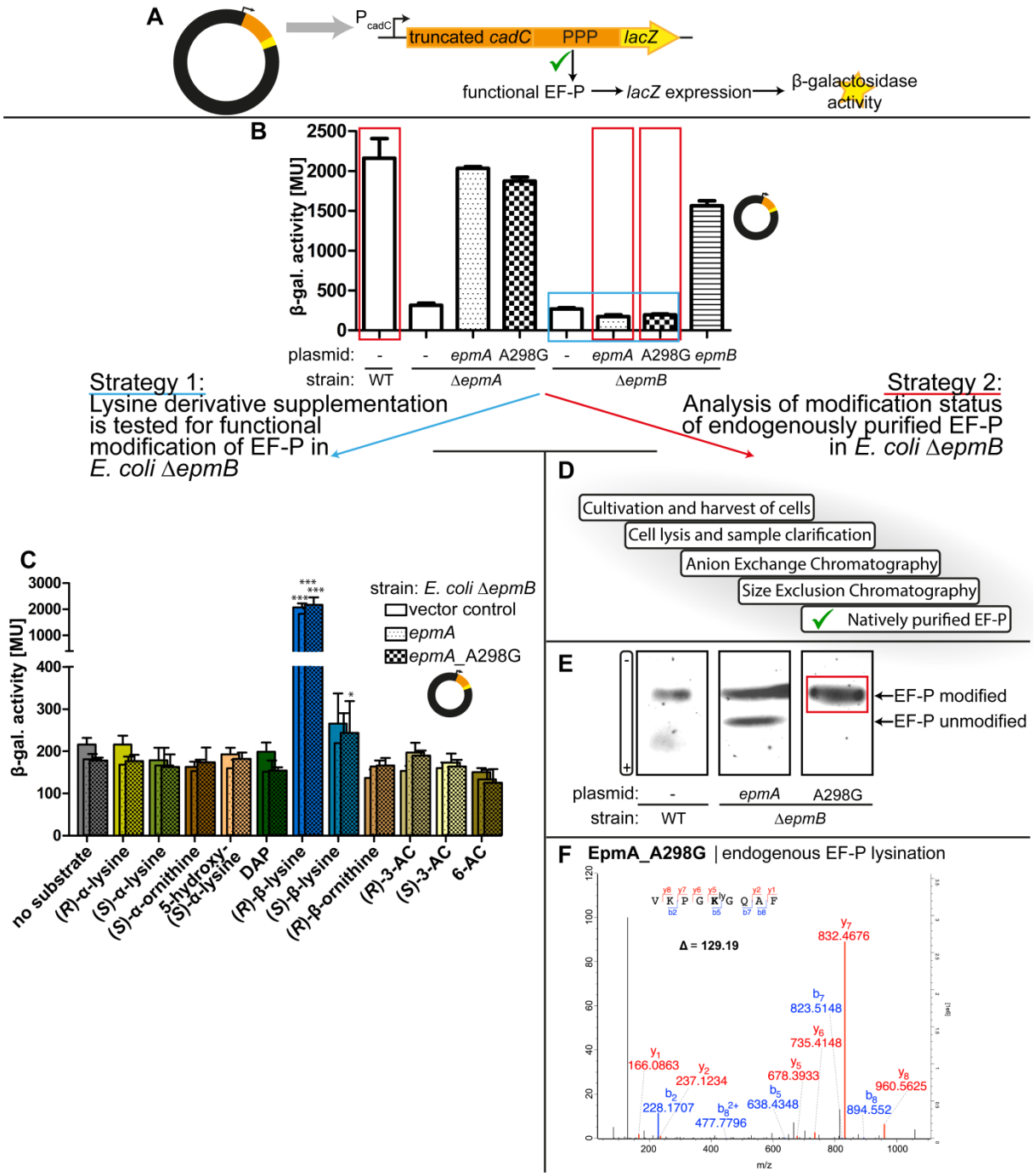

Figure 29: Translation of PPP-LacZ in *E. coli* BW25113 WT, Δ*epmA* and Δ*epmB*. (A) Schematic depiction of the EF-P-dependent *in vivo* reporter assay. A triproline translation motif (RPPP) requires functional EF-P for robust translation of truncated CadC linked to LacZ, whose translation was detected as β-galactosidase activity [16]. All strains mentioned in this figure were transformed with the described plasmid. (B) β-galactosidase activity in *E. coli* WT, Δ*epmA* and Δ*epmB*. Introduction of a second plasmid (-: empty vector) enables expression of either *epmA*, *epmA*_A298G or *epmB*. Complementation of the deletion phenotypes was successful, cross-complementation of Δ*epmB* phenotype was not. Here, overexpression of *epmA* or *epmA*_A298G was not sufficient to convert EF-P into the functional state. At least three independent samples were measured. Error bars indicate s.e.m.. (C) β-galactosidase activity in *E. coli* Δ*epmB* grown in LB medium supplemented with different lysine derivatives at a concentration of 10 mM. Irrespective of additional expression of *epmA* (dotted bars) or *epmA*_A298G (squared bars), EF-P modified with (*R*)-β-lysine *in vivo* exhibited superior efficiency of protein translation. The concentration of (*S*)-β-lysine was ~0.25 mM. (*R*)-3-AC was supplemented in a concentration of 1 mM due to growth defects at higher concentrations. At least five independent samples were

measured. Results of the two-tailed t-test are indicated as following ***: p < 0.001, *: p < 0.05. (D) Schematic depiction of purification strategy of endogenous EF-P. (E) Vertical IEF of natively purified EF-P from WT control and *E. coli* Δ*epmB* with subsequent overexpression of *epmA* and *epmA*_A298G. Two bands, corresponding to unmodified and modified EF-P, were found in *E. coli* Δ*epmB* overexpressing *epmA*. EF-P was even completely in the modified state when *epmA*_A298G was overexpressed. This indicates an attached but non-functional non-cognate PTM of EF-P *in vivo*. (F) MS spectra of the samples framed in red. (E) Fragmentation spectra of the EF-P peptide containing the critical K34 is shown to be modified with a lysine residue. The MS spectra were searched for all other tested modifications without positive result. This confirms that lysylation is indeed the endogenously occurring modification of EF-P in *E. coli* Δ*epmB* overproducing EpmA_A298G.

Despite the fact that K_m for (*R*)-β-lysine is magnitudes higher than for (*S*)-α-lysine regarding EpmA_A298G *in vitro*, β-galactosidase activity *in vivo* of the first-mentioned substrate was enhanced by a factor of 13 compared to (*S*)-α-lysine (Figure 29C). This fact indicates that in *E. coli* Δ*epmA* complemented with EpmA_A298G, EF-P is modified with (*R*)-β-lysine instead of the high affinity substrate (*S*)-α-lysine, even though intracellular concentration of (*R*)-β-lysine is likely to be low compared to (*S*)-α-lysine. When (*R*)-β-lysine pathway was deleted, EpmA_A298G attached its high affinity substrate (*S*)-α-lysine to EF-P. (*R*)-β-lysine supplementation of LB complex medium presumably leads to complete modification with (*R*)-β-lysine because otherwise Δ*epmA* phenotype could only be restored partially by complementation with EpmA_A298G.

As second strategy to elucidate unnatural EF-P modifications *in vivo*, endogenous EF-P from *E. coli* Δ*epmB* was natively purified and subjected to IEF and MS analysis (Figure 29D-F). The purification protocol for endogenous EF-P includes anion exchange chromatography and gel filtration to yield untagged, natively modified EF-P. By this rapid and convenient method EF-P from the WT control and *E. coli* Δ*epmB* transformed with an inducible plasmid for overexpression of EpmA or EpmA_A298G was isolated (Figure 29B, red frames). The three indicated samples were subjected to vertical IEF followed by Anti-EF-$P_{E.c.}$ Western Blotting to verify abundance of EF-P and to elucidate the modification status. Figure 29E nicely shows complete modification in the WT strain as positive control but interestingly also clear bands at the same height than the modified EF-P control band for both *E. coli* Δ*epmB* samples. This suggests a modification with additional positive charge compared to K34 like it is the case for a PTM with two amino groups. In addition, a band at the height of unmodified EF-P was visible when EpmA was overproduced. The samples were subjected to chymotrypsin digest and LC-MS/MS analysis and it was found that indeed, overproduction of EpmA_A298G in *E. coli* Δ*epmB* led to a modification at K34 at the loop of EF-P (peptide

PGKG, Figure 29F). This modification with the mass of 129.19 Da potentially originated from (*S*)-α-lysine. In the present study, the aim was to find unnatural EF-P modifications *in vivo*. As result the lysylation of EF-P was detected when EpmA_A298G was overproduced although *epmB* was deleted in *E. coli*.

3.4 Modification of EF-P in *B. subtilis* and other Firmicutes

3.4.1 Modification status of EF-P$_{B.s.}$ during different growth phases

In contrast to EpmA which establishes (*R*)-β-lysylation in a single step, the PTM of *B. subtilis* EF-P seems to be developed in a yet unsolved multi-step process. Here, a precursor is attached to EF-P at an early stage of the modification pathway that is then subject to ongoing development in the bound form. The complex pathway is postulated to include at least four different enzymes [36]. This may lead to a situation contrary to *E. coli*, where EpmA and EF-P were balanced in all growth phases to ensure full PTM. To elucidate the ratio of unmodified-to-modified EF-P at different growth phases, cells were collected at eight time points and lysed. Application of the same procedure as described for *E. coli* EF-P was unsuccessful because bands on the IEF gels were invisible or not pleasantly resolved (not shown). Therefore, an additional protein precipitation step with TCA/acetone was included and the IEF gel was rehydrated in presence of urea/thiourea to increase their solubility in general and to avoid aggregation of proteins at their pIs. Urea is a solubilizing agent that prevents hydrogen bonds and consequently, unwanted protein aggregation formation that affects mobility in a negative way and impedes sharp band resolution [109]. Additional thiourea ensured denaturation by cleavage of disulfide bridges. As some proteins require detergent solubilization, the zwitterionic detergent CHAPS (3-[(3-cholamidopropyl)dimethylammonio]-1-propanesulfonate) was used.

Figure 30 shows that during all growth phases of *B. subtilis*, two distinct EF-P bands are visible, one at the height of the control (EF-P^{unmod}) and one that is shifted towards the cathode of the gel, indicating an additional positively charged group. Proportion of EF-P^{mod} is predominant during all phases although it seems to decrease over time. Witzky *et al*. found that 5-aminopentanol, hydroxypentanone and pentanone are attached to K32 of EF-P in WT cells [36]. Out of these three compounds, only 5-aminopentanol exhibits the positively charged group detected by IEF analysis shown in Figure 30.

Consequently, the majority of EF-P is 5-aminopentanolated during all growth phases.

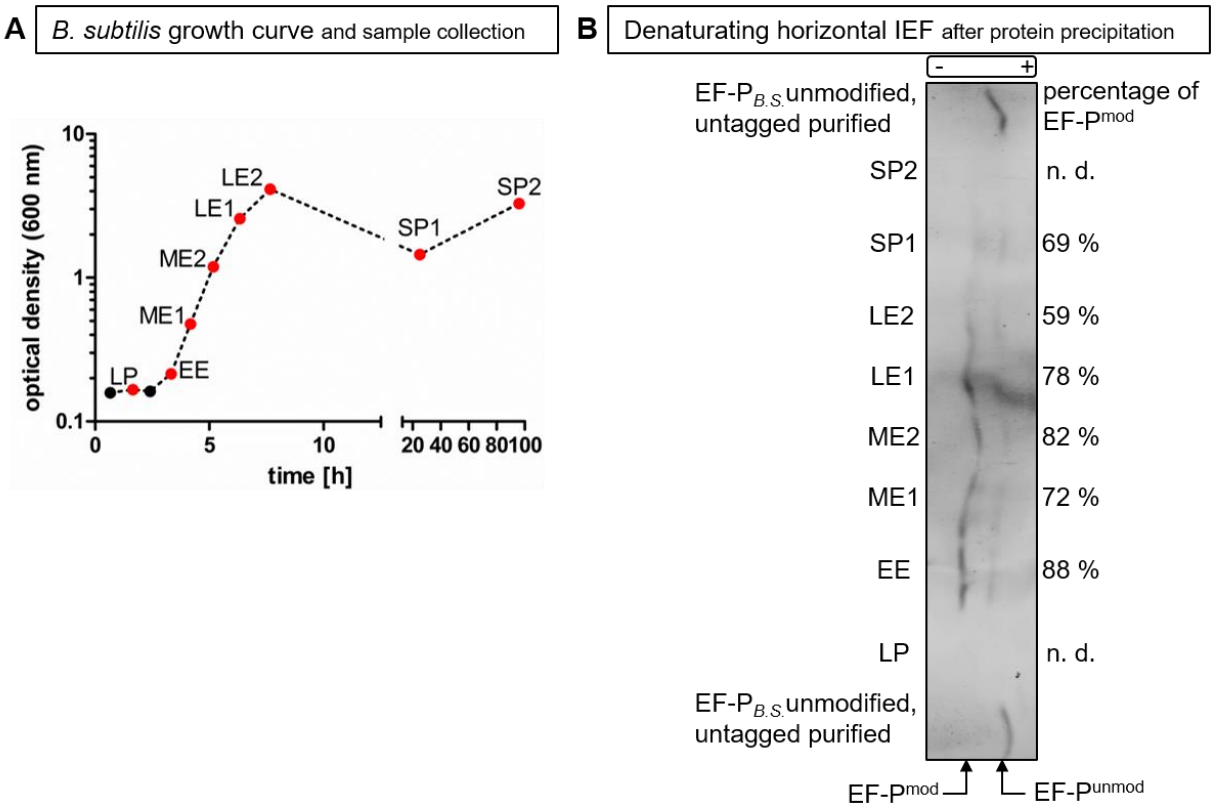

Figure 30: Denaturating horizontal IEF reveals modification status of *B. subtilis* EF-P during different growth phases. LP: lag phase, EE/ME/LE: early/middle/late exponential phase, SP: stationary phase. (A) Eight time points of the growth curve were chosen (highlighted in red) and cell lysates were subjected to protein precipitation. (B) Denaturating horizontal IEF (20 – 100 µg total protein per lane). Western Blot analysis using Anti-EF-P$_{B.s.}$ shows two EF-P variants (ratio indicated at the right) with distinct pI values corresponding to unmodified and modified EF-P. n. d.: ratio EF-P modified-to-unmodified not estimable.

3.4.2 Aminotransferases potentially involved in the post-translational modification of EF-P$_{B.s.}$

The PTM of *B. subtilis* EF-P develops in EF-P bound form to finally yield 5-aminopentanolated EF-P. It appears likely that one reaction step is catalyzed by an aminotransferase (transaminase) which donates the amino group. 13 described or postulated aminotransferases were chosen, and their corresponding deletion strains analyzed regarding behavior of their EF-Ps in a pH gradient by denaturating horizontal IEF. Results are shown in Figure 31 (bottom). Here, especially GsaB, EpsN and IlvK seem to be interesting candidates for further study because a band at the height of unmodified EF-P was found and WT band was absent.

It was reported that deletion of *efp* in *B. subtilis* leads to impaired swarming motility that is caused by a negative impact on flagellar biosynthesis [110]. Swarming is differentiated from swimming by participation of a surface and increased involvement

of flagella. Therefore, also swarming behavior of the 13 aminotransferase deletion strains was analyzed.

In Figure 31, the 13 aminotransferase deletion strains are shown to exhibit distinct swarming abilities. Here, especially *B. subtilis* Δ*yhdR*, Δ*dat* and Δ*yaaO* exhibit similar low swarming diameters compared to *B. subtilis* Δ*efp*.

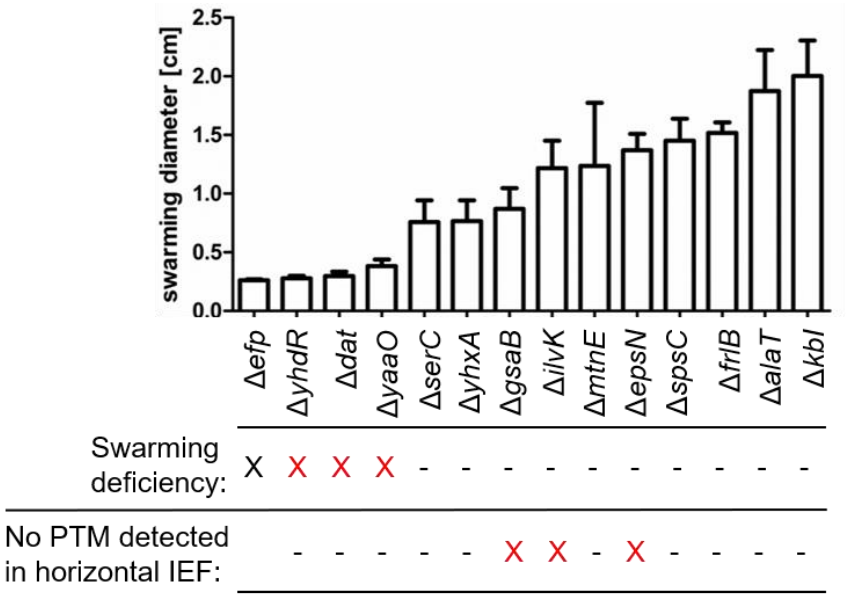

Figure 31: 13 aminotransferase deletion mutants are subjected to swarming assay and analyzed regarding their modification status. Swarming behavior of the aminotransferase mutants are compared to *B. subtilis* Δ*efp* to elucidate potential enzymes involved in EF-P PTM pathway. Red crosses highlight the aminotransferase mutants which exhibit a swarming deficiency, or which contain EF-P in the unmodified state.

Characterization of 13 aminotransferase deletion strains of *B. subtilis* regarding their EF-P modification status and their swarming phenotypes suggested three candidates each, potentially involved in PTM of EF-P. To resolve whether these effects are direct or indirect more research is required in the future.

4 Discussion

4.1 Unnatural post-translational modifications of EF-P

In this study it was shown that EF-P in *E. coli* Δ*epmB* is unfunctional but not necessarily unmodified. This contradicts the commonly accepted opinion, that deletion of *epmA* or *epmB* in *E. coli* leads to completely unmodified EF-P and that these cells phenocopy Δ*efp* strains. When endogenous EF-P was purified from a strain overproducing EpmA or EpmA_A298G, vertical IEF unexpectedly revealed a band at similar height to modified EF-P. Expression of the WT ligase led to similar amounts of unmodified and modified EF-P, whereby expression of *epmA*_A298G exhibited complete modification with a non-cognate EpmA substrate. MS revealed that EF-P was modified with a PTM of 129.19 Da at β3/β4 loop which corresponds to lysylation. β-lysine is neither known to be abundant in the (*S*)- (no pathway known) nor the (*R*)-configuration (known pathway deleted). With a concentration of 0.4 mM (*S*)-α-lysine is a highly abundant metabolite in the cell, whereas the nonproteinogenic amino acid (*R*)-α-lysine is not [92]. In addition, the catalytic pocket of EpmA_A298G is optimized for (*S*)-α-lysine. Therefore, it is concluded that (*S*)-α-lysine is the non-cognate PTM of EF-P in *E. coli* Δ*epmB* (Figure 32AC).

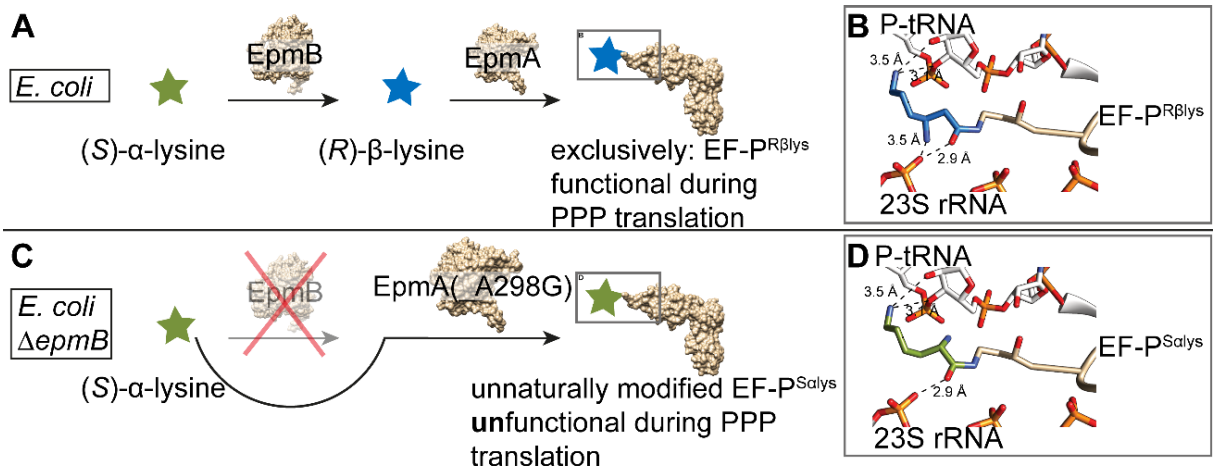

Figure 32: Endogenous modification of EF-P in *E. coli* (A, B) and *E. coli* Δ*epmB* (C, D). (A, C) Schematic pathway of post-translational modification with or without conversion of (*S*)-α-lysine by EpmB. (B, D) Structural insights into the translation of a polyproline motif. Interaction of modified EF-P with the CCA end of the P-site tRNA and 23S rRNA as determined by Cryo-EM [14]. If (*R*)-β-lysine is absent due to deletion of *epmB*, EF-P is nevertheless post-translationally modified by EpmA(_A298G). Then, (*S*)-α-lysine is attached. Fewer contacts with the ribosome are possible for EF-P$^{S\alpha lys}$, EF-P is unfunctional during polyproline translation.

Unnoticed by investigators, Peil *et al*. found 2 % modified EF-P (mass shift +128 Da) in *E. coli* Δ*epmB* [33]. In this thesis, 64 % modification at subsequent *epmA*

overexpression and complete modification of EF-P at *epmA*_A298G overexpression was detected. One might claim that deletion of *epmB* does not resemble an inherently occurring situation in *E. coli*. But Schmidt *et al*. could not detect EpmB in every cell of *E. coli*, grown in LB medium to stationary phase. 78 % (after 1 day) and 97 % (after 3 days) of cells exhibit no EpmB copy at all, indicating at least low abundance of the protein [1].

Cryo-EM structures of a ribosome stalled at a polyproline motif either with or without EF-$P_{E.c.}$ revealed lability of the P-site $tRNA^{Pro}$ in the latter case [14]. EF-P interacts with $tRNA^{Pro}$ via Y183 and with the 30S subunit via R186. Domain III of EF-P (G144, D145, T146) interacts with the mRNA and ribosomal protein S7. Moreover, (*R*)-β-lysylhydroxylysine enables additional interaction: First, the hydroxy group at C4 of K34 forms hydrogen bonds with the first cytosin of the CCA end of P-site $tRNA^{Pro}$. Second, the terminal amino group at C6 of the (*R*)-β-lysyl residue is in proximity to the phosphate backbone of CCA (Figure 32B). Third, both the carbonyl group at C1 and the amino group at C3 of (*R*)-β-lysine form hydrogen interactions with the ribosome (A2439). The last-mentioned interaction is missing in EF-$P^{Sαlys}$ (Figure 32D) and the modified EF-P is unfunctional in rescue of polyproline stalled ribosomes. This indicates the stabilizing effect on the CCA end of P-site $tRNA^{Pro}$ through various interactions of EF-$P^{Rβlys}$, which enables its optimal positioning for peptide bond formation between prolines [14].

The described mischarging of EF-P with (*S*)-α-lysine *in vivo*, mediated by EpmA(_A298G) and found in *E. coli* Δ*epmB* leads to modified but unfunctional EF-P. This does not seem to be advantageous at first sight, but recent research identified states in which reliance on functional EF-P is low and here, non-cognate modification may not be disadvantageous. Tollerson *et al.* reported recently, that Δ*epmA*, Δ*epmB* and Δ*efp* phenotypes (like slow growth, increased antibiotic sensitivity, loss of virulence [111–114]) are dependent on the growth state, indicating demand on functional EF-P especially in high growth rate conditions. Interestingly, reduction of temperature for *E. coli* growth leads to clear reduction of the Δ*efp* phenotype in many ways (polyproline translation, polysome ratios, antibiotics susceptibility). This matches the findings of Klee *et al.* who compared the growth behavior of plant pathogen *E. amylovora* WT and Δ*epmB* strain [113]. Remarkably, they found a growth defect only in LB rich medium (pH 7.0) whereas in minimal medium (M9, pH 7.0) both strains

grew comparably well [113]. Apparently, EF-P reliance is not only caused by abundance of XPPX motifs but also influenced or even regulated by external stimuli or conditions. Putatively, EF-P is modified with (*S*)-α-lysine in these informal EF-P states, meaning states where EF-P in the unfunctional form is tolerated, such as in slow growth states (e. g. 25 °C), when disadvantageous Shine-Dalgarno sequences are present or unfavorable start codons are chosen. In all these cases dependence on functional EF-P is low due to reduced protein translation need or low translation initiation rates that prevent ribosome queuing in general [112]. Therefore, the non-cognate EpmA mediated lysylation of EF-P potentially resembles EF-P status in growth phases of low EpmB copy number or in states where reliance on functional EF-P is negligible.

An interesting way of decreasing dependency on functional EF-P is reported in *E. amylovora*. In a recent study a suppression strategy of *efp*, *epmA* and *epmB* deletion phenotypes is proposed [90]. Here, colony size as well as virulence was restored in these deletion mutants by additional *hrpA3* deactivation or deletion [90]. HrpA3 is a DEAH family RNA helicase-like protein with predicted ATP-dependent RNA helicase function but its mode of action remains unclear. In *E. coli* HrpA3 is associated with the degradosome [115] so it can be speculated that *hrpA3* deletion leads to a delay in mRNA degradation at stalled ribosomes and thereby provides a larger time window for translation processes [90].

Consequently, the question was addressed which substrate EpmA_A298G prefers to transfer to EF-P *in vivo* when (*R*)-β-lysine and (*S*)-α-lysine are present (*E. coli* Δ*epmA*). The first mentioned substrate was supplemented to LB medium in a concentration of 10 mM, whereby the intracellular concentration of (*S*)-α-lysine was determined elsewhere to be 0.4 mM [92]. The phenotype of *E. coli* Δ*epmA* was complemented (87 % compared to WT) by overexpression of *epmA*_A298G when the translation level of PPP-LacZ was examined. As (*S*)-α-lysylated EF-P was shown to be unfunctional in rescue of polyproline stalled ribosomes, the phenotype is complemented by preference of (*R*)-β-lysine over the low K_m substrate of EpmA_A298G. Apparently, assurance of EF-P functionality is number one priority.The research shown in this thesis expands our understanding and sensitizes for the differentiation between deleted, unmodified, unnaturally modified and modified functional EF-P.

In line with expectations, EF-P is not functional in *E. coli* Δ*epmB* and therefore translation of PPP-LacZ was drastically reduced compared to WT. This finding is also not altered by overexpression of *epmA*(_A298G) to facilitate modification of EF-P in this (*R*)-β-lysine pathway deletion strain. Weakening of the deletion phenotype was tested by addition of 11 different lysine derivatives to the cultivation medium and only successful using the cognate EpmA substrate and its enantiomer (*S*)-β-lysine, whereas other (*R*)-β-lysine like compounds supplemented to the medium had no effect. Nevertheless, results show that lysine derivatives were successfully transported into the cell. It cannot be excluded that different uptake abilities affect intracellular lysine derivative concentrations and thereby indirectly manipulate EF-P modification efficiency. Two lysine transport systems are characterized in *E. coli*: the lysine-arginine-ornithine (LAO) system [HisQ][HisP]$_2$[HisM][ArgT] and the lysine-specific permease (LysP) [116]. As *E. coli* amino acid transport is proven for α-lysine and ornithine and indicated for (*R*)-β-lysine, it is likely that the other tested substances were also transported. This assumption was also corroborated by similar growth behaviors (not shown). (*R*)-3-AC provided a notable exception because a reduction of the LB supplementation from 10 mM to 1 mM was necessary to enable growth. As concentration-dependent inhibition of EpmA(_A298G) was induced by (*R*)-3-AC *in vitro* it might be possible that this compound also inhibited other enzymes of *E. coli* leading to this severe growth defect at concentrations higher than 2 mM.

Having documented that EpmA unnaturally post-translationally modifies EF-P with (*S*)-α-lysine and - when added to the medium - also with (*S*)-β-lysine *in vivo*, further substrates were found that were attached to EF-P *in vitro*. EpmA forms the adenylate of its cognate substrate (*R*)-β-lysine and of five non-cognate substrates but excludes *in vitro* activation of four other tested lysine derivatives. This shows that not all chemical groups of (*R*)-β-lysine are equally important for recognition, binding and activation by EpmA. Only lysine derivatives with 6-atom carbon chains were activated by EpmA (no activation of ornithines), whereby the ε-terminus was tolerated to be free of chemical groups ((*R*)-3-AC) or to exhibit an amino group, but not to be bulky (DAP). Moreover, an amino group is required either at ε- (6-AC), β- ((*R*)-β-lysine, (*R*)-3-AC) or α- ((*R*/*S*)-α-lysine, 5-hydroxy-(*S*)-α-lysine) position which enables interaction with amino acid residues of the catalytic pocket of EpmA.

Beside these configurational requirements, stereochemical demands were elucidated by the fact that K_m value increases drastically by a factor of ~40 when (*S*)-β-lysine is compared to (*R*)-β-lysine as substrate. Even more severe, EpmA selectively activated (*R*)- but not (*S*)-3-AC. The biochemical characterization of EpmA revealed the negative effect of an additional hydroxy group, nevertheless, 5-hydroxy-(*S*)-α-lysine was also activated by EpmA.

Backmutation of EpmA's catalytic pocket to resemble its evolutionary origin LysRS deepened the understanding of the interplay between amino acid residues of the catalytic pocket and the donor substrate ligand. The anticipated preference for (*S*)-α-lysine was achieved, moreover EpmA_A298G explicitly preferred substrates with α-amino groups ((*R*/*S*)-α-lysine, (*S*)-α-ornithine, 5-hydroxy-(*S*)-α-lysine) which manifested in lower K_m values towards all these substrates compared to WT EpmA. EpmA_A298G requires an α- or β-amino group at its substrate. 6-AC, which exhibits just an ε-amino group, was not activated by the variant. Also here, hydroxylation of the substrate was detrimental which is shown by increase of the K_m value by a factor of 100 when comparing (*S*)-α-lysine with its 5-hydroxylated version. The K_m value towards (*S*)-α-lysine decreased by a factor of 80 compared to EpmA. At the same time and in line with expectations the K_m towards (*R*)-β-lysine increased by a factor of 60. This is a finding that contradicts Roy *et al*. who found similar K_m values towards (*R*)-β-lysine for both enzyme variants [32]. Notably, this study provides a much more detailed and completive substrate spectrum analysis than found in [32] and demonstrates EpmA(_A298G)'s pronounced donor substrate promiscuity.

The hypothesis that enzyme promiscuity especially allows for innovative enzyme functions is supported by ancestral sequence reconstructions that find ancestral enzyme forms to exhibit broader substrate specificities [117]. Beside considering a promiscuous enzymatic activity as starting point for the evolution of a new enzyme it can also be employed by protein engineers and synthetic biologists. Urgent problems of our time are tackled like bio-based instead of petroleum-based manufacturing (e. g. vanillin production [118]) or degradation of anthropogenic pollutants [119]. Enzyme promiscuity is also used in chemical industry, naming just one example from BASF, where *Burkholderia plantarii* lipase is used to produce enantiopure (*R*)-phenylethylamine, a platform chemical for production of pharmaceuticals and pesticides [120]. Here, individual industrial applications or even the creation of novel

metabolic pathways are conceived on the base of promiscuous enzymes which are optimized during directed evolution approaches [52]. High-throughput approaches identified promiscuous enzymes that stood in for essential proteins or gave rise to resistance against antibiotics or toxins [52]. Therefore, it becomes clear why Copley *et al.* designated promiscuity as the fuel of evolutionary innovation [52]. Not least it forms the basis of EF-P modification with non-cognate substrates demonstrated in this thesis.

All amino acid derivatives which were activated by EpmA were also transferred to EF-P which implies that the first substep is the bottleneck of the reaction and determines the expanse of promiscuity. It is also clarified that pre-transfer editing is observed, and post-transfer editing is absent. (*S*)-3-AC, DAP and (*R*)-β-ornithine were not activated by EpmA *in vitro* to form the adenylate and also not attached to EF-P *in vitro*. In contrast, the artificial modification of EF-P was successfully performed by EpmA(_A298G) *in vitro* to create EF-$P_{E.c.}$ modified with (*S*)-β-lysine, (*R*/*S*)-α-lysine, (*S*)-α-ornithine, 5-hydroxy-(*S*)-α-lysine, (*R*)-3-AC or 6-AC (Figure 33A). It must be noted that modification of EF-P was incomplete (EF-P^{unmod} present) in the case of 5-hydroxy-(*S*)-α-lysine attached by EpmA as well as (*R*)-α-lysine and (*S*)-α-ornithine attached by EpmA_A298G. As K_m values for these combinations are high, incubation with higher concentrations of the non-cognate substrate potentially leads to complete modification.

In conclusion, the variety of known natural PTMs of EF-P (and its homologs a/eIF5A) which all elongate the tip between β-strands 3 and 4 by addition of (*R*)-β-lysine, rhamnose, 5-aminopentanol or by formation of hypusine (eukaryotes, archaea) was expanded by seven synthetic PTMs using EpmA(_A298G). Nevertheless, these EF-Ps were shown to be unfunctional in the rescue of polyproline stalled ribosomes *in vitro*. It was made use of the commercially available kit for cell-free synthetic biology (CFSB), the PURE system. Apparently, the elongated tip of EF-P at K34 does not exhibit the correct orientation or charge condition to enable optimal interplay with the PTC of the ribosome. Instead, modification of EF-P by (*R*)-β-lysine *in vivo* or *in vitro* is superior to all synthetically modified variants of EF-P which explains its evolutionary selection.

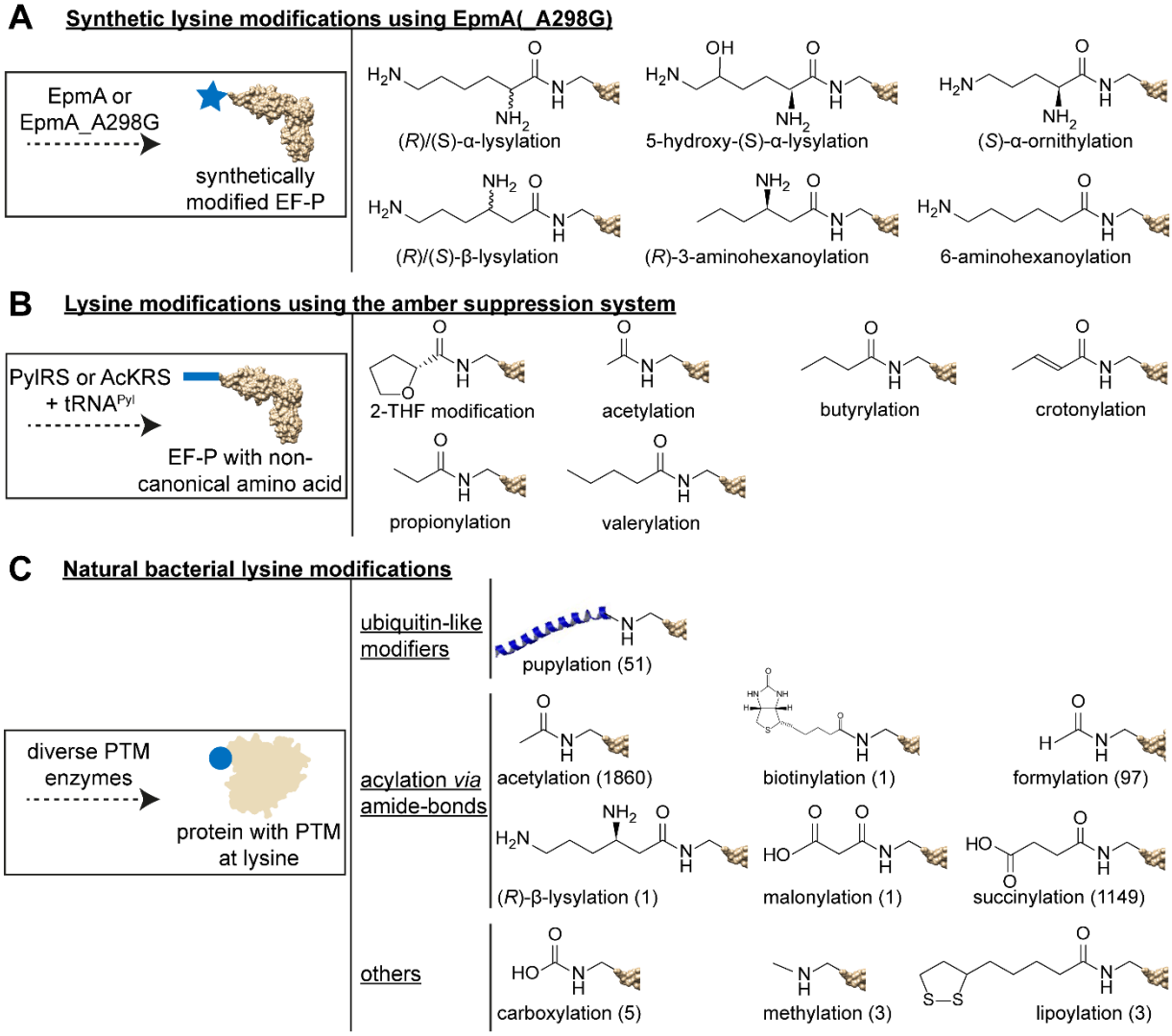

Figure 33: Overview of natural and synthetic lysine modifications. (A) Synthetic post-translational modifications of EF-P. The indicated lysine derivatives were activated and transferred by EpmA or EpmA_A298G. (B) Lysine modifications successfully introduced using the amber suppression system. Results are partially derived from [121]. (C) Lysine PTMs in *E. coli* according to PLMD database. The ε-terminal lysine modifiers are grouped and schematically depicted. The number behind the modification corresponds to the number of proteins modified by that compound in *E. coli*. The figure is derived from [122].

Interestingly, EF-P modified with enantiomer (*S*)-β-lysine exhibits different behavior *in vitro* and *in vivo*. Using the PURE system, no stimulating effect on PPP-Nluc translation was observed. In contrast, addition of (*S*)-β-lysine to *E. coli* Δ*epmB* growing in LB medium led to significantly increased translation of PPP-LacZ compared to unsupplemented medium. Thereby, (*S*)-β-lysine is either the only non-cognate substrate in this study leading to functional EF-P when attached to K34 or a yet unknown enzyme partially converts (*S*)-β-lysine into (*R*)-β-lysine in *E. coli*. The compound naturally occurs in the (*S*)-α-lysine degradation via acetate pathway which is catalyzed by L-lysine 2,3-aminomutase KamA (PDB: 2A5H [123]) in organisms like

Clostridium subterminale or *B. subtilis* [124, 125]. While KamA and EpmB share the same substrate and both produce one specific enantiomer of β-lysine, the two enzymes vastly differ in activity. The turnover number of *E. coli* EpmB is 5.0 min^{-1} which indicates its low activity and leads to the conclusion that (*R*)-β-lysine is produced in small amounts [42]. Apparently, low intracellular concentration of this specialized molecule is enough to be accepted by the cytosolic protein EpmA and to maintain adequate EF-P modification. In contrast to that, KamA takes over an important role in lysine metabolism, explaining its high activity.

EF-P was shown not to be modified with (*S*)-glutamine and (*S*)-arginine by EpmA(_A298G) *in vitro*, although it is reported that $tRNA^{Lys}$ is mischarged by LysRS with non-cognate amino acids including arginine [54]. The biochemical characterization revealed that bulky terminal groups impede activation (like it is the case in DAP and (*S*)-arginine) and carbon chain shortening (like in ornithine and (*S*)-glutamine) compared to lysine is not tolerated, so exclusion of the two amino acids is explainable.

Compounds like this need to be tackled with a different strategy, namely the amber suppression system utilizing PylRS and its variant AcKRS (Figure 33B). It is used for bulky residues and here, different carbon chain lengths are tolerated. Therefore, the amber suppression strategy complements the described use of the inherent substrate promiscuity of EpmA to synthetically modify EF-P *in vitro* (Figure 33A). This reported strategy is suitable for close (*R*)-β-lysine analogs. Synergy of both approaches not only yields a pool of unnatural lysine modifications on EF-P to study polyproline formation mechanism but also creates diverse potential applications for incorporation of noncanonic amino acids, β-amino acids and derivatizable groups into peptides.

The amber suppression system manipulates protein structure and function by site-specific incorporation of noncanonic amino acids. Derivatization of lysine at the ε-terminal amino group is used to alter physical, chemical, or biological properties of the peptide and to enable incorporation of photocrosslinkers, fluorescent probes, spin labels, redox active groups, heavy atoms, and reactive groups [126]. To do so, an orthogonal aaRS/tRNA pair is used which does not interfere with the biosynthetic machinery of the host cell but recognizes the little used stop codon UAG (amber). PylRS, originating from *Methanosarcina mazei*, is an example of an aaRS showing untypically high substrate promiscuity. The PylRS/$tRNA^{Pyl}$ set utilizes lysine derivatives which exhibit an ε-terminal carbonyl group and a hydrophobic, bulky moiety [126].

Volkwein could show that this amber suppression system is suitable to introduce 2-THF-, butyryl-, crotonyl-, propionyl-, and valeryllysine instead of K34 of EF-$P_{E.\ c.}$ when mutating the respective site to TAG [121]. Therefore, the tip of EF-P is successfully elongated in a PTM-independent, single translation step. Nevertheless, all these synthetic variants were unfunctional at polyproline stalled ribosomes. Also, (*R*)-β-lysyllysine was not accepted as substrate by PylRS and therefore not incorporated into the nascent peptide chain so only a truncated variant of EF-P was observed. Promiscuity of PylRS together with its low selectivity towards the $tRNA^{Pyl}$ anticodon offers the opportunity to easily engineer PylRS for applications in synthetic biology approaches [127]. Change of substrate specificity of PylRS towards (*R*)-β-lysyllysine and its close analogs is conceivable but intercepted by the new approach to use EpmA for synthetic EF-P modification.

In this thesis, a variant of PylRS, acetyllysyl-tRNA-synthetase (AcKRS), enables incorporation of acetyllysine into proteins using the amber suppression system [66]. Lysine acetylation of proteins is a common and reversible PTM in eukaryotes and bacteria. Eukaryotic cells acetylate lysine residues enzymatically by lysine acetyltransferases (KATs) and lysine deacetylases (KDACs) or non-enzymatically with acetyl-CoA representing the acetyl donor [108]. The PTM specific antibody recognizing acetylated lysine enabled immunoprecipitation and in combination with high-resolution mass spectrometry-based proteomics identified 2,000 human proteins being acetylated at lysines and involved in all kinds of cellular processes, also in cancer progression. Several KATs, KDACs and acetyllysine recognizing proteins (bromodomain-containing proteins) are associated with cancer development and are targets of small molecules to provide potential cancer therapies [108]. In bacteria, most of the lysine acetylations are implemented non-enzymatically and mediated by acetyl phosphate. Therefore, this interesting lysine derivative was included into the study. For production of acetylated EF-P *in vitro*, Nε-acetyl-L-lysine was incorporate at amber codon position (TAG), which replaced the AAA codon coding for K34. The deacetylation reaction catalyzed by CobB was inhibited by addition of nicotinamide. Also this synthetically modified EF-P was found to be unfunctional in stimulation of PPP-Nluc translation.

Independent of the strategy used – post-translational modification with EpmA or amber suppression – both aim for EF-P tip elongation and subsequently, a better

understanding of the structural mechanism of polyproline motif translation. Despite profitable structural insight by Cryo-EM structures, the detailed mechanism of peptide bond formation and the critical role of the distinct PTMs remain elusive. Deeper understanding of differently shaped PTMs fulfilling the same function at the ribosome is only possible by synthetic alteration of the conserved central residue of β3/β4 loop in EF-P. For example, (*R*)-β-lysylation, 5-aminopentanolation and hypusination have in common that the conserved lysine in β3/β4 loop is elongated by 4-6 carbon atoms, ending up in a terminal amino group in all cases. In contrast to that, the central moieties of the β3/β4 loop shown in Figure 33B do not contain a positively charged, terminal amino group. This underlines its critical role in stabilizing the P-site tRNA by interacting with the phosphate backbone of its CCA end.

Due to the described preference of PylRS for bulky lysine derivatives, the PTM-independent introduction of rhamnose via amber suppression should be tested in the future. This is especially interesting, as cross-complementation of EF-P$_{E.c.}$ with rhamnose, when an arginine residue at position 34 and EarP as modification enzyme are present, was published recently [38]. Here, it was reported that proline at the -2 position compared to the conserved residue is favorable for lysylation and obstructive for rhamnosylation. Additional variation of the -2 proline to serine enabled EF-P functionality at the ribosome (at least when modified by EarP of *S. oneidensis*) leading to the conclusion that composition of the seven amino acids long β3/β4 loop of EF-P has direct influence on accessibility of the PTM enzyme as well as performance at the ribosome when stalling motifs are encountered. Further studies should take this into account no matter which approach is focused on, PTM-independent amber suppression or PTM-dependent modification via PTM enzymes. By that, further post-translational modifications of lysine become accessible. Lysine is designated as hotspot for enzymatic and chemical PTMs. It is the most frequently modified amino acid and also the one with the widest range of different modifications [128].

Lysine, arginine and histidine are the three basic amino acids encoded by the genetic code. Their positively charged groups at physiological pH positions these amino acids more frequently at the surface of proteins which makes the reactive group accessible for PTM [128]. The manifold PTMs of lysine are summarized in the ‘protein lysine modification database’ PLMD [129]. For example, EpmA is acetylated at K166, EpmC is acetylated at K28, EF-P is modified at five lysine residues with succinyl, acetyl or

hydroxyl groups. Among the 20 different lysine modifications are ubiquitin-like modifiers, the big group of acylations which result in amide-bound derivatives and others. For *E. coli*, the occuring lysine modifications and their abundance are summarized in Figure 33C.

4.2 New insights into post-translational modification of EF-P in *E. coli*

In this thesis, EF-P copy number was determined to be 7,360 per cell at stationary phase of an ON culture which agrees with previous research performed by Schmidt *et al*. who found 8,323 EF-Ps/cell [1]. Several growth conditions of *E. coli* were shown to exhibit higher copy numbers, naming just the exceptionally high value of ~35,000 EF-Ps/cell in LB medium after 5 h of growth. This value is explainable by generally 90 % higher protein biosynthesis rates during late exponential phase than during stationary phase [130].

Even more interesting than the exact copy number is the ratio of EF-P-to-EpmA and its impact on the degree of PTM. As expected, EF-P was completely in the unmodified state in *E. coli* Δ*epmA* and in the modified state when *efp*, *epmA* and *epmB* were overexpressed in parallel. Further variation of EF-P and EpmA copy numbers revealed that doubling of *efp* by introduction of a second chromosomal copy led to 50 % (*R*)-β-lysylation of EF-P at endogenous EpmA levels, the rest remained unmodified. This important finding leads to two conclusions. On the one hand, excess of EpmA is avoided and it can be speculated that EpmA's copy number is capped due to promiscuity of this enzyme and thereby prevents (*S*)-α-lysine modification of EF-P *in vivo* because this variant is unfunctional in polyproline rescue. On the other hand, the finding of 50 % PTM status suggests that translation of EpmA is not governed by EF-P-mediated regulation. Instead, *epmA* and *efp* seem to be globally regulated. This is indicated by stable copy number ratios in *E. coli* at different growth conditions. Here, ~550 EF-Ps per EpmA were measured at 21 conditions, whereby one outlier value pertains to slow growth conditions (chemostat, μ = 0.12) [1]. The stable copy number ratio between EF-P and EpmA becomes even more visible when the same 22 growth conditions are applied and EF-P-to-EpmB ratios are analyzed. Values vary between 338 and 277,875.

Now, numbers are added to the proposal established by Navarre *et al*. who suggested that low levels of *epmA* expression are satisfactory for high levels of function [111].

The stable correlation of EF-P and EpmA is also expressed by the exhaustive PTM state of EF-P *in vivo* throughout all growth phases.

Unbalancing these EpmA-to-EF-P levels could potentially affect pathogenicity, as it is known that PTMs play a role in fundamental metabolic reactions. Many cellular signaling states which are relevant for diseases are associated with higher modification status ratio [131]. Therefore, EpmA serves as potential target for intervention and piloting to alter the ratio of modification in clinically relevant strains. *In vivo*, the coordinated interplay between EpmA, EpmB and EpmC is necessary for functionality of EF-P and thereby indirectly for relief of polyproline stalled ribosomes and unimpaired protein synthesis. Two examples show that fast protein synthesis as response to changing environments is a requirement for the successful host invasion of pathogenic bacteria [9]. Therefore, EF-P exhibits relevance in possible future medical applications. The pathogen *E. coli* O157:H7 was shown to strongly rely on EF-P since this *E. coli* strain exhibits the highest number of PPX motifs. The zoonotic, facultative intracellular pathogen *S. enterica* was shown to be hypersusceptible to a variety of growth inhibitors (antibiotics, detergents, heavy metals) and exhibited attenuated virulence in mice due to changes in expression of pathogenicity island SPI-I proteins upon lack of functional EF-P [44, 46, 111].

Unintendedly, the role of hydroxylation at the C4 atom of K34, catalyzed by EpmC, is further elucidated in this study. Chapter 3.2.1 shows that deletion of *epmC* led to unhydroxylated EF-P, as expected, but interestingly also 45 % of EF-P was in the unmodified state. Analysis of endogenous, immune-precipitated EF-P was reported to be 1.3 % modified but unhydroxylated (+129 Da), whereby the vast majority of EF-P exhibited the complete PTM (+144 Da) [33]. As hydroxylation as last step of the PTM pathway of EF-P is negligible for function [16, 20, 132] the stabilizing hydrogen bond interaction with the P-tRNA postulated by Peil *et al*. seems to be absent or of minor importance [14, 33]. Instead it can be speculated about a potential protective function of the hydroxyl group for the PTM as absence of the hydroxylation may facilitate cleavage of the lysylation of K34.

Sir2-like deacetylase CobB was shown to unspecifically cleave amide bonds which link the lysine residue of a peptide to its PTM such as propionylation, succinylation, crotonylation, acetylation or modification with one of the 20 amino acids [129, 133, 134]. Therefore, CobB was recently designated as general amidase in *E. coli* which

could be used to release unknown amide-bound lysine modifiers [134]. Wei *et al*. also demonstrated that neither the N-terminal amine-derived amide bonds nor peptide bonds within the protein backbone were altered [129, 134]. Therefore, it is possible that hydroxylation of K34 protects the PTM against promiscuous deacetylase CobB, but more research is necessary to verify the role of EpmC.

4.3 Promiscuity of EpmA unlocks the enzyme's potential

In this study, EpmA was shown to activate non-natural α-, β-amino acids and lysine derivatives. Together with the knowledge on EpmA_A298G it can be made use of the intrinsic features and advantages of EpmA, EpmA_A298G and LysRS. The first is optimized for a β-amino acid, the second exhibits a similar catalytic pocket and favoured substrate than LysRS and the third serves for tRNA charging and therefore catalyzes the precursor step for incorporation of amino acids into peptides (Figure 34).

During transition from the RNA world to establishment of the genetic code in the protein world, early aaRSs had to adapt specificity for their amino acids by shaping the binding pocket and reinforcing it with polar and nonpolar interaction partners [135]. Beside the canonical function of aaRS other novel and critical functions are described that illustrate evolutionary plurality and variability of aaRSs. Broad genome sequencing efforts revealed "footprints of aminoacyl-tRNA synthetases are everywhere", so many enzymes include domains of aaRS which catalyze various reactions [136].

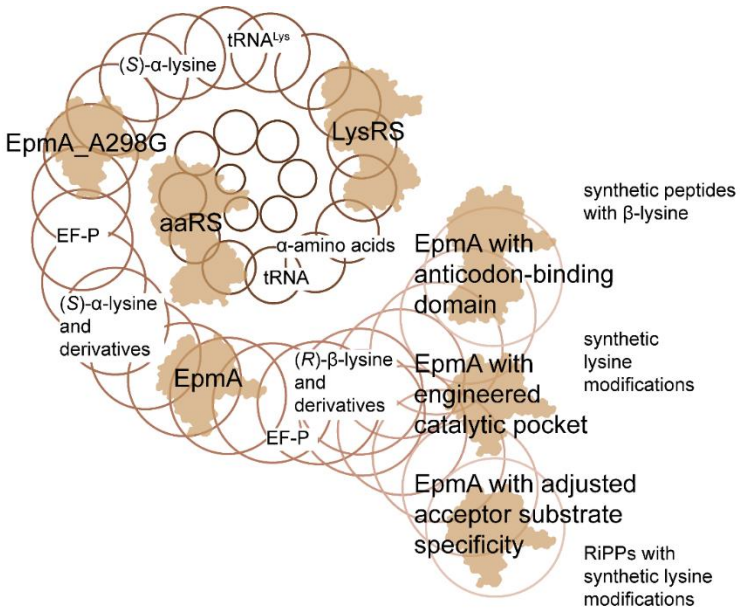

Figure 34: Progression from aminoacyl-tRNA synthetase to EpmA with possible further developments. Although optimized for their cellular function (substrates shown in small font), a certain degree of substrate promiscuity is preserved during progression from aaRS to EpmA. Engineering of EpmA can lead to several future applications.

Among them are several examples of tRNA-binding domain truncated proteins [137–139]. Ofir-Birin *et al.* described a transcriptional instead of translational role of LysRS in the human allergic response, represented by immune-stimulated mast cells [140]. Although aaRS act as potent protectors of the genetic code due to acceptor substrate specificity and editing ability He *et al*. demonstrated the ability of aaRSs to post-translationally modify a lysine residue with amino acids [129, 141]. They modified the ε-terminal amino group of lysine within a peptide with all 20 amino acids *in vitro*, whereby each reaction was catalyzed by its corresponding aaRS. The addition of cognate tRNA was only necessary for attachment of arginine, glutamine or glutamic acid to lysine [129]. This demonstrates that aaRSs can deal with variable acceptor substrates, for example LysRS accepts a synthetic peptide instead of $tRNA^{Lys}$.

The evolution of EpmA can be backtracked to LysRS due to their homology. Conserved among these proteins are active site residues of the catalytic pocket, either involved in lysine or ATP recognition and binding [51]. Differences are lack of the aminoterminal anticodon binding domain and a replaced region of five amino acids following motif I [51]. An interesting approach that should be considered in the future traces back evolution to the point where the anticodon binding domain of LysRS was lost. Addition of this aminoterminal domain to EpmA could restore the capability of aminoacylating $tRNA^{Lys}$ (Figure 34). Even more striking it could be charged with (*R*)-β-lysine. Actual research in synthetic biology lays a strong focus on introduction of β-amino acids into a nascent protein chain. Here, the advantageous qualities of LysRS and EpmA can be combined to ultimately provide a versatile enzyme which unfolds its specificity for a β-amino acid during the process of protein translation.

Variation of EpmA's catalytic pocket, in particular at the amino acid residue 298, had direct and comprehensible effect on donor substrate specificity. Backmutation of this residue to match the catalytic pocket of LysRS (G298) resulted in a clear preference for α-amino acids. In the future, further engineering of EpmA's catalytic pocket optimizes substrate specificity toward other linear compounds with amino group. By formation of the aminoadenylate their reactivity is increased and chemical bond formation with the desired acceptor substrate is facilitated.

It is demonstrated in this thesis, that EpmA is specific towards its acceptor substrate EF-P. The exchange of the central amino acid at the tip of the β3/β4 loop by arginine resulted in unmodified EF-P, even when *epmA* was overexpressed to support

substrate promiscuity. In this way, EpmA is shown to distinguish between K34 as cognate PTM position and another lysine residue at -3 position. Nevertheless, EpmA was shown to enlarge the spectrum of modification and introduces PTMs to side chains leaving the peptide terminus (site-selectivity) and other residues (chemoselectivity) unaltered. By that it has the potential to serve as a tool for synthetic biology demands. Further studies should focus on testing, adapting and applying EpmA to catalyze lysine modification of several relevant proteins or synthetic peptides instead of just EF-P as acceptor. By that the scope of application of EpmA broadens drastically. The derivatization of lysine in synthetic peptides is an actual task of synthetic biology because PTMs transform the folding and functional properties of proteins and unlock important regulation abilities. From the chemist's point of view this is a challenge because the N-terminus and cysteine residues are more reactive due to their lower pK_a values and nucleophilicities, respectively [142]. Commercially accessible peptides containing post-translationally modified lysine are only available with acetyl, malonyl, succinyl and methyl as modification (e. g. from JPT). EpmA can help to expand this spectrum and enable synthetic lysine modifications, for example in the so-called RiPPs (Ribosomally synthesized and post-translationally modified peptides). Especially the diversification of antimicrobial peptides can have wide therapeutic applications in the future [143]. Moreover, antibody-drug conjugates are often linked via lysine modifiers [144]. Exemplary applications are the lysine labeling of peptide hormone insulin and the eukaryotic peptide hormone analog octreotide with a fluorescent moiety or drug which was made possible by specifically modifying lysine with N-phenylvinylsulfonamide derivatives [142]. Octreotide is a somatostatin analog that has been intensively used for conjugation with toxic drugs for targeted delivery into somatostatin receptor-selective cancer cells [142]. Lysine of insulin chain B is modified with a fatty acid (myristic acid or a C_{16}-fatty acid) in the FDA approved drugs named detemir and degludec, respectively [142].

Taken together, the promiscuity of EpmA unlocks its potential. It should be subject for engineering and directed evolution approaches to meet customized characteristics. Thereby, engineered EpmA variants can yield an enzyme capable of incorporation of β-amino acids, activation of non-natural amino acids, and modification of synthesized peptides.

4.4 Modification of EF-P in *Bacillus*

This thesis shows that while EF-P was in the fully modified state during all growth phases of *E. coli*, EF-$P_{B.s.}$ separated in a denaturating horizontal IEF gel in unmodified and modified versions. Here, 59 – 88 % of EF-P was in the modified state. It can be speculated that the unresolved modification pathway in *B. subtilis* and other Firmicutes is not as efficient or not as fast as the EpmABC pathway, which is also indicated by the complexity of the unknown pathway that is postulated to include at least four different enzymes [36].

In this study different (predicted) aminotransferases were found to be potentially involved in the modification pathway. EF-Ps of *B. subtilis* Δ*ilvK*, Δ*epsN* and Δ*gsaB* exhibited the same pI value than unmodified EF-P did. The latter strain was also examined by Witzky *et al*. with the same result [36]. Three of the 13 tested aminotransferase deletion strains exhibited reduced swarming motility, indicating an impaired EF-P modification pathway. Among them are *B. subtilis* Δ*yhdR*, Δ*dat* and Δ*yaaO*. In the same way, swarming motility of *B. subtilis* Δ*efp* is reported to be negatively affected compared to WT because diproline motifs - which are accumulated in flagellar genes - require functional EF-P for proper translation [34, 145]. Consequently, flagellar number is decreased in *B. subtilis* Δ*efp* [110]. In addition, *B. subtilis* Δ*ymfI* is unable to swarm due to the intermediate modification status of EF-P and accumulation of aminopentanone-modified EF-P [36]. Together with the results obtained by Witzky *et al.* [36], the hypothetical pathway, potential modification enzymes as well as influencing genes shown in Figure 35 can be derived.

YmfI is reported to be the enzyme which catalyzes the final PTM step that is reduction of 5-aminopentanone to 5-aminopentanol [146]. Witzky *et al.* created a transposon mutagenized library of *B. subtilis* lacking the *ymfI* gene [36]. Interestingly, some genes they found to be transposon insertion suppressors of *ymfI* and therefore were able to swarm, were also found in this study by IEF analysis beforehand. *B. subtilis* Δ*yaaO* showed contradicting phenotypes in the two studies regarding swarming behavior and IEF band position. Witzky *et al*. suggested an indirect role of YaaO due to the fact that 5-aminopentanolated EF-P is still found in this strain, admittedly in lower yield.

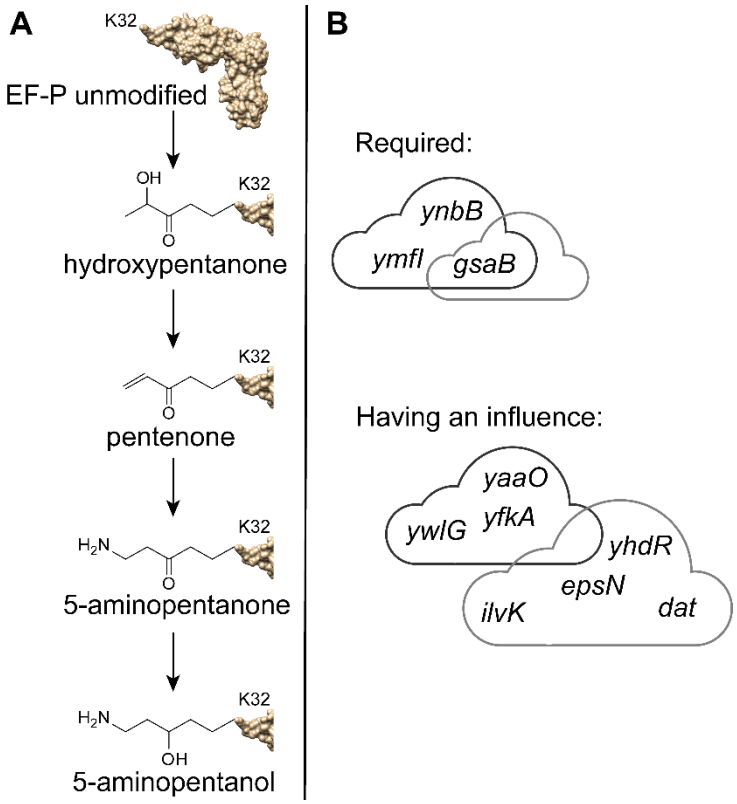

Figure 35: Post-translational modification of EF-P from *B. subtilis*. (A) Hypothetical pathway provided by Witzky *et al.* [36]. (B) Required genes for complete PTM found by Witzky *et al.* [36] (dark cloud) and in this study (light cloud). In addition, candidates with direct or indirect influence are listed.

It was beyond the scope of this thesis to elucidate enzymes involved in the modification pathway of EF-P in *Bacillus* in detail. Nevertheless, candidates are presented that establish the basis for further studies. Those are added to *ynbB*, *gsaB* and *ymfI* which are believed to be involved in this pathway, as deletion of each of the genes abolished 5-aminopentanolation of EF-P [36]. Moreover, it is likely that *B. subtilis hydR*, *dat* and *yaaO* are either directly involved in PTM of EF-P and thereby phenocopy *B. subtilis* Δ*efp*, or indirectly influence EF-P or the pathway, or affect swarming motility in other ways.

Analysis of EF-$P_{B.s.}$ during different phases showed that EF-P seemed to be underrepresented in low division phases like lag and stationary phase. Fittingly, *B. subtilis* was the first organism reported that does not exhibit a growth defect upon deletion of *efp* [34]. Despite its important role during translation, one should have in mind that *efp* is not essential in bacteria. The reason is, that translation of proline motifs is ten times faster in the presence of functional EF-P, nevertheless it is not completely abolished in absence of the translation factor [7]. Moreover, there are several other possible reasons for decreased translation speed such as occurrence of stalling

peptides like C-terminal proline residues, secretion monitor leader peptides (e. g. SecM) or stalling sequences like FXXYXIWPP and others, which induce programmed stalling during their own translation to regulate expression of downstream genes [21, 147]. These regulatory programmed stalling incidents are explained by direct effects like encounter of polyproline motifs but also by indirect mechanisms like interactions of the nascent peptide with residues from the exit tunnel or the PTC [148, 149]. Here, positively charged stretches (lysine and arginine rich motifs) in the nascent peptide chain can interact with the negatively charged ribosomal exit tunnel when they are in 10 - 20 Å distance from the PTC. Thereby, electrostatic interactions influence the translation rates [150]. Interestingly, nascent peptides that delay protein synthesis in bacteria are not rescued by EF-P [21]. Dependence on EF-P is lowered in phases of decreased general translation rates. Moreover, *B. subtilis* Δ*efp* phenotype (swarming defect) suppressor strategies are reported like mutation of a stalling motif to decrease the translational pause (SPP mutated to APP in FliY) or mutation of genes involved in ribosome-associated factors and ribosomal proteins [110].

4.5 Detection of EF-P for elucidation of new post-translational modifications

Methods for evaluation of PTMs which do not necessarily require an enrichment step are rare. In this thesis, two of those methods were provided and applied to EF-P (Chapters 3.1 and 3.2). It transpired that 1D-IEF is a suitable tool for modification status detection of EF-P and the method was successfully established in Prof. K. Jung laboratory during the practical work for this thesis. Consequently, the detailed IEF guideline in Table 8 summarizes the distinct applications of native horizontal, denaturating horizontal and vertical IEF. It includes information on sample preparation, gel treatment, resolution optimization and possible staining methods.

Table 8: IEF techniques and their distinct applications.

	Native horizontal IEF	**Denaturating horizontal IEF**	**Vertical IEF**
Cross-reference	Chapters 2.6.3 and 3.2.2	Chapters 2.6.2, 2.6.4 and 3.4	Chapters 2.6.5, 3.3.1 and 3.3.3.3
Application	*E. coli* lysates	*B. subtilis* lysates	Purified proteins
Sample preparation	Wash/lysis: 10 mM Tris, 250 mM sucrose, pH 7.0		
		Protein precipitation with TCA/acetone, resolve ON in solubilization mix	
Gel variant	CleanGel IEF (GE)	GE: CleanGel IEF SERVA: Blank FocusGel 24S	SERVA*Gel* IEF 4 - 7

Gel rehydration	1.1 g D-sorbitol, 820 µL Pharmalyte 4 - 6.5 ad 11 mL, incubate 1 h	GE gel: solubilization mix without BPP, incubate ≥2 h Serva Gel: 12.84 g urea, 4.65 g thiourea, 2.46 mL Pharmalyte 4 - 6.5, 1.28 g CHAPS, 0.32 g DTT ad 32 mL, incubate 2 h	-
Loading amount	Lysates: 20 µL OD_{600}=10 Pure protein: 5 µg	20 - 150 µg	1 µg
Loading buffer	10X: 50 v% glycerol, 10 mg/mL BPP	Not required (= solubilization mix)	2X IEF Sample Buffer
Running buffer	-	-	SERVA IEF Anode Buffer + Cathode Buffer 3 - 10
Sample application	Large volume: filter paper next to cathode Small volume: directly	Large volume: small filter paper stripe next to the cathode Small volume: silicone application strip	Directly
Temperature	10 °C	15 °C	4 °C
Focusing conditions			
Prefocusing	350 V 6 mA 8 W, 20 min		-
Sample transition	250 V 4 mA 8 W, 20 min		50 V 10 mA 10 W, 1 h
Main focusing	1,000 V 7 mA 14 W, 4 h		200 V 30 mA 10 W, 1 h
Band sharpening	1,250 V 7 mA 18 W, 10 min		500 V 40 mA 20 W, 40 min
Gel processing	Remove gel from plastic film using a metal wire		-
	Silver Staining or Western Blotting		Coomassie/Silver Staining or Western Blotting

Contrary to the hypothesized association, different descendants of the IEF technique (vertical / native horizontal / denaturating horizontal) were necessary for different organisms and sample types. Purified EF-P was easily detected by vertical IEF, native horizontal IEF was used to analyze lysates of Gram-negative *E. coli*. Gram-negative *B. subtilis* lysates required a preceding protein precipitation step with TCA/acetone before analysis by denaturating IEF. The gel was rehydrated using urea which leads to denaturating conditions, decreases the speed of separation by increasing gel viscosity [79] and at the same time claims a defined temperature management during gel processing.

Unanticipatedly, protein tags caused a more drastic pI shift, than hypothesized based on the theoretical calculation. This was shown for His_6- or SUMO-tagging. Also single amino acid exchanges like K34R and P32S affect the position of the band in the IEF gel. This practical issue was addressed by careful selection of the reference protein.

Establishing the IEF method and gaining expertise allowed useful insights into different aspects of EF-P research which were published by Pfab *et al.* [67], Pinheiro *et al.* [35] and Volkwein *et al.* [38]. It could be shown that endogenously and recombinantly produced EF-P from *Corynebacterium glutamicum*, *Mycobacterium smegmatis* and *Steptomyces coelicolor* exhibit the same pI value and are naturally unmodified [35]. Together with other Actinobacteria they form a new subfamily of EF-Ps which are functional without PTM. Research on switching the PTM of *P. putida* (rhamnosylation) to *E. coli* EF-P (naturally (*R*)-β-lysylated) included interaction studies with EarP from *P. putida* and EF-P from *E. coli*. Here, the technique of vertical IEF was used to ensure that EF-P was in the unmodified state to qualify it for the experiment. Subsequently, ^{15}N NMR relaxation experiments could be performed. Titration revealed facilitated interaction between the non-cognate PTM partners especially when K34 is exchanged by arginine to resemble the conserved residue of EF-P from *P. putida* (results published in [38]).

The techniques of horizontal and vertical IEF presented in this thesis are not necessarily limited to EF-P or a specific PTM. Instead, the guideline for IEF of EF-P is generalizable for application to proteins from all domains of life. Therefore, the guideline contributes to microbiological methodology, especially in laboratories in which MS instruments are not available.

Chapter 3.1 presents the creation, characterization and application of universal EF-P antibodies. Two amino acid sections of EF-P were identified which are highly conserved among different bacteria and accessible for an antibody at the same time. Corresponding peptide antibodies P68/P69 successfully detected EF-P of diversely shaped bacteria such as Gram-negative (*E. coli*, *S. oneidensis*) as well as Gram-positive cocci (*M. luteus*), bacilli (*B. subtilis*) and filamentous bacteria (*Streptomyces*). At the same time the antibodies were specific, as a single band corresponding to EF-P was detected from bacterial lysates.

Here, also copy number determination during different growth phases can be helpful, which was also demonstrated in this thesis. Determination of EF-P copy numbers was possible because the created EF-P antibodies showed a broad sector of linear correlation between band intensity and EF-P amount. In the same way that EF-P copy numbers per cell were determined for *E. coli* (7,360) and *B. subtilis* (6,717), they can

be derived for bacteria not equally well studied because literature values of EF-P copy numbers are rare.

Juxtaposition of P68 and P69 during antibody characterization revealed that P69 was slightly more sensitive than P68 regarding *E. coli* and *S. oneidensis*. Comparison of the sequence identity of the three model organisms with the peptide sequence used for rabbit immunization and antibody purification was performed in Table 9. It shows that the raw numbers of sequence identity do not necessarily explain this fact and also not why EF-$P_{S.o.}$ was undetectable from lysate but needed to be concentrated prior to SDS-PAGE and Western Blot analysis. For example, EF-$P_{B.s.}$ was sensitively detected by P69 (53 % sequence identity), whereas EF-$P_{S.o.}$ was hard to detect using P68 (60 % sequence identity). Therefore, sensitivities of the universal antibodies for bacterial EF-Ps are not predictable and should be tested individually. Optimal conditions (antibody, dilution and incubation time) determined for standard organisms are listed in Table 9.

Table 9: Sequence identity between peptide antibodies P68/P69 and model organism EF-Ps. Theoretical sequence identity between antibody peptide and EF-P sequence do not inevitably represent antibody effectivity. Antibody characterization results and final antibody usage suggestions are summarized in the right column.

	Theoretical result		**Experimental result/ Recommendation**
	Peptide antibody P68	**Peptide antibody P69**	
Peptide sequence	NH_2- C+ TEPGVKGDTAGGTKP -$CONH_2$	NH_2- C+ VPLFINEGEKIKVDT -$CONH_2$	
EF-P sequence (% identity)			
E. coli	DPGLKGDTAGTGGKP **(73 %)**	VPLFVQIGEVIKVDT **(73 %)**	P69 ON 1:1,000
B. subtilis	TEPGIKGDTASGGTKP **(93 %)**	VPFFVNEGDTLVVNT **(53 %)**	Very sensitive, Mix 1:10,000
S. oneidensis	EPSARGDTSGKVMKP **(60 %)**	VADFVKVGDKIEIDT **(47 %)**	Only for purified proteins > 0.25 µg P69 1:1,000 ON

The spectrum of EF-P antibodies is broadened. Antibodies are located on the one side of the spectrum that were raised against the PTM as single epitope (anti-EF-P^{Rha} [39, 41], anti-acetyllysine ([151], now commercially available, e. g. ImmuneChem), anti-propionyllysine [152], anti-butyryllysine (commercially available, e. g. PTM Biolabs), anti-succinyllysine [153]). Despite their advantages, they only provide a yes-or-no answer regarding the modification status and are inconvenient tools to identify novel

PTMs and novel modified sites by immunoblotting. For model organisms like *E. coli*, *S. oneidensis*, *B. subtilis* or *T. thermophilus* antibodies are available that detect the native protein. The cross-reactivity of *B. subtilis* EF-P antibody with *Mycobacterium phlei* EF-P is ascertained by our group (unpublished) and the detection of *Neisseria meningitides* EF-P is reported using a polyclonal *E. coli* EF-P antibody purchased from Keari Bio [154]. On the other side of the spectrum is the universal EF-P antibody reported here, that serves as elegant tool for analysis of diverse EF-Ps without necessitating a protein enrichment step.

Further studies should consider that immunoprecipitation is a centerpiece technique of PTM analysis because here, low-abundant proteins with PTM are targeted and enriched. Therefore, antibodies that specifically bind the target protein or PTM are conjugated to solid beads and enable affinity purification. The universal EF-P antibody presented in this study can be used in immunoprecipitation to enrich EF-P from different bacteria not sufficiently addressed to date.

EF-P modification enzymes are predominantly unknown in Gram-positive bacteria for which P68/P69 performs particularly well. There is also only little research on the archaeal ortholog of EF-P, but it was shown that archaeal translation initiation factor 5A (aIF5A) of the crenarchaeum *Sulfolobus solfataricus* forms complexes with deoxyhypusine synthase and is modified with hypusine just like the eukaryotic representative eIF5A [30]. Interestingly it was found that besides its activity in protein synthesis aIF5A also exhibits moonlighting function in RNA metabolism as it exhibits endoribonucleolytic activity [155]. Moonlighting describes the ability of a protein to bear more than one physiological function. This distinct activity is often applied in different places or times and must not originate from genetic fusion, splice variants or fragmentation [52]. Moonlighting and promiscuity are opposed, as the latter is defined by performance of a physiologically irrelevant secondary reaction. The newly available antibodies P68/P69 detect EF-P independent of its modification status and can therefore be used to study possible new functions of EF-P or its potential regulatory role in unstudied strains.

5 References

1. Schmidt A, Kochanowski K, Vedelaar S, Ahrné E, Volkmer B, Callipo L, Knoops K, Bauer M, Aebersold R & Heinemann M (2016). The quantitative and condition-dependent *Escherichia coli* proteome. *Nat Biotechnol* **34,** 104–110.

2. Bremer H & Dennis PP (2008). Modulation of chemical composition and other parameters of the cell at different exponential growth rates. *EcoSal Plus* **3**.

3. Forchhammer J & Lindahl L (1971). Growth rate of polypeptide chains as a function of the cell growth rate in a mutant of *Escherichia coli* 15. *J Mol Biol* **55,** 563–568.

4. Rodnina MV (2016). The ribosome in action: Tuning of translational efficiency and protein folding. *Protein Sci* **25,** 1390–1406.

5. Rodnina MV & Wintermeyer W (2016). Protein elongation, co-translational folding and targeting. *J Mol Biol* **428,** 2165–2185.

6. LadyofHats (29.09.2008) Translation: Illustrates how a ribosome a mRNA and lots of tRNA molecules work together to produce peptides or proteins. https://commons.wikimedia.org/w/index.php?curid=4889777.

7. Woolstenhulme CJ, Guydosh NR, Green R & Buskirk AR (2015). High-precision analysis of translational pausing by ribosome profiling in bacteria lacking EFP. *Cell Rep* **11,** 13–21.

8. Komar AA (2009). A pause for thought along the co-translational folding pathway. *Trends Biochem Sci* **34,** 16–24.

9. Qi F, Motz M, Jung K, Lassak J & Frishman D (2018). Evolutionary analysis of polyproline motifs in *Escherichia coli* reveals their regulatory role in translation. *PLoS Comput Biol* **14,** e1005987.

10. Lu P, Vogel C, Wang R, Yao X & Marcotte EM (2007). Absolute protein expression profiling estimates the relative contributions of transcriptional and translational regulation. *Nat Biotechnol* **25,** 117–124.

11. Wohlgemuth I, Brenner S, Beringer M & Rodnina MV (2008). Modulation of the rate of peptidyl transfer on the ribosome by the nature of substrates. *J Biol Chem* **283,** 32229–32235.

12. Doerfel LK, Wohlgemuth I, Kubyshkin V, Starosta AL, Wilson DN, Budisa N & Rodnina MV (2015). Entropic contribution of elongation factor P to proline positioning at the catalytic center of the ribosome. *J Am Chem Soc* **137,** 12997–13006.

13. Pavlov MY, Watts RE, Tan Z, Cornish VW, Ehrenberg M & Forster AC (2009). Slow peptide bond formation by proline and other N-alkylamino acids in translation. *Proc Natl Acad Sci USA* **106,** 50–54.

14. Huter P, Arenz S, Bock LV, Graf M, Frister JO, Heuer A, Peil L, Starosta AL, Wohlgemuth I, Peske F, Nováček J, Berninghausen O, Grubmüller H, Tenson T, Beckmann R, Rodnina MV, Vaiana AC & Wilson DN (2017). Structural basis for

polyproline-mediated ribosome stalling and rescue by the translation elongation factor EF-P. *Mol Cell* **68,** 515-527.e6.

15. Peil L, Starosta AL, Lassak J, Atkinson GC, Virumae K, Spitzer M, Tenson T, Jung K, Remme J & Wilson DN (2013). Distinct XPPX sequence motifs induce ribosome stalling, which is rescued by the translation elongation factor EF-P. *Proc Natl Acad Sci USA* **110,** 15265–15270.

16. Ude S, Lassak J, Starosta AL, Kraxenberger T, Wilson DN & Jung K (2013). Translation elongation factor EF-P alleviates ribosome stalling at polyproline stretches. *Science* **339,** 82–85.

17. Gutierrez E, Shin B-S, Woolstenhulme CJ, Kim J-R, Saini P, Buskirk AR & Dever TE (2013). eIF5A promotes translation of polyproline motifs. *Mol Cell* **51,** 35–45.

18. Starosta AL, Lassak J, Peil L, Atkinson GC, Woolstenhulme CJ, Virumäe K, Buskirk A, Tenson T, Remme J, Jung K & Wilson DN (2014). A conserved proline triplet in Val-tRNA synthetase and the origin of elongation factor P. *Cell Rep* **9,** 476–483.

19. Bailly M & Crécy-Lagard V de (2010). Predicting the pathway involved in post-translational modification of elongation factor P in a subset of bacterial species. *Biol Direct* **5,** 3.

20. Doerfel LK, Wohlgemuth I, Kothe C, Peske F, Urlaub H & Rodnina MV (2013). EF-P is essential for rapid synthesis of proteins containing consecutive proline residues. *Science* **339,** 85–88.

21. Woolstenhulme CJ, Parajuli S, Healey DW, Valverde DP, Petersen EN, Starosta AL, Guydosh NR, Johnson WE, Wilson DN & Buskirk AR (2013). Nascent peptides that block protein synthesis in bacteria. *Proc Natl Acad Sci USA* **110,** E878-87.

22. Hanawa-Suetsugu K, Sekine S-i, Sakai H, Hori-Takemoto C, Terada T, Unzai S, Tame JRH, Kuramitsu S, Shirouzu M & Yokoyama S (2004). Crystal structure of elongation factor P from *Thermus thermophilus* HB8. *Proc Natl Acad Sci USA* **101,** 9595–9600.

23. Blaha G, Stanley RE & Steitz TA (2009). Formation of the first peptide bond: the structure of EF-P bound to the 70S ribosome. *Science* **325,** 966–970.

24. Yanagisawa T, Sumida T, Ishii R, Takemoto C & Yokoyama S (2010). A paralog of lysyl-tRNA synthetase aminoacylates a conserved lysine residue in translation elongation factor P. *Nat Struct Mol Biol* **17,** 1136–1143.

25. Park J-H, Johansson HE, Aoki H, Huang BX, Kim H-Y, Ganoza MC & Park MH (2012). Post-translational modification by β-lysylation is required for activity of *Escherichia coli* elongation factor P (EF-P). *J Biol Chem* **287,** 2579–2590.

26. Park MH, Cooper HL & Folk JE (1981). Identification of hypusine, an unusual amino acid, in a protein from human lymphocytes and of spermidine as its biosynthetic precursor. *Proc Natl Acad Sci USA* **78,** 2869–2873.

27. Park MH, Nishimura K, Zanelli CF & Valentini SR (2010). Functional significance of eIF5A and its hypusine modification in eukaryotes. *Amino acids* **38,** 491–500.

28. Melnikov S, Mailliot J, Shin B-S, Rigger L, Yusupova G, Micura R, Dever TE & Yusupov M (2016). Crystal structure of hypusine-containing translation factor eIF5A bound to a rotated eukaryotic ribosome. *J Mol Biol* **428,** 3570–3576.

29. Dever TE, Gutierrez E & Shin B-S (2014). The hypusine-containing translation factor eIF5A. *Crit Rev Biochem Mol Biol* **49,** 413–425.

30. Bassani F, Romagnoli A, Cacciamani T, Amici A, Benelli D, Londei P, Märtens B, Bläsi U & La Teana A (2018). Modification of translation factor aIF5A from *Sulfolobus solfataricus*. *Extremophiles* **22,** 769–780.

31. Prunetti L, Graf M, Blaby IK, Peil L, Makkay AM, Starosta AL, Papke RT, Oshima T, Wilson DN & Crécy-Lagard V de (2016). Deciphering the translation initiation factor 5A modification pathway in halophilic archaea. *Archaea* **2016,** 7316725.

32. Roy H, Zou SB, Bullwinkle TJ, Wolfe BS, Gilreath MS, Forsyth CJ, Navarre WW & Ibba M (2011). The tRNA synthetase paralog PoxA modifies elongation factor-P with (*R*)-β-lysine. *Nat Chem Biol* **7,** 667–669.

33. Peil L, Starosta AL, Virumae K, Atkinson GC, Tenson T, Remme J & Wilson DN (2012). Lys34 of translation elongation factor EF-P is hydroxylated by YfcM. *Nat Chem Biol* **8,** 695–697.

34. Rajkovic A, Hummels KR, Witzky A, Erickson S, Gafken PR, Whitelegge JP, Faull KF, Kearns DB & Ibba M (2016). Translation control of swarming proficiency in *Bacillus subtilis* by 5-amino-pentanolylated elongation factor P. *J Biol Chem* **291,** 10976–10985.

35. Pinheiro B, Scheidler CM, Kielkowski P, Schmid M, Forné I, Ye S, Reiling N, Takano E, Imhof A, Sieber SA, Schneider S & Jung K (2020). Structure and function of an elongation factor P subfamily in actinobacteria. *Cell Rep* **30,** 4332-4342.e5.

36. Witzky A, Hummels KR, Tollerson R, Rajkovic A, Jones LA, Kearns DB & Ibba M (2018). EF-P posttranslational modification has variable impact on polyproline translation in *Bacillus subtilis*. *mBio* **9**.

37. Lassak J, Keilhauer EC, Fürst M, Wuichet K, Gödeke J, Starosta AL, Chen J-M, Søgaard-Andersen L, Rohr J, Wilson DN, Häussler S, Mann M & Jung K (2015). Arginine-rhamnosylation as new strategy to activate translation elongation factor P. *Nat Chem Biol* **11,** 266–270.

38. Volkwein W, Krafczyk R, Jagtap PKA, Parr M, Mankina E, Macošek J, Guo Z, Fürst MJL, Pfab M, Frishman D, Hennig J, Jung K & Lassak J (2019). Switching the post-translational modification of translation elongation factor EF-P. *Front Microbiol* **10,** 2100.

39. Li X, Krafczyk R, Macošek J, Li Y-L, Zou Y, Simon B, Pan X, Wu Q-Y, Yan F, Li S, Hennig J, Jung K, Lassak J & Hu H-G (2016). Resolving the α-glycosidic linkage of

arginine-rhamnosylated translation elongation factor P triggers generation of the first Arg^{Rha} specific antibody. *Chem Sci* **7,** 6995–7001.

40. Rajkovic A, Erickson S, Witzky A, Branson OE, Seo J, Gafken PR, Frietas MA, Whitelegge JP, Faull KF, Navarre W, Darwin AJ & Ibba M (2015). Cyclic rhamnosylated elongation factor P establishes antibiotic resistance in *Pseudomonas aeruginosa*. *mBio* **6,** e00823.

41. Krafczyk R, Macošek J, Jagtap PKA, Gast D, Wunder S, Mitra P, Jha AK, Rohr J, Hoffmann-Röder A, Jung K, Hennig J & Lassak J (2017). Structural basis for EarP-mediated arginine glycosylation of translation elongation factor EF-P. *mBio* **8**.

42. Behshad E, Ruzicka FJ, Mansoorabadi SO, Chen D, Reed GH & Frey PA (2006). Enantiomeric free radicals and enzymatic control of stereochemistry in a radical mechanism: the case of lysine 2,3-aminomutases. *Biochemistry* **45,** 12639–12646.

43. Kobayashi K, Katz A, Rajkovic A, Ishii R, Branson OE, Freitas MA, Ishitani R, Ibba M & Nureki O (2014). The non-canonical hydroxylase structure of YfcM reveals a metal ion-coordination motif required for EF-P hydroxylation. *Nucleic Acids Res* **42,** 12295–12305.

44. Zou SB, Hersch SJ, Roy H, Wiggers JB, Leung AS, Buranyi S, Xie JL, Dare K, Ibba M & Navarre WW (2012). Loss of elongation factor P disrupts bacterial outer membrane integrity. *J Bacteriol* **194,** 413–425.

45. Marman HE, Mey AR & Payne SM (2014). Elongation factor P and modifying enzyme PoxA are necessary for virulence of *Shigella flexneri*. *Infect Immun* **82,** 3612–3621.

46. Zou SB, Roy H, Ibba M & Navarre WW (2011). Elongation factor P mediates a novel post-transcriptional regulatory pathway critical for bacterial virulence. *Virulence* **2,** 147–151.

47. Schimmel P (1987). Aminoacyl tRNA synthetases: General scheme of structure-function relationships in the polypeptides and recognition of transfer RNAs. *Annu Rev Biochem* **56,** 125–158.

48. Smith TF & Hartman H (2015). The evolution of class II aminoacyl-tRNA synthetases and the first code. *FEBS Lett* **589,** 3499–3507.

49. Wolf YI, Aravind L, Grishin NV & Koonin EV (1999). Evolution of aminoacyl-tRNA synthetases-analysis of unique domain architectures and phylogenetic trees reveals a complex history of horizontal gene transfer events. *Genome Res* **9,** 689–710.

50. Kong L, Fromant M, Blanquet S & Plateau P (1991). Evidence for a new *Escherichia coli* protein resembling a lysyl-tRNA synthetase. *Gene* **108,** 163–164.

51. Ambrogelly A, O'Donoghue P, Söll D & Moses S (2010). A bacterial ortholog of class II lysyl-tRNA synthetase activates lysine. *FEBS Lett* **584,** 3055–3060.

52. Copley SD (2017). Shining a light on enzyme promiscuity. *Curr Opin Struct Biol* **47,** 167–175.

53. Schimmel P & Schmidt E (1995). Making connections: RNA-dependent amino acid recognition. *Trends Biochem Sci* **20,** 1–2.

54. Jakubowski H (1999). Misacylation of $tRNA^{Lys}$ with noncognate amino acids by lysyl-tRNA synthetase. *Biochemistry* **38,** 8088–8093.

55. Splan KE, Musier-Forsyth K, Boniecki MT & Martinis SA (2008). In vitro assays for the determination of aminoacyl-tRNA synthetase editing activity. *Methods* **44,** 119–128.

56. Baldwin AN & Berg P (1966). Transfer ribonucleic acid-induced hydrolysis of valyladenylate bound to isoleucyl ribonucleic acid synthetase. *J Biol Chem* **241,** 839–845.

57. Guth E, Farris M, Bovee M & Francklyn CS (2009). Asymmetric amino acid activation by class II histidyl-tRNA synthetase from *Escherichia coli*. *J Biol Chem* **284,** 20753–20762.

58. Hati S, Ziervogel B, Sternjohn J, Wong F-C, Nagan MC, Rosen AE, Siliciano PG, Chihade JW & Musier-Forsyth K (2006). Pre-transfer editing by class II prolyl-tRNA synthetase: role of aminoacylation active site in "selective release" of noncognate amino acids. *J Biol Chem* **281,** 27862–27872.

59. Burkholder PR & Giles NH (1947). Induced biochemical mutations in *Bacillus subtilis*. *Am J Bot* **34,** 345–348.

60. Studier FW & Moffatt BA (1986). Use of bacteriophage T7 RNA polymerase to direct selective high-level expression of cloned genes. *J Mol Biol* **189,** 113–130.

61. Baba T, Ara T, Hasegawa M, Takai Y, Okumura Y, Baba M, Datsenko KA, Tomita M, Wanner BL & Mori H (2006). Construction of *Escherichia coli* K-12 in-frame, single-gene knockout mutants: the Keio collection. *Mol Syst Biol* **2,** 2006.0008.

62. Platt R, Drescher C, Park SK & Phillips GJ (2000). Genetic system for reversible integration of DNA constructs and *lacZ* gene fusions into the *Escherichia coli* chromosome. *Plasmid* **43,** 12–23.

63. Guzman LM, Belin D, Carson MJ & Beckwith J (1995). Tight regulation, modulation, and high-level expression by vectors containing the arabinose P_{BAD} promoter. *J Bacteriol* **177,** 4121–4130.

64. Blattner FR, Plunkett G, Bloch CA, Perna NT, Burland V, Riley M, Collado-Vides J, Glasner JD, Rode CK, Mayhew GF, Gregor J, Davis NW, Kirkpatrick HA, Goeden MA, Rose DJ, Mau B & Shao Y (1997). The complete genome sequence of *Escherichia coli* K-12. *Science* **277,** 1453–1462.

65. Venkateswaran K, Moser DP, Dollhopf ME, Lies DP, Saffarini DA, MacGregor BJ, Ringelberg DB, White DC, Nishijima M, Sano H, Burghardt J, Stackebrandt E & Nealson KH (1999). Polyphasic taxonomy of the genus *Shewanella* and description of *Shewanella oneidensis* sp. nov. *Int J Syst Bacteriol* **49 Pt 2,** 705–724.

66. Volkwein W, Maier C, Krafczyk R, Jung K & Lassak J (2017). A versatile toolbox for the control of protein levels using Nε-acetyl-L-lysine dependent amber suppression. *ACS Synth Biol* **6,** 1892–1902.

67. Pfab M, Kielkowski P, Krafczyk R, Volkwein W, Sieber SA, Lassak J & Jung K (2020). Synthetic post-translational modifications of elongation factor P using the ligase EpmA. *FEBS J*., doi:10.1111/febs.15346.

68. Ude S (05.03.2013) The role of elongation factor EF-P in translation and in copy number control of the transcriptional regulator CadC in *Escherichia coli*. Dissertation, Munich.

69. Dubendorff JW & Studier FW (1991). Controlling basal expression in an inducible T7 expression system by blocking the target T7 promoter with lac repressor. *J Mol Biol* **219,** 45–59.

70. Artimo P, Jonnalagedda M, Arnold K, Baratin D, Csardi G, Castro E de, Duvaud S, Flegel V, Fortier A, Gasteiger E, Grosdidier A, Hernandez C, Ioannidis V, Kuznetsov D, Liechti R, Moretti S, Mostaguir K, Redaschi N, Rossier G, Xenarios I & Stockinger H (2012). ExPASy: SIB bioinformatics resource portal. *Nucleic Acids Res* **40,** W597-603.

71. Kelley LA, Mezulis S, Yates CM, Wass MN & Sternberg MJE (2015). The Phyre2 web portal for protein modeling, prediction and analysis. *Nat Protoc* **10,** 845–858.

72. Pettersen EF, Goddard TD, Huang CC, Couch GS, Greenblatt DM, Meng EC & Ferrin TE (2004). UCSF Chimera-a visualization system for exploratory research and analysis. *J Comput Chem* **25,** 1605–1612.

73. Schneider CA, Rasband WS & Eliceiri KW (2012). NIH Image to ImageJ: 25 years of image analysis. *Nat Methods* **9,** 671–675.

74. Li S-J & Hochstrasser M (1999). A new protease required for cell-cycle progression in yeast. *Nature* **398,** 246–251.

75. Mossessova E & Lima CD (2000). Ulp1-SUMO crystal structure and genetic analysis reveal conserved interactions and a regulatory element essential for cell growth in yeast. *Mol Cell* **5,** 865–876.

76. Gallego-Jara J, Écija Conesa A, Diego Puente T de, Lozano Terol G & Cánovas Díaz M (2017). Characterization of CobB kinetics and inhibition by nicotinamide. *PLoS One* **12,** e0189689.

77. Laemmli UK (1970). Cleavage of structural proteins during the assembly of the head of bacteriophage T4. *Nature* **227,** 680–685.

78. Ladner CL, Yang J, Turner RJ & Edwards RA (2004). Visible fluorescent detection of proteins in polyacrylamide gels without staining. *Anal Biochem* **326,** 13–20.

79. Westermeier R (30. September 2016) Elektrophorese leicht gemacht: Ein Praxisbuch für Anwender, 2nd edn. Wiley-VCH, Weinheim.

80. Chen X, Ma J-J, Tan M, Yao P, Hu Q-H, Eriani G & Wang E-D (2011). Modular pathways for editing non-cognate amino acids by human cytoplasmic leucyl-tRNA synthetase. *Nucleic Acids Res* **39,** 235–247.

81. Tetsch L, Koller C, Haneburger I & Jung K (2008). The membrane-integrated transcriptional activator CadC of *Escherichia coli* senses lysine indirectly via the interaction with the lysine permease LysP. *Molecular microbiology* **67,** 570–583.

82. Jeffrey H. Miller (1972) Experiments in molecular genetics. Cold Spring Harbor Laboratory, New York.

83. Benson DA, Karsch-Mizrachi I, Clark K, Lipman DJ, Ostell J & Sayers EW (2012). GenBank. *Nucleic Acids Res* **40,** D48-53.

84. Larkin MA, Blackshields G, Brown NP, Chenna R, McGettigan PA, McWilliam H, Valentin F, Wallace IM, Wilm A, Lopez R, Thompson JD, Gibson TJ & Higgins DG (2007). Clustal W and Clustal X version 2.0. *Bioinformatics* **23,** 2947–2948.

85. T. A. Hall (1999). BioEdit: a user-friendly biological sequence alignment editor and analysis program for Windows 95/98/NT. *Nucl Acids Symp* **41,** 95–98.

86. Crooks GE, Hon G, Chandonia J-M & Brenner SE (2004). WebLogo: a sequence logo generator. *Genome Res* **14,** 1188–1190.

87. Muntel J, Fromion V, Goelzer A, Maaβ S, Mäder U, Büttner K, Hecker M & Becher D (2014). Comprehensive absolute quantification of the cytosolic proteome of *Bacillus subtilis* by data independent, parallel fragmentation in liquid chromatography/mass spectrometry (LC/MS(E)). *Mol Cell Proteomics* **13,** 1008–1019.

88. Kang HA, Schwelberger HG & Hershey JW (1993). Translation initiation factor eIF-5A, the hypusine-containing protein, is phosphorylated on serine in *Saccharomyces cerevisiae*. *J Biol Chem* **268,** 14750–14756.

89. Torgyn Laas, Ingmar Olsson & Lennart Söderberg (1980). High-voltage temperature isoelectric distribution, focusing with pharmalyte: Field strength and temperature distribution, zone sharpening, isoelectric spectra and pl determinations. *Anal Biochem* **101,** 449–461.

90. Klee SM, Sinn JP, Holmes AC, Lehman BL, Krawczyk T, Peter KA & McNellis TW (2019). Extragenic suppression of elongation factor P gene mutant phenotypes in *Erwinia amylovora*. *J Bacteriol* **201**.

91. Gilreath MS, Roy H, Bullwinkle TJ, Katz A, Navarre WW & Ibba M (2011). β-Lysine discrimination by lysyl-tRNA synthetase. *FEBS Lett* **585,** 3284–3288.

92. Bennett BD, Kimball EH, Gao M, Osterhout R, van Dien SJ & Rabinowitz JD (2009). Absolute metabolite concentrations and implied enzyme active site occupancy in *Escherichia coli*. *Nat Chem Biol* **5,** 593–599.

93. Kreimeyer A, Perret A, Lechaplais C, Vallenet D, Médigue C, Salanoubat M & Weissenbach J (2007). Identification of the last unknown genes in the fermentation pathway of lysine. *J Biol Chem* **282,** 7191–7197.

94. Chen I-C, Lin W-D, Hsu S-K, Thiruvengadam V & Hsu W-H (2009). Isolation and characterization of a novel lysine racemase from a soil metagenomic library. *Appl Environ Microbiol* **75,** 5161–5166.

95. Otzen M, Palacio C & Janssen DB (2018). Characterization of the caprolactam degradation pathway in *Pseudomonas jessenii* using mass spectrometry-based proteomics. *Appl Microbiol Biotechnol* **102,** 6699–6711.

96. Mitchell DJ, Kim DT, Steinman L, Fathman CG & Rothbard JB (2000). Polyarginine enters cells more efficiently than other polycationic homopolymers. *J Pept Res* **56,** 318–325.

97. Weiler J, Gausepohl H, Hauser N, Jensen ON & Hoheisel JD (1997). Hybridisation based DNA screening on peptide nucleic acid (PNA) oligomer arrays. *Nucleic Acids Res* **25,** 2792–2799.

98. Lim J-H, Kim M-S, Kim H-E, Yano T, Oshima Y, Aggarwal K, Goldman WE, Silverman N, Kurata S & Oh B-H (2006). Structural basis for preferential recognition of diaminopimelic acid-type peptidoglycan by a subset of peptidoglycan recognition proteins. *J Biol Chem* **281,** 8286–8295.

99. Hara R, Yamagata K, Miyake R, Kawabata H, Uehara H & Kino K (2017). Discovery of lysine hydroxylases in the clavaminic acid synthase-like superfamily for efficient hydroxylysine bioproduction. *Appl Environ Microbiol* **83**.

100. Perdivara I, Yamauchi M & Tomer KB (2013). Molecular characterization of collagen hydroxylysine O-glycosylation by mass spectrometry: Current status. *Aust J Chem* **66,** 760–769.

101. Kanehisa M & Goto S (2000). KEGG: kyoto encyclopedia of genes and genomes. *Nucleic Acids Res* **28,** 27–30.

102. Francklyn CS, First EA, Perona JJ & Hou Y-M (2008). Methods for kinetic and thermodynamic analysis of aminoacyl-tRNA synthetases. *Methods* **44,** 100–118.

103. Michaelis L, Menten ML, Johnson KA & Goody RS (2011). The original Michaelis constant: translation of the 1913 Michaelis-Menten paper. *Biochemistry* **50,** 8264–8269.

104. Zaher HS & Green R (2009). Quality control by the ribosome following peptide bond formation. *Nature* **457,** 161–166.

105. Beyer H & Walter W (1991) Lehrbuch der organischen Chemie, 22nd edn. S. Hirzel Verlag, Stuttgart.

106. Haynes WM, ed (2017) CRC handbook of chemistry and physics: A ready-reference book of chemical and physical data, 97th edn. CRC Press, Boca Raton, London, New York.

107. Rodionov DA, Vitreschak AG, Mironov AA & Gelfand MS (2003). Regulation of lysine biosynthesis and transport genes in bacteria: yet another RNA riboswitch? *Nucleic Acids Res* **31,** 6748–6757.

108. Gil J, Ramírez-Torres A & Encarnación-Guevara S (2017). Lysine acetylation and cancer: A proteomics perspective. *J Proteomics* **150,** 297–309.

109. AES Electrophoresis Society Isoelectric focusing. http://www.aesociety.org/areas/isoelectric_focusing_orig.php.

110. Hummels KR & Kearns DB (2019). Suppressor mutations in ribosomal proteins and FliY restore *Bacillus subtilis* swarming motility in the absence of EF-P. *PLoS Genet* **15,** e1008179.

111. Navarre WW, Zou SB, Roy H, Xie JL, Savchenko A, Singer A, Edvokimova E, Prost LR, Kumar R, Ibba M & Fang FC (2010). PoxA, yjeK, and elongation factor P coordinately modulate virulence and drug resistance in *Salmonella enterica*. *Mol Cell* **39,** 209–221.

112. Tollerson R, Witzky A & Ibba M (2018). Elongation factor P is required to maintain proteome homeostasis at high growth rate. *Proc Natl Acad Sci USA* **115,** 11072–11077.

113. Klee SM, Mostafa I, Chen S, Dufresne C, Lehman BL, Sinn JP, Peter KA & McNellis TW (2018). An *Erwinia amylovora yjeK* mutant exhibits reduced virulence, increased chemical sensitivity and numerous environmentally dependent proteomic alterations. *Mol Plant Pathol* **19,** 1667–1678.

114. Kaniga K, Compton MS, Curtiss R & Sundaram P (1998). Molecular and functional characterization of *Salmonella enterica* serovar typhimurium *poxA* gene: effect on attenuation of virulence and protection. *Infect Immun* **66,** 5599–5606.

115. Carabetta VJ, Silhavy TJ & Cristea IM (2010). The response regulator SprE (RssB) is required for maintaining poly(A) polymerase I-degradosome association during stationary phase. *J Bacteriol* **192,** 3713–3721.

116. Steffes C, Ellis J, Wu J & Rosen BP (1992). The *lysP* gene encodes the lysine-specific permease. *J Bacteriol* **174,** 3242–3249.

117. Hochberg GKA & Thornton JW (2017). Reconstructing ancient proteins to understand the causes of structure and function. *Annu Rev Biophys* **46,** 247–269.

118. Hansen EH, Møller BL, Kock GR, Bünner CM, Kristensen C, Jensen OR, Okkels FT, Olsen CE, Motawia MS & Hansen J (2009). De novo biosynthesis of vanillin in fission yeast (*Schizosaccharomyces pombe*) and baker's yeast (*Saccharomyces cerevisiae*). *Appl Environ Microbiol* **75,** 2765–2774.

119. Copley SD (2009). Evolution of efficient pathways for degradation of anthropogenic chemicals. *Nat Chem Biol* **5,** 559–566.

120. Drauz K, Gröger H & May O, eds (2012) Enzyme catalysis in organic synthesis. Wiley-VCH-Verl., Weinheim.

121. Volkwein W (08.09.2014) Synthetische Aktivierung des Elongationsfaktors P. Master's Thesis, Munich.

122. Xu H, Zhou J, Lin S, Deng W, Zhang Y & Xue Y (2017). PLMD: An updated data resource of protein lysine modifications. *J Genet Genomics* **44,** 243–250.

123. Lepore BW, Ruzicka FJ, Frey PA & Ringe D (2005). The x-ray crystal structure of lysine-2,3-aminomutase from *Clostridium subterminale*. *Proc Natl Acad Sci USA* **102,** 13819–13824.

124. Chirpich TP, Zappia V, Costilow RN & Barker HA (1970). Lysine 2,3-aminomutase. Purification and properties of a pyridoxal phosphate and S-adenosylmethionine-activated enzyme. *J Biol Chem* **245,** 1778–1789.

125. Müller S, Hoffmann T, Santos H, Saum SH, Bremer E & Müller V (2011). Bacterial abl-like genes: production of the archaeal osmolyte Nε-acetyl-β-lysine by homologous overexpression of the yodP-kamA genes in *Bacillus subtilis*. *Appl Microbiol Biotechnol* **91,** 689–697.

126. Yanagisawa T, Ishii R, Fukunaga R, Kobayashi T, Sakamoto K & Yokoyama S (2008). Multistep engineering of pyrrolysyl-tRNA synthetase to genetically encode Nε-(o-azidobenzyloxycarbonyl) lysine for site-specific protein modification. *Chem Biol* **15,** 1187–1197.

127. Wan W, Tharp JM & Liu WR (2014). Pyrrolysyl-tRNA synthetase: an ordinary enzyme but an outstanding genetic code expansion tool. *Biochim Biophys Acta* **1844,** 1059–1070.

128. Azevedo C & Saiardi A (2016). Why always lysine? The ongoing tale of one of the most modified amino acids. *Adv Biol Regul* **60,** 144–150.

129. He X-D, Gong W, Zhang J-N, Nie J, Yao C-F, Guo F-S, Lin Y, Wu X-H, Li F, Li J, Sun W-C, Wang E-D, An Y-P, Tang H-R, Yan G-Q, Yang P-Y, Wei Y, Mao Y-Z, Lin P-C, Zhao J-Y, Xu Y, Xu W & Zhao S-M (2018). Sensing and transmitting intracellular amino acid signals through reversible lysine aminoacylations. *Cell Metab* **27,** 151-166.e6.

130. Wada A, Igarashi K, Yoshimura S, Aimoto S & Ishihama A (1995). Ribosome modulation factor: stationary growth phase-specific inhibitor of ribosome functions from *Escherichia coli*. *Biochem Biophys Res Commun* **214,** 410–417.

131. Barber KW & Rinehart J (2018). The ABCs of PTMs. *Nat Chem Biol* **14,** 188–192.

132. Bullwinkle TJ, Zou SB, Rajkovic A, Hersch SJ, Elgamal S, Robinson N, Smil D, Bolshan Y, Navarre WW & Ibba M (2013). (R)-β-lysine-modified elongation factor P functions in translation elongation. *J Biol Chem* **288,** 4416–4423.

133. Colak G, Xie Z, Zhu AY, Dai L, Lu Z, Zhang Y, Wan X, Chen Y, Cha YH, Lin H, Zhao Y & Tan M (2013). Identification of lysine succinylation substrates and the succinylation regulatory enzyme CobB in *Escherichia coli*. *Mol Cell Proteomics* **12,** 3509–3520.

134. Wei Y, Yang W-J, Wang Q-J, Lin P-C, Zhao J-Y, Xu W, Zhao S-M & He X-D (2019). Cell-wide survey of amide-bonded lysine modifications by using deacetylase CobB. *Biol Proced Online* **21,** 23.

135. Guo M & Schimmel P (2013). Essential nontranslational functions of tRNA synthetases. *Nat Chem Biol* **9,** 145–153.

136. Schimmel P & Ribas De Pouplana L (2000). Footprints of aminoacyl-tRNA synthetases are everywhere. *Trends Biochem Sci* **25,** 207–209.

137. Sissler M, Delorme C, Bond J, Ehrlich SD, Renault P & Francklyn C (1999). An aminoacyl-tRNA synthetase paralog with a catalytic role in histidine biosynthesis. *Proc Natl Acad Sci USA* **96,** 8985–8990.

138. Brevet A, Chen J, Lévêque F, Blanquet S & Plateau P (1995). Comparison of the enzymatic properties of the two *Escherichia coli* lysyl-tRNA synthetase species. *J Biol Chem* **270,** 14439–14444.

139. Roy H, Becker HD, Reinbolt J & Kern D (2003). When contemporary aminoacyl-tRNA synthetases invent their cognate amino acid metabolism. *Proc Natl Acad Sci USA* **100,** 9837–9842.

140. Ofir-Birin Y, Fang P, Bennett SP, Zhang H-M, Wang J, Rachmin I, Shapiro R, Song J, Dagan A, Pozo J, Kim S, Marshall AG, Schimmel P, Yang X-L, Nechushtan H, Razin E & Guo M (2013). Structural switch of lysyl-tRNA synthetase between translation and transcription. *Mol Cell* **49,** 30–42.

141. Holman KM, Puppala AK, Lee JW, Lee H & Simonović M (2017). Insights into substrate promiscuity of human seryl-tRNA synthetase. *RNA* **23,** 1685–1699.

142. Chen H, Huang R, Li Z, Zhu W, Chen J, Zhan Y & Jiang B (2017). Selective lysine modification of native peptides via aza-Michael addition. *Org Biomol Chem* **15,** 7339–7345.

143. Baumann T, Nickling JH, Bartholomae M, Buivydas A, Kuipers OP & Budisa N (2017). Prospects of in vivo incorporation of non-canonical amino acids for the chemical diversification of antimicrobial peptides. *Front Microbiol* **8,** 124.

144. Chaubet G, Thoreau F & Wagner A (2018). Recent, non-classical, approaches to antibody lysine modification. *Drug Discov Today Technol* **30,** 21–26.

145. Kearns DB, Chu F, Rudner R & Losick R (2004). Genes governing swarming in *Bacillus subtilis* and evidence for a phase variation mechanism controlling surface motility. *Mol Microbiol* **52,** 357–369.

146. Hummels KR, Witzky A, Rajkovic A, Tollerson R, Jones LA, Ibba M & Kearns DB (2017). Carbonyl reduction by YmfI in *Bacillus subtilis* prevents accumulation of an inhibitory EF-P modification state. *Mol Microbiol* **106,** 236–251.

147. Tanner DR, Cariello DA, Woolstenhulme CJ, Broadbent MA & Buskirk AR (2009). Genetic identification of nascent peptides that induce ribosome stalling. *J Biol Chem* **284,** 34809–34818.

148. Nakatogawa H & Ito K (2002). The ribosomal exit tunnel functions as a discriminating gate. *Cell* **108,** 629–636.

149. Wilson DN, Arenz S & Beckmann R (2016). Translation regulation via nascent polypeptide-mediated ribosome stalling. *Curr Opin Struct Biol* **37,** 123–133.

150. Lu J & Deutsch C (2008). Electrostatics in the ribosomal tunnel modulate chain elongation rates. *J Mol Biol* **384,** 73–86.

151. Qiang L, Xiao H, Campos EI, Ho VC & Li G (2005). Development of a PAN-specific, affinity-purified anti-acetylated lysine antibody for detection, identification, isolation, and intracellular localization of acetylated protein. *J Immunoassay Immunochem* **26,** 13–23.

152. Cheng Z, Tang Y, Chen Y, Kim S, Liu H, Li SSC, Gu W & Zhao Y (2009). Molecular characterization of propionyllysines in non-histone proteins. *Mol Cell Proteomics* **8,** 45–52.

153. Zhang Z, Tan M, Xie Z, Dai L, Chen Y & Zhao Y (2011). Identification of lysine succinylation as a new post-translational modification. *Nat Chem Biol* **7,** 58–63.

154. Yanagisawa T, Takahashi H, Suzuki T, Masuda A, Dohmae N & Yokoyama S (2016). *Neisseria meningitidis* translation elongation factor P and its active-site arginine residue are essential for cell viability. *PLoS One* **11,** e0147907.

155. Bassani F, Zink IA, Pribasnig T, Wolfinger MT, Romagnoli A, Resch A, Schleper C, Bläsi U & La Teana A (2019). Indications for a moonlighting function of translation factor aIF5A in the crenarchaeum *Sulfolobus solfataricus*. *RNA Biol* **16,** 675–685.

Acknowledgements

First of all, I would like to thank Kirsten for her support and funding, for advice in labmeetings and organization of talks and seminars. Moreover, thank Jürgen for insightful comments and a head of ideas.

I would like to thank excellence cluster CIPSMwomen for enabling personal and professional growth by giving me a position that includes administration and communication responsibilities, by funding of conference participation and by organizing interesting talks at ‘CIPSM Scientific Oktoberfest’s.

Hereby, I would like to honor the rabbits SY7620 and SY7621 that produced my peptide antibodies.

A lot of positive people I will definitely miss are my buddies Elli and Simone, office colleagues Angi, Jannis, Urte, lab colleagues Bruno, Korinna, Ingrid, Lena, best conversation partners Franzi, Julia, Ralph, Wolfram and the MiBi running group Dan, Larissa, Marina, Michelle, Steffi, Sophie.

My rock in the sea Max Liedl for creating a relationship that feels like home. Ben, I’m looking forward to support you in all the small and large challenges life brings up.

Thanks to all the people who created active rests from preparation of this thesis, namely Isolde Preuss with Molly for panorama walks in the Austrian Alps and several rounds in the heated outdoor pool, my parents and Matthias for action on alpine and skating ski and for their support in any case, and Heather Robertson for keeping me fit.

Moreover, I would like to mention the song “Dance Monkey” by Tones And I which was played in the 1 hour loop uncountable times during writing and preparation of figures for this thesis.

„Mögen alle Menschen, Tiere und Lebewesen glücklich und frei sein. Mögen alle meine Worte, Taten und Gedanken zu diesem Glück und zu dieser Freiheit beitragen.“ Lokah Samastah Sukhino Bhavantu

Curriculum Vitae

Personal Information

Name: Miriam Pfab

Date of Birth: 13.09.1990

Place of Birth: München

Higher Education and Research Experience

05/2016 - 10/2019	**PhD student**, Ludwig-Maximilians-Universität Munich (LMU), Germany Group: Prof. Kirsten Jung Subject: Post-translational modification of elongation factor P
10/2013 - 02/2016	**Master of Science (Chemistry)**, Technical University Munich (TUM), Germany Specialization: Technical Chemistry, Construction Chemistry Master thesis: “Modelling of Glycosidic Bond Cleavage using SiO_2/ZrO_2 Catalysts for Hydrolysis of Cellobiose“
10/2012 - 09/2013	**Bachelor of Science (Chemistry)**, Technical University Munich (TUM), Germany Bachelor thesis: “The synthesis of Co, Ni, Rh, Ru, Pt, Pd Catalysts and their Application in Biomass Conversion“
09/2010 - 09/2012	**Study of Food Chemistry**, Technical University Munich (TUM), Germany